DELFT UNIVERSITY OF TECHNOLOGY

MASTER THESIS

Investigation of the sand losses which occur during construction of a closure dam in a tidal inlet

Author
Joost Willems

Graduation committee
Prof. dr. ir. M.J.F. Stive
R.J. Labeur
G.L.M. van der Schrieck
C. Langeveld
J. Kroon

November 8, 2013

Preface

After the two closures of 'Maasvlakte 2', the demand originated for extra knowledge to predict sand losses during the construction of sand closures. I am the lucky one who is elected to do the first step in the investigation to the processes which occur during sand closures.

In March I started with a research in literature, followed by an analysis of the important parameters and processes in the system of a sand closure and a tidal basin. The final phase consisted of the development of a tool to predict the sand losses. This was a braincracker, because in my expectation I would solve the problem and be able to build a tool which predicts the sand losses really good for all the different cases. Unfortunately this was a bridge too far for a graduation project, which felt a bit like a loss for me. It became a real struggle when I discovered that I could not build an optimal tool to predict the sand losses.

Despite the disappointment, a good first step is taken in the investigation to the processes which occur during the construction of a sand closure. I am convinced that with the results of this thesis and a next step the tool can be optimized or new tool can be made, which gives a good prediction of the sand losses.

This report could not be established without the help of different people. First I would like to thank the people of my graduation committee for their help and the time they spend to help me in my investigation. I would like two persons especially. Cuno, thanks for providing the opportunity to do my graduation project at Van Oord and Anna, thanks for for the helpful meetings and the time you spend to improve the process and the result of my research.

Besides my committee I would like to thank my parents for their support during the process and their help in the final phase when the pressure became high. The next person I want to thank is my brother, just because you are my brother. I also want to thank you for your support during the heavy final weeks of the research. Rein, Mieke en Mareijn, especially in the week before I had to hand in my concept report for the green light meeting, you were very helpful. The many phone calls helped me through this period.

I would like to thank Dirk, Willem, Max, Constant, Jimmy and Maarten for the nice time we had during our graduation project at our office at Van Oord. I would not have missed the coffee sessions along the water and the world improving discussions after some drinks. Thank you guys for the nice time we had during our graduation project.

Regards,

Joost Willems

Abstract

At the construction of 'Maasvlakte 2', two sand closures were constructed. Sand is in most cases the most profiting construction material. But in the processes which occur during the construction of a closure and the amount of sand losses, a large uncertainty is present. In order to construct a closure, the production of sand has to be larger than the sand losses. The current calculation tool for the sand losses is presented in the 'CUR 157, Sand Closures'. This book presents a feasibility study, but the calculated sand losses show a large uncertainty. For future closures it is demanded to improve the accuracy of the predictions of the sand losses.

This thesis contains two goals. Investigate the processes which occur during the construction of a sand closure and construct a tool to calculates the sand losses. In order to perform this research, answer is found to the research question: "How can the processes during construction of a sand closure be described and modelled to improve the prediction of the sand losses over time?"

For the analysis of the processes which are important an analytical description of the flow through a tidal inlet is used. Subsequently the flow through the gap and the interaction between the flow and the bed are analysed to calculate the changes in the geometry of the closure gap. In the analysis, the formulation of the CUR 157 is compared with the Van Rhee formulation. The theory of Van Rhee describes the interaction between the flow and the bed. The most important concept of his theory is that, as a consequence of the friction which the flow exerts to the bed, the soil dilates and water is flowing in the soil layer. This inflow of water hinders the erosion of the bed. This process becomes more significant when the flow velocities increase.

After the analysis, the Van Rhee formulation is used in a 1-dimensional numerical model to calculate the sand losses. This model is calibrated using one of the closures of 'Maasvlakte 2' and calibrated on three other cases. Finally the results of the model are compared with the sand losses calculated with the formulation of the CUR 157.

From the analysis of the processes which occur in a closure gap can be concluded that the flow depends on resistance over the closure gap, the tidal forcing and the storage surface of the basin. The resistance over the gap depends on the geometry of the closure gap. A long sill (in flow direction) increases the friction over the gap and in order to increase the friction, a vertical closure is preferred above horizontal closure. The interaction between the bed and the flow depends on the flow velocity and the soil properties. An important process is the hindering of the erosion due to the inflow of water. The hindering becomes larger if the porosity and the permeability of the bed are smaller.

The 1-dimensional model provides results with an uncertainty, comparable to the CUR 157 formulation. An improvement pertaining to the CUR 157 calculation is that the 1-dimensional model takes into account more physical processes. However the model contains two shortcomings. The first one is that the model performs a vertical closure downstream of the sections where the production takes place to close the dam horizontally. This is a consequence of the

deficiency that the model does not take into account the 2-dimensional processes. The second shortcoming is that the model shows unstable behaviour when the flows become critical. In the end, the extra physical processes which are taken into account are promising. When the shortcomings are solved in future research an extra improvement of the calculation of the sand losses is possible.

Contents

List of symbols

Symbol	Description	Units
β	Angle of the bed of the closure gap	$[rad]$
Δ	Relative density	$[-]$
Γ	Dimensionless coefficient which contains all the parameters which determine the geometry of a closure gap and the tidal forcing in Battjes' method	$[-]$
$\gamma_{L,R}$	Angle of respectively the left and right bank of a closure gap	$[rad]$
$\zeta_{0,b}$	water levels respectively at sea (subscript 0) and in the basin (subscript b)	$[m]$
θ	Shields number/dimensionless value of the friction velocity	$[-]$
θ_{cr}	Critical shields parameter or initiation of motion	$[-]$
θ_{cr}^1	Critical shields parameter according to Van Rhee	$[-]$
μ	Dimensionless coefficient for in and outflow losses	$[-]$
ν	Kinematic viscosity	$[m^2/s]$
ξ	Relative crest length of the sill in a closure gap	$[-]$
ξ_{in}	Friction loss during inflow from the sea or the basin	$[-]$
$\xi_{in_{HC}}$	Friction loss during inflow at the horizontal closure	$[-]$
ξ_{out}	Friction loss during the outflow in the sea or the basin	$[-]$
$\xi_{out_{HC}}$	Friction loss during the outflow at the horizontal closure	$[-]$
ξ_{total}	Total resistance over the closure gap	$[-]$
ρ_s	Density of sand	$[kg/m^3]$
ρ_w	Density of water	$[kg/m^3]$
σ	Courant number	$[-]$
τ	Relaxation time of the system of a tidal inlet and tidal basin	$[s]$
Φ	Dimensionless flow parameter	$[-]$
ϕ	Angle of internal friction of a soil layer	$[rad]$
ϕ_e	Net dimensionless pick up	$[-]$
$\phi_{e,T}$	Net dimensionless pick up, averaged over a tidal period	$[-]$
ϕ_p	Dimensionless pick up rate	$[-]$
ϕ_p^1	Dimensionless pick up rate calculated using the Van Rhee formula	$[-]$
ϕ_s	Dimensionless sedimentation rate	$[-]$
χ	Dimensionless friction term, used in Battjes' method	$[-]$
Ψ	Dimension less transport parameter	$[-]$
ψ	Reduction factor for submerged flows	$[-]$
ω	Angular frequency of a wave	$[s^{-1}]$
ω_0	Eigenfrequency of the system of a tidal inlet and a basin	$[s^{-1}]$

A_b	Surface area of the water basin	$[m^2]$
A_c	Cross-sectional area of the closure gap	$[m^2]$
a, b	Dimensionless regression coefficients in the formula of the CUR 157	$[-]$
a_0	Tidal amplitude	$[m]$
C	Chézy coefficient	$[m^{\frac{1}{2}}/s]$
C_d	Discharge coefficient for super-critical flows	$[-]$
C_{prod}	Added volumetric concentration by production	$[-]$
C_{ero}	Eroded sand that becomes in suspension expressed in a volumetric concentration	$[-]$
c	Volumetric concentration of sediment in the water	$[-]$
c_{wave}	Celerity or the propagation velocities of waves	$[m/s]$
c_f	Dimensionless friction coefficient	$[-]$
c_{nb}	Near bed volumetric sediment concentration	$[-]$
D_{15}		$[m]$
D_{50}	Median grain size	$[m]$
D_{90}		$[m]$
D_*	The dimensionless diameter of a sand grain	$[-]$
d	Water depth	$[m]$
E	Erosion rate	$[kg/m^2 s]$
E_{EH}	Sediment transport rate calculated with the Engelund and Hansen formula	$[m^3/sm]$
E_m	Sand loss per meter closure gap width in the main stream of the closure gap	$[m^3/ms]$
E_t	Sand loss per meter width of the bank in the vortex street	$[m^3/ms]$
F_g	Gravitational force on a sand grain under water	$[N]$
F_i	Force on a soil layer exerted by the hydraulic gradient	$[N]$
F_s	Shear force which the water exerts on the bed	$[N]$
Fr	Froude number	$[-]$
g	Gravitational acceleration	$[m/s^2]$
H_0	Energy level upstream of the closure gap	$[m]$
ΔH_v	Energy loss over a closure gap	$[m]$
h_b	Water level at the basin, above N.A.P.	$[m]$
h_0	Water level at sea, above N.A.P.	$[m]$
h_{sill}	Bed level of the sill of the closure gap below N.A.P.	$[m]$
h_t	Water level downstream referred to the height of the sill of a closure dam	$[m]$
h_w	Water level in the closure gap referred to N.A.P.	$[m]$
i	Hydraulic gradient in a soil layer	$[m/m]$
k	Permeability of a soil layer	$[m/s]$
k_s	Roughness of the bed of the closure gap	$[m]$
L	Length of the closure gap in flow direction	$[m]$
L_a	Adaptation length	$[m]$
L_{wave}	Wave length	$[m]$
n	A parameter to determine the reduction factor for submerged flows	$[-]$
n_0	Porosity of the bed	$[-]$

n_l	Loose porosity of the bed after dilatancy	$[-]$
P	Wetted perimeter of the closure gap	$[m]$
Q	Discharge	$[m^3/s]$
Q_F	Discharge of a free flow over a weir	$[m^3/s]$
Q_{pipe}	Discharge of the sand-water mixture through the pipe	$[m^3/s]$
q	Flow through a soil layer	$[m/s]$
R	Hydraulic radius	$[m]$
r	Ratio between the amplitude off shore and in the tidal basin	$[-]$
S	Sedimentation rate	$[kg/m^2s]$
T	Wave period	$[s]$
T_a	Adaptation time	$[s]$
t	Time	$[s]$
u	Flow velocity of the water	$[m/s]$
u_*	Friction velocity	$[m/s]$
v_{bed}	Bed velocity	$[m/s]$
v_e	Erosion velocity of the bed	$[m/s]$
v_{sed}	Sedimentation velocity of the bed	$[m/s]$
W	Width of the closure gap	$[m]$
w	Height of a sill above the bottom	$[m]$
w_s	Settling velocity of sediment particles in the water	$[m/s]$
y_L	Modular limit ratio, used to determine whether a free flow occurs or not	$[-]$
y_t	Transition-submergence ratio	$[-]$
z_b	Bed level of the bed in the closure gap	$[m]$

List of Figures

List of Tables

Chapter 1

Introduction

A closure dam is a hydraulic structure which blocks the water flow between two river branches or a tidal basin and the sea. It benefits to use sand as construction material for closure dams, because it is often available close to the construction site and thereby the mining, placing and transport is relatively easy compared with rock, concrete blocks or clay. The disadvantage is that sand erodes more easily than gravel, rock or clay. When flow velocities become large, the erosion becomes high and a lot of sand production is needed to close the dam, which includes a higher risk of failure and ultimately higher costs. This thesis investigates the processes which occur during the construction of a closure dam in tidal areas, in order to calculate the sand losses. The sand losses are defined as the amount of sand that is transported out of the closure gap and does not contribute to the closure dam. This is the quantity of sand which has to be produced additionally during a construction step to reduce the closure gap and continue to the next construction phase.

The relevance of this research is that a lot of money and risk is involved in closure operations. When a sand closure is constructed, the contractor wants to know whether it is possible to close the dam and how much sand has to be produced. To calculate the sand losses, it is important to know the processes which occur and be able to predict what will happen during the closure. With an improvement of the accuracy of the calculation method and model, the risk of failure is smaller and therewith the closure operation can be tendered cheaper to make a competitive offer.

The calculation method that currently is used to calculate sand losses, which stems from 1992, is described in the 'CUR 157, Sand Closures'. This book presents a feasibility study for sand closures and a formula to calculate the sand losses during closure. However, a large uncertainty is incorporated in the calculation technique, described in the CUR 157. To increase the certainty of the amount of sand losses an improvement to this calculation method is necessary.

Problem statement

In the calculation method of the CUR 157, the physical processes are not taken into account sufficiently. The CUR 157 uses a transport formula which is made for relative low flow velocities and the transport capacity of the water is calculated using an equilibrium situation of the flow. To appropriately use this formulation to describe the sand losses which occur in practice, a calibration is done using a limited range of grain sizes. The hypothesis is that if the interaction between the bed and the continuous varying flow is taken into account, the sand losses can be calculated more accurately for a wide range of grain sizes. Especially important are the processes which occur during high flow velocities.

Goal of the study

This thesis contains two goals. The first goal is to analyse the processes which determine the amount of sand losses which occur during the construction of a closure dam. The second goal of this study is to use the analysed processes to develop a 'simple to use' tool to calculate the sand losses. This tool should be applicable to a wide range of grain sizes. This thesis aims to answer the following question: "How can the processes during construction of a sand closure be described and modelled to improve the prediction of the sand losses over time?"

Methodology

This thesis considers the construction of a closure gap in the inlet of a tidal basin. To describe the system of a closure gap in a tidal inlet, two different methods are used. For a qualitative description of the processes which occur during the construction of a closure gap, an analytical description of the system is used. For the calculation of the sand losses a numerical model is used. The numerical model is calibrated using data from 'Maasvlakte 2'. Finally the 1-dimensional model is verified quantitatively using two cases from 'CUR 157' with different conditions as at 'Maasvlakte 2'.

Structure of the report

Chapter 2 presents a description of the construction methods for sand closures and the processes which occur during closure. At the end of chapter 2, the present calculation technique is explained. Chapter 3 presents an analytical calculation model. This model consists a flow model and a model for losses and is used to analyse the processes which occur during the construction of a closure dam. This is presented in chapter 4. Chapter 5 presents a 1-dimensional model which is calibrated and verified in chapters 6 and 7. Finally in chapter 8, the conclusions and recommendations of this thesis are discussed.

Chapter 2

Sand closures

This chapter gives an introduction in closure dams and sand closures in particular. First tidal basins and the execution methods for closure dams are discussed. This is followed by a description of the processes of the flow and the interaction between the flow and the geometry. Subsequently the effects of the processes on the stability of a closure gap are described, together with an example to get an idea of the order of magnitude of closure gaps. Finally a description is given of the calculation technique that is currently used.

2.1 Tidal basins and inlets

Closure dams are used to close tidal basins, reservoirs or river branches. This thesis focusses on the closure of tidal basins. There are three types of tidal basins: tidal lagoons, tidal bays and estuaries. The biggest difference between the different basins is the amount of fresh water run-off and the wave impact. Table 2.1 gives an overview of the three types of tidal inlets.

Environment	Distinctive attributes
Tidal bays	High level of wave energy dissipation; little freshwater run-off
Tidal lagoons	Waves excluded by barriers; tidal flows via passes; infilling wetlands; little freshwater run-off
Estuaries	Waves possibly excluded by barriers or sand shoals; high freshwater run-off

Table 2.1: Different environments of tidal basins [Bosboom and Stive,2011]

The different parts of a tidal basin are presented in figure 2.1. The tidal basin is connected to the sea by a tidal inlet. The river inflow, tidal fluctuations and the tidal basin are discussed below. The tidal inlet and the closure of a tidal inlet is discussed separately in section 2.2.

River inflow

The river inflow has a couple of consequences for the dynamics of a tidal inlet. First the water that flows into the tidal basin has to be discharged through the tidal inlet. This causes an asymmetry of the flow through the inlet, with a larger flow into the sea and a smaller flow into the basin. So, over a tidal period a net discharge is flowing out through the tidal inlet.
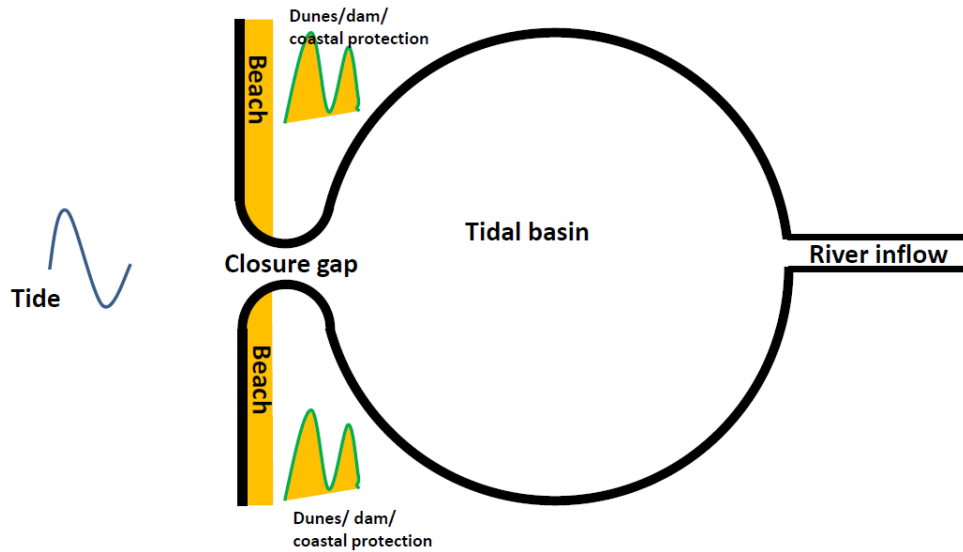
Figure 2.1: An overview of a tidal basin connected with sea, with a river flowing in

The second important process which take place if a river flows into the basin is the difference between salt water in the sea and the fresh water run off from the river. This difference can cause stratification in the channel. An example of stratification at a tidal inlet is a salt wedge which flows underneath the fresh water from the river. This salt wedge can move forward and backward as a consequence of the tidal fluctuation and is discussed in more detail in section 2.3.

Tidal fluctuations

The sun and the moon attract the water, which causes a raise and decrease of the water level. The earth rotates around its own axis and the moon rotates around the earth. These movements cause the propagation of the tidal wave around the earth. At a certain location, high and low water can be observed, which are known as the tidal fluctuations. Since the movement of the earth around its own axis and the moon around the earth are periodic, the tide can be seen as a periodic movement of high and low water. For example the lunar tide is semi-diurnal and has a period of 12 hours and 25 minutes.

When the earth, moon and the sun are in one line the tidal amplitude is larger. This is the so called spring tide. On the other hand, when the sun, earth and moon make an angle of about 90 degrees with each other the amplitude is lower, the so called neap tide. Besides spring and neap tide, a difference is observed between the amplitude within a day. This is called the daily inequality and is caused by the orientation of the rotation axis of the earth and the location of the moon. The geometry of the sea also influences the tide and can cause skewness of the tidal wave or a difference in the tidal period.

Tidal basin

The geometry of the basin is important for the propagation of a tidal wave into the basin and thereby the flow through a tidal inlet. For a long basin, the tidal wave propagates into the basin until it reaches the end where the wave reflects. The water level fluctuations in the basin become a sum of the incident and the reflected tidal wave. The tidal wave also experiences

friction from the bottom. So the amplitude reduces while propagating into the basin. The propagating velocity and the friction which the tidal wave experiences, depend on the depth of the basin. For smaller basins the tidal wave doesn't propagate through the basin, but the water level in the basin is approximately the same everywhere. In such a case the water level in the basin fluctuates along with the fluctuations at sea. However if the tidal inlet is small, a delay and damping of the fluctuations is observed.

Whether a basin is considered small or large depends on the length of a tidal wave and the surface of the area. The length of the tidal wave propagating through the basin depends on the depth of the basin. Equation 2.1 presents the relation between the length of the propagating tidal wave through the basin and the tidal period. This relation is valid in very shallow water ($d << L_{wave}$) [Holthuijsen,2007]. For a basin with a water depth of 15m and a semi-diurnal tide, the wave length becomes about 500km. A basin is considered as small if it is 20 times smaller than the wave length. In this case a basin is called small if the length is smaller than 25km.

$$L_{wave} = c_{wave}T = \sqrt{gd}T \tag{2.1}$$

In which:

L_{wave} = the wave length of the propagating tidal wave in the basin $[m]$
c_{wave} = the celerity or propagation speed of a wave $[m/s]$
T = the wave period $[s]$
d = the depth of the tidal basin $[m]$

2.2 Construction of a closure dam

The size of a tidal inlet is reduced during closure till the water can not flow in and out the basin any more. During construction, the tidal inlet is called a closure gap. Different methods exist to reduce the closure gap size. This section first discusses the different methods of construction, followed by the equipment which is used during construction of a closure dam.

Methods of construction

To close a tidal basin, three different methods of construction can be distinguished, namely horizontal closure, vertical closure and a combination of both. During a vertical closure operation, a sill is build up till the bed of the gap reaches the water surface and the basin is closed, see figure 2.2-A. During horizontal closure, the edge of the dam is extended to reduce the closure gap size and finally close the gap. The horizontal closure can be performed as a one-sided closure, see figure 2.2-B or as a two-sided closure, figure 2.2-C. In practice often a combination of vertical and horizontal closure is used to construct a closure dam. In that case first a sill is constructed till a certain depth below the water level. After the sill is constructed, the dam is closed horizontally as shown in figure 2.2-D.
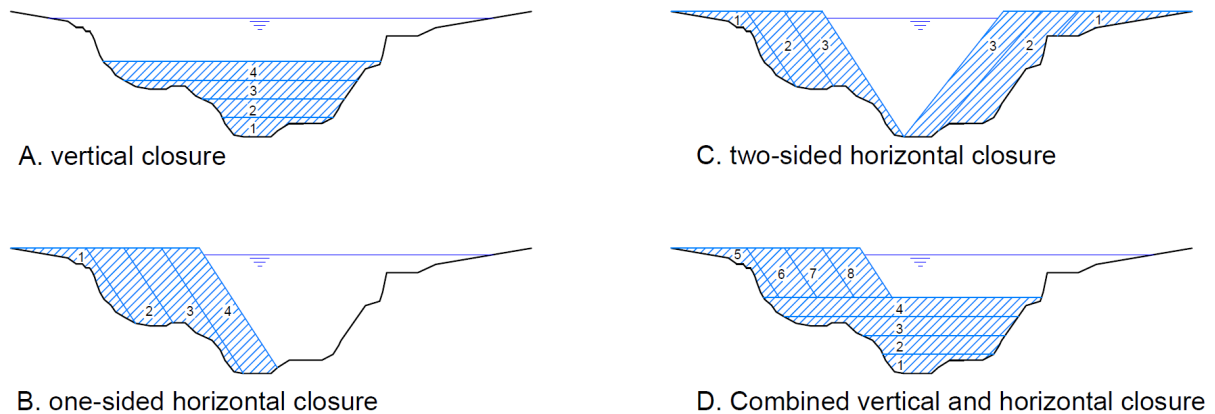
Figure 2.2: The different closure methods

Consequences of different closure methods

The flow through a closure gap experiences a force caused by the water level gradient over the gap, which accelerates the water. The bed and banks cause resistance, which slows down the flow. Different closure methods influence the geometry of, and the flow through, the closure gap. A larger wetted perimeter means a larger area where the friction takes place. In most cases, before the closure operation starts, the width of the closure gap is much larger than the depth. This implies that during vertical closure the wetted perimeter remains larger than during horizontal closure. For this reason the vertical closure is preferred above the horizontal closure method to increase the resistance over the gap. For wide closure gaps it is not possible to perform the final closure stage vertically, so often a combination between horizontal and vertical closure is used to construct a dam.

Equipment

To place the sand in the body of the dam, the sand has to be dredged, transported and finally brought in place. For the different production phases different equipment is available.

Sand winning and transport

The sand winning is mostly done by a dredger. Two types of dredgers are used for this job, a cutter suction dredger or a trailing suction hopper dredger. A cutter is not suitable for transporting sand over long distances, while a trailing suction hopper dredger can also do the transport of the sand to the construction site. A cutter pumps the sand through a pipeline towards the construction site or into a hopper barge which sails the sand towards the location of the dam. Whether a pipeline is used or hopper barges depend on the available equipment, distance between the winning area and the construction site. For small distances a pipeline seems to be more efficient, while for large distances mostly hoppers are used.

Deposition of sand

Sand can be placed in the dam using different methods. For a vertical closure, a hopper barge can place the sand on the location of the dam. A split barge releases the sand quite fast, but the barge has to be able to sail above the sill. When the water depth is smaller than the draught

of the barge, a hopper must bring the sand in place by rainbowing. For horizontal closure sand can be placed on the land and the dam body by rainbowing or by a land pipeline. Subsequently the sand is brought in position by land equipment; bulldozers, and excavators.

2.3   The flow through the closure gap

Reducing the cross sectional area of a closure gap hinders the flow through the gap. This leads to tidal jets flowing in and out the basin through the closure gap, which is shown in figure 2.3. An important physical mechanism of tidal jets is that they hold a lot of momentum which can lead to a vortex street from the tip of the partly constructed dam and gyres at the downstream side of the closure dam.
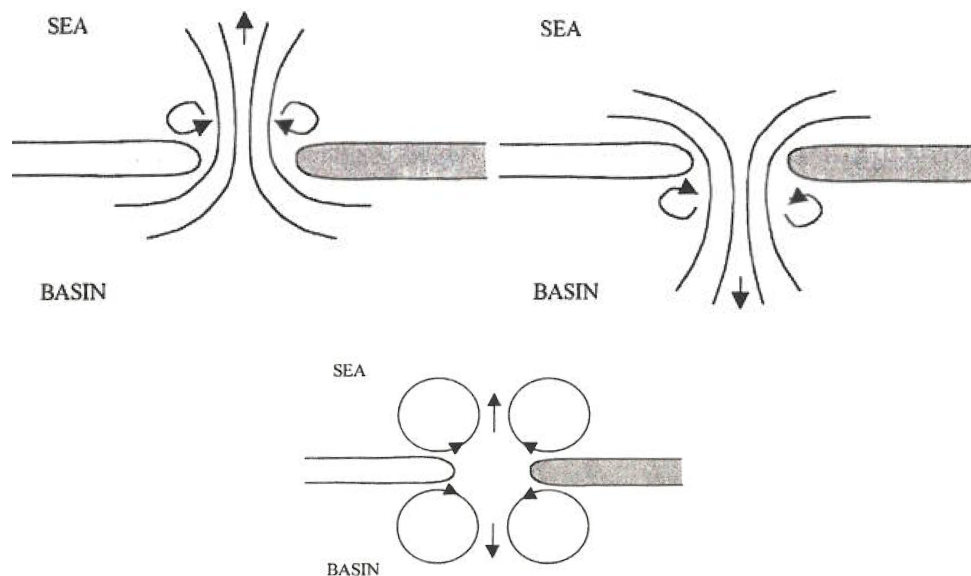
Figure 2.3: The upper panel shows the tidal jets and the lower panel presents the gyres at the outflow of the closure currents [Bosboom and Stive,2011]

When the flow area becomes smaller, the flow accelerates toward the closure gap. At the downstream side of the dam, the flow decelerates again. The acceleration and deceleration depend on the geometry of the closure gap and the hydraulic gradient. The hydraulic gradient and the geometry change over time during production. The continuing changes in the flow have the consequence that the flow doesn't reach an equilibrium. This is important since most of the sediment transport formulations use an equilibrium of the flow to determine whether erosion or sedimentation occurs.

The flow over time

The magnitude of the discharge depends on the geometry of the closure gap, the storage area of the tidal basin, the tide and whether there are other tributaries which discharge into the tidal basin. If the tide is the only forcing, the flow is a consequence of the tidal fluctuation and the response of the water level in the basin. In this case the flow over time follows the tidal fluctuations. This is shown in the upper panel of figure 2.4. The lower panel shows the discharge if a river discharges in the tidal basin. As figure 2.4 shows, the maximum discharge

during outflow becomes larger and smaller during inflow. This difference influences the amount of erosion and or sedimentation of sand during a tidal cycle.
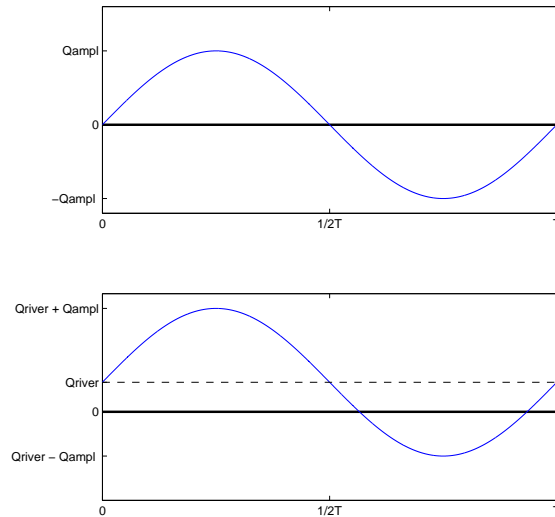
Figure 2.4: Influence of a river on the discharge through a closure gap

Density currents

When the run off from the river is large and the tidal basin consists of mainly fresh water, the tide causes a salt wedge flowing in the basin. The salt wedge flows underneath the fresh water flow. The length over which the salt wedge penetrates into the basin depends on the size of the fluctuations and the discharge of the river. The larger the discharge and the smaller the fluctuations the smaller the salt wedge becomes. If the discharge of fresh water is small, the salt wedge reaches the water level and the water surface around the closure gap (or even the whole basin) becomes salt. In that case, the fresh water flows into the basin and mixes with the salt water. A schematic view of a salt wedge is shown in figure 2.5.
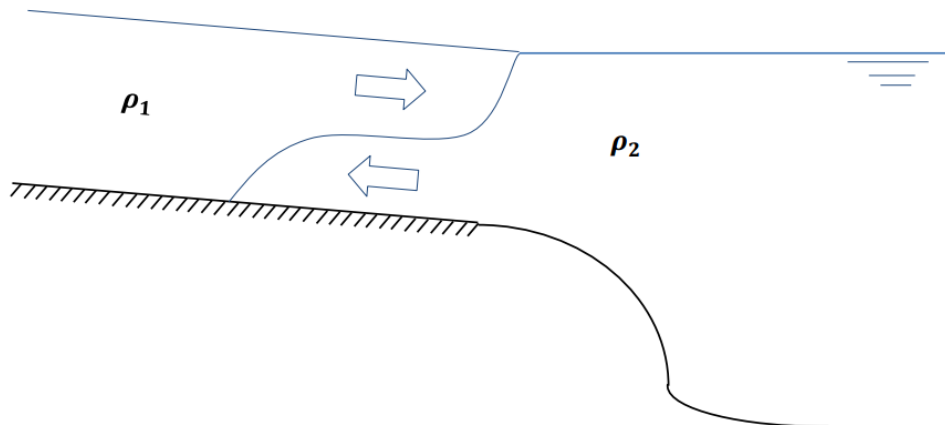
Figure 2.5: A schematic view of a salt wedge intruding into a basin, with: $\rho_2 > \rho_1$

Critical and free flows

When a closure gap becomes smaller, the maximum gradient over the closure gap increases, which leads to higher flow velocities. At a certain moment the water level at sea or in the basin becomes lower than the sill of the dam. In that case a free flow occurs and the flow over the gap becomes critical. A property of a critical flow is that the Froude number is equal to one, see equation 2.2. When the Froude number is larger than one, the flow is supercritical and if the Froude number is lower than one, the flow is subcritical. A free flow is a critical flow and is shown in figure 2.6.

$$Fr = \frac{|u|}{\sqrt{gd}} \tag{2.2}$$

In which:

Fr = the Froude number $[-]$
u = the flow velocity of the water $[m/s]$
d = the water depth $[m]$
g = the gravitational acceleration $[m/s^2]$
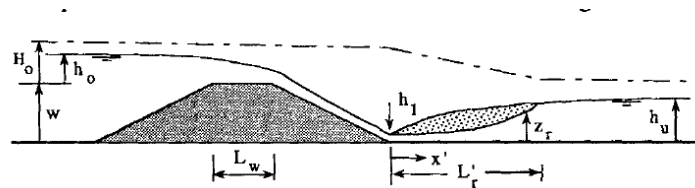
Figure 2.6: Schematic view of a free overflow over a weir [Fritz and Hager,1998]

Downstream of a weir with a free overflow, a hydraulic jump can occur. When the downstream water level rises, the following states of the flows occur. When the water is just a little higher than the sill of a dam or weir, a plunging jet occurs, see figure 2.7-a. Increasing the water level downstream of the dam a little more, a surface jet flow occurs. Raising the water level even more to a water level almost equal to the water level upstream, a surface jet occurs, see figure 2.7-b. Which flow regime occurs depends on the length of the sill and the degree of submergence (the water level at the downstream side of the closure gap). The submergence of the dam also has a consequence for the discharge through the closure gap. The influence is given in equation 2.3 [Fritz and Hager,1998].
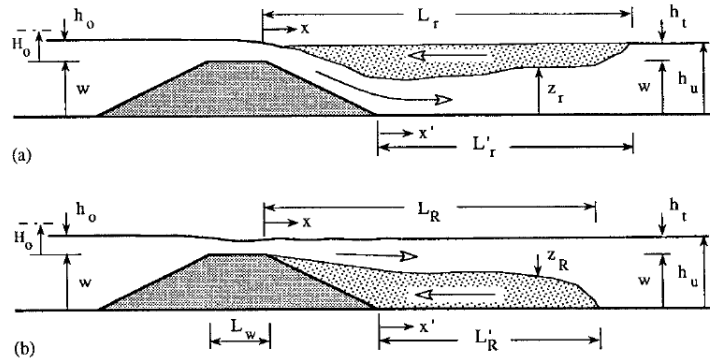
Figure 2.7: Different states of the tailwater flow. In a, the plunging jet and in b, the surface jet [Fritz and Hager,1998]

$$Q = \psi Q_F = \left(1 - \frac{y_t - y_L}{1 - y_L}\right)^{1/n} Q_F \qquad (2.3)$$

In which:

Q_F = the discharge of a free flow, calculated using the formula for critical flows $[m^3/s]$
ψ = the reduction factor for submergence of a weir $[-]$
y_t = $\frac{h_t}{H_0}$ $[-]$
y_L = $0.85 - 0.5\frac{H_0}{H_0+L_0}$ $[-]$
H_0 = The energy head upstream of the closure gap $[m]$
h_t = the water level downstream of the closure gap $[m]$
L_0 = the length of the weir $[m]$
n = is a function of the relative crest length ξ $\left(= \frac{H_0}{H_0+L_0}\right)$, given by the values:

$n(\xi = 0.25)$ = 7
$n(\xi = 0.67)$ = 6
$n(\xi = 1)$ = 4

2.4 Change of the geometry
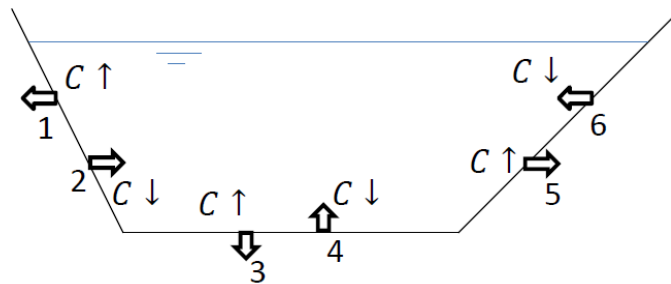
Figure 2.8: The interaction between the geometry and the flow

Figure 2.8 shows the interaction between the bed and banks of the closure gap and the flowing water. The geometry of the closure gap can change due to erosion and sedimentation. The arrows show the movement of the bed. So situation 1, 3 and 5 represent erosion, while situation 2, 4 and 6 represent sedimentation. Figure 2.8 also shows the consequence for the concentration of sediments in the water when erosion or sedimentation occurs. As can be seen, an increase of the concentration occurs during erosion. The process of erosion and sedimentation is treated below.

Erosion

In literature erosion is described according to two mechanisms, the single particle mode and the continuum mode. The single particle approach considers the erosion of circular particles, which are picked up one by one, while in the continuum mode erosion of a soil layer is considered. In this section an overview is presented of the external forces on the grains on top of a sand bed. In chapter 3, the pick up formula of Van Rhee is presented. This formula calculates the erosion and takes into account the permeability of the soil layer which erodes and is applicable to high flow velocities.

Sand particles only start to move if the external forces (mostly exerted by the water) are larger than the internal friction. The balance of forces acting on a particle determines the ability to move. Figure 2.9 shows the drag and lift forces, exerted by the flow of water. The gravitational force, F_g, of a particle under water is equal to $(\rho_s - \rho_w)gV$, where V is the volume of the particle and $\rho_{s,w}$ are respectively the relative density of the sand and the water. The momentum balance around pivot point A (the point where the grain hits the other grains in the bed at the downstream side of the grain) shows that the forces are balanced when the following relation is obtained.
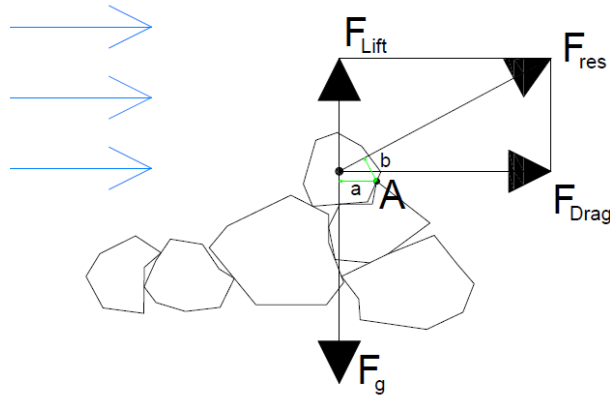
Figure 2.9: Forces acting on a single grain

$$F_{res}b = F_g a \tag{2.4}$$

If $F_{res}b > F_g a$, the sand particle is picked up from its position in the bed and erosion takes place. If the flow takes the particle to a place further away downstream, sediment transport is a fact. In literature the friction of the flow is expressed in a dimensionless friction velocity, which is also called the shields parameter, θ, see equation 2.5 [Shields,1936]. The moment the sediments start to move is called the initiation of motion. Van Rijn described a method to determine the

initiation of motion using the so called critical shields parameter, θ_{cr}. If the shields parameter is equal to the critical shields parameter, the resistance of the bed is equal to the friction force of the water. When the friction becomes larger the sediment particles start to move. The critical shields parameter depends on the sediment size and the viscosity of the water. A method to determine the initiation of motion is described in appendix A.

$$\theta = \frac{F_s}{F_g} = \frac{u_*^2}{\Delta g D} \tag{2.5}$$

$$\theta_{cr} = tan\phi \tag{2.6}$$

In which:

θ = the dimensionless value of the friction velocity, also called the shields parameter $[-]$
F_s = the shear or drag force which the flow exerts on the bed $[N]$
u_* = the friction velocity $[m/s]$
Δ = the relative density $[-]$
g = the gravitational acceleration $[m/s^2]$
D = the grain size $[m]$
ϕ = the angle of internal friction of the bed $[rad]$

Sedimentation

If sedimentation occurs, sediments which are in suspension settle on top of the bed. The sedimentation rate depends on the settling velocity (or fall velocity), w_s, which is the downward velocity of a particle under water. The settling velocity for a single particle in the water can be calculated when the drag force and gravity force are in equilibrium. For different grain sizes, the settling velocity is calculated differently. Van Rijn formulated the settling velocity as shown in equation 2.7. [Van Rijn,1993].

$$w_s = \begin{cases} \frac{\Delta g d^2}{18\nu} & \text{for } 1 < d \le 100\mu m \\ \frac{10\nu}{d}\left[\sqrt{1 + \frac{0.01\Delta g d^3}{\nu^2}} - 1\right] & \text{for } 100 < d \le 1000\mu m \\ 1.1\sqrt{\Delta g d} & \text{for } d \ge 1000\mu m \end{cases} \tag{2.7}$$

In a sand-water mixture, the effect of hindered settling reduces the fall velocity. Richardson and Zaki [Van der Schrieck,2012] found experimentally relations between the settling velocity and the hindered settling velocity. This resulted in a reduction coefficient of the fall velocity given in equation 2.8

$$\frac{w_s(c)}{w_s} = (1 - c)^{\beta} \tag{2.8}$$

In which:

$w_s(c)$ = the fall velocity in the mixture with a sediment concentration $[m/s]$
w_s = the single particle fall velocity in water $[m/s]$
c = the concentration of sediments in the sand water mixture $[-]$
β = a dimensionless coefficient $[-]$

The parameter β gives the power of the reduction of the fall velocity in a mixture. The values of beta depend on the particle Reynolds number, see equation 2.9, and the different values of β are given in table 2.2 [Miedema and Vlasblom,1996].

$$Re_d = \frac{w_s d}{\nu} \tag{2.9}$$

Particle Reynolds number	β-coefficient
For $Re_d < 0.2$	4.65
For $0.2 < Re_d < 1$	$4.35 \cdot Re_d^{-0.03}$
For $1 < Re_d < 200$	$4.45 \cdot Re_d^{-0.1}$
For $Re_d > 200$	2.39

Table 2.2: The β-values for the fall velocity in a mixture

Sediment transport

When particles are suspended in the water, they flow along with the water. Sediment transport can be determined in different ways. Most of the transport models calculate the sedimentation and the erosion by comparing the actual transport with a transport capacity. In this approach it is assumed that the water has a maximum transport capacity. When the actual transport is smaller than the maximum capacity, erosion occurs till the transport reaches the maximum transport capacity. On the other hand, when the transport is larger than the transport capacity, sedimentation occurs. The adaptation time is the time that is needed to reach the maximum transport capacity. If the adaptation time is multiplied by the velocity of the water, the length is obtained which is needed to reach the maximum capacity. This is shown in equation 2.10 and 2.11. Over this length and time the flow has to be the same to reach the maximum capacity [De Vriend,2011].

$$T_a \approx \frac{h}{w_s} \tag{2.10}$$

$$L_a \approx \frac{uh}{w_s} \tag{2.11}$$

In which:

L_a = the adaptation length $[m]$
u = the flow velocity of the water $[m/s]$
h = the water depth $[m]$
w_s = settling velocity of sand in water $[m/s]$
T_a = the adaptation time $[s]$

2.5 The stability of tidal inlets and closure gaps

To show the effect of the processes of erosion and sedimentation during different stages of the construction of a sand closure so called closure and equilibrium curves are used [Escoffier,1940]. An example of these curves are given in figure 2.10. The horizontal axis represents a parameter, which becomes larger for an increasing cross section, such as the width, height or the flow surface of the gap itself. In this example this parameter is the flow surface of the closure gap, but it can

also be the width to describe a horizontal closure for example. On the vertical axis the maximum velocity in the inlet is given during a tidal cycle for the associated closure gap geometry. For the given tidal forcing and geometry, the closure curve represents the maximum velocity which occurs during a tidal period. The equilibrium velocity curve represents the maximum velocity within a tidal period for which the erosion over a tidal period is equal to the sedimentation. In practice for different inlets, the equilibrium curve is determined empirically over a longer time than one tidal period. So seasonal influences, waves and long shore currents are taken into account. Besides, the equilibrium curve is different for closures with different circumstances and geometries. Closure gaps are constructed within a couple of days or weeks, so the seasonal influences can be left out of the analysis and the equilibrium curve can be determined only by the tidal flow, sedimentation and erosion.
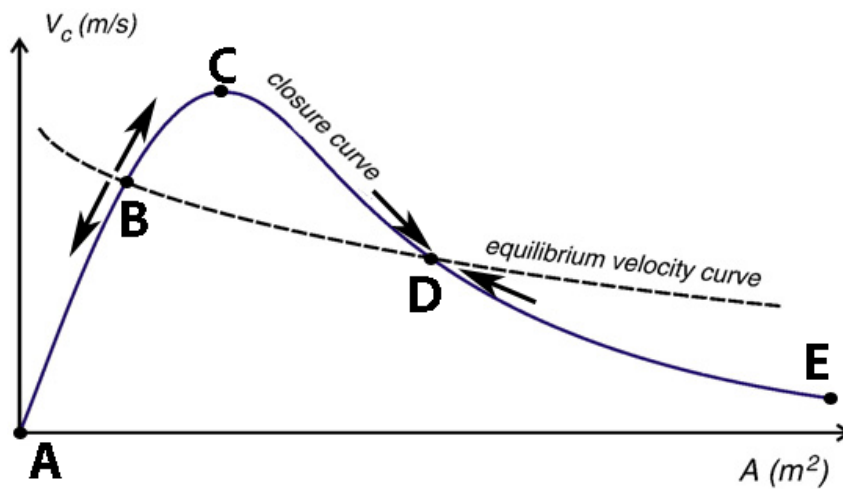
Figure 2.10: Closure Curve with an equilibrium velocity curve [Tran,2012]

The points B and D are intersections between the closure curve and the equilibrium velocity curve. Point B represents an unstable equilibrium condition, which means that a little deviation of the cross section means that the inlet increases or decreases, depending on the direction of the deviation. Point D represents a stable equilibrium condition, which means that if the cross sectional area is between point B and D, as well as larger than D, the size changes in such a way that it moves along the curve towards point D.

The construction of a closure gap can be described as a movement along the x axis towards point A, starting somewhere around the natural equilibrium, point D. The maximum velocity of the flow through the gap follows the closure curve. When point B is passed, the dam closes itself. In practice the slope between point A and B is very steep or even vertical, so point B is reached at a very small closure gap surface or sometimes even at closure.

The challenge during the construction of a closure dam is to overcome the most critical phase around point C. The dam is closed more easily if the equilibrium velocity is higher and the velocities of the closure curves are smaller. The height of point C gives the difficulty of the closure, while the distance between point B and D determine the duration of the closure. When the closure curve remains below the equilibrium curve for all the closure gap surfaces, the closure gap is unstable and closes naturally.

2.6   CUR 157, Sand closures

In 1992 the CUR published a feasibility study for sand closures based on the closures performed in the years prior to the publication. The calculation method presented in the CUR 157, Sand Closures is discussed in this section [CUR157].

Calculation method

For the calculation of the sand losses, the velocity in the closure gap is important. The CUR 157 proposes to use a submerged weir discharge relation to calculate the velocity for a 0-dimensional basin capacity model. This discharge relation is given in equation 2.12.

$$\frac{Q}{A} = \mu\sqrt{2g\Delta h} \qquad (2.12)$$

In which:

$\quad Q \quad$ = the discharge through the closure gap $[m^3/s]$
$\quad A \quad$ = the flow area of the closure gap $[m^2]$
$\quad \mu \quad$ = a discharge coefficient $[-]$
$\quad \Delta h \quad$ = the water level difference over the closure gap $[m]$

To calculate the sand losses, the CUR makes a distinction between horizontal closure and vertical closure. During vertical closure, only the bed can erode and the banks are stable. During the horizontal closure, a distinction is made in the flow patterns, namely a main stream and a vortex street (for a two-sided closure, there are two vortex streets). An explanation of the flow lines is given in figure 2.11. The formulas to calculate the losses are based on the equilibrium transport formulation of Engelund and Hansen and are shown in equation 2.13 and 2.14.

$$E_m = \frac{au^5}{C^3 D_{50}\Delta^2(1-n_0)\sqrt{g}} \qquad (2.13)$$

$$E_t = \frac{au^{3.5}}{C^{1.5} D_{50}^{0.25}\Delta^{1.25}(1-n_0)\sqrt{g}} \qquad (2.14)$$

In which:

$\quad E_m \quad$ = the sand loss per meter closure gap width in the main stream $[m^3/ms]$
$\quad E_t \quad$ = the sand loss per meter bank width in the vortex street $[m^3/ms]$
$\quad a \quad$ = a regression factor, which is 0.05 for a vertical closure, 0.06 for the main stream and 0.34 for the vortex street in a horizontal closure. During vertical closure the a for the vortex street is 0, so no vertex street occurs $[-]$
$\quad u \quad$ = the velocity in the closure gap averaged over the gap $[m/s]$
$\quad C \quad$ = the Chezy coefficient $[m^{\frac{1}{2}}/s]$
$\quad D_{50} \quad$ = the median grain diameter $[m]$
$\quad \Delta \quad$ = $\frac{\rho_s - \rho_w}{\rho_w}$ = the relative density $[-]$
$\quad n_0 \quad$ = the porosity of the bed $[-]$
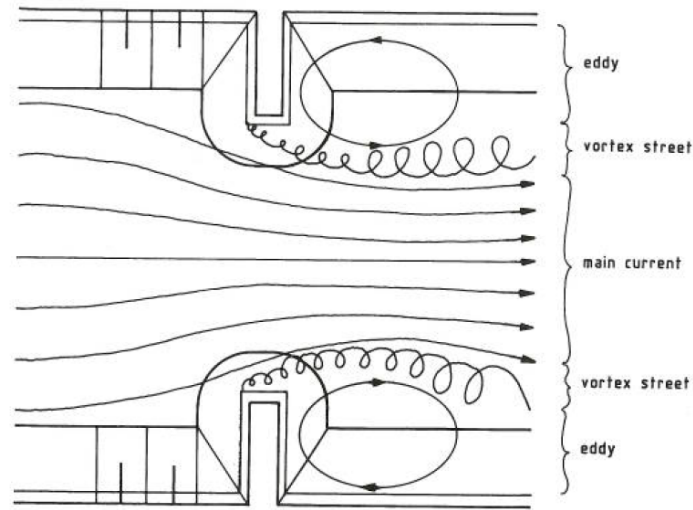
Figure 2.11: An overview of the flow lines during closure [CUR157]

The transport formulations for the main stream and the vertical closure are calibrated in such a way that the whole width of the sill/bottom of the closure gap has to be taken into account. For the vortex street only 30% of the length of the banks in the flow direction has to be taken into account as shown in figure 2.12.
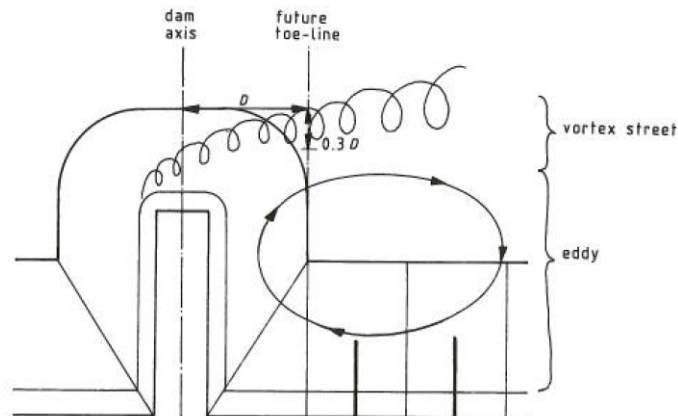
Figure 2.12: Overview of the vortex street and the development over the distance [CUR157]

Derivation of the CUR formulas

The formulas are derived from the Engelund and Hansen formulation and are developed in two steps. First a dimensionless transport and velocity parameter are equalized as in equation 2.15.

$$\Phi \frac{g}{C^2} = a\Psi^b \tag{2.15}$$

In which:

$\Phi \quad = \frac{u^2}{C^2 \Delta D_{50}} \quad$ = the dimensionless velocity parameter $[-]$

$\Psi \quad = \frac{s}{\sqrt{g\Delta D_{50}^3}} \quad$ = the dimensionless transport parameter [$-$]

$a, b \quad =$ regression factors [$-$]

Thereafter the b is determined based on sand transport measurements by use of ASTM's (Acoustic Sand Transport Meters) at the closures of Slaak (1986), Tolense Gat (1986) and Krammer (1987). The measurements were taken at the flow over a sill, at the vortex street and the main current of a vertical and horizontally constricted closure gap. The second step is to determine the regression factor a by evaluating the cubic losses after the closure was constructed.

Shortcomings

Velocity

The velocity is a very important parameter. Most of the sediment transport formulas are calibrated for river flows and are applicable for velocities of about 1m/s or smaller and for equilibrium conditions. Because the Engelund and Hansen formula gives overall the best performances, the CUR 157 uses this formula. But for different velocities, other formulas might provide better results. Especially at high velocities the soil properties become important and seem to hinder the erosion.

Grain sizes

The grain size is stated in the formulas which are derived in the CUR 157, however the formulas are calibrated on a narrow range of grain sizes. Therefore it is questionable if the formulas are directly applicable outside this bandwidth and a recalibration is necessarily. The closures which are used for the calibration all (except one) had a median grain size in a range between $120\mu m$ and $220\mu m$.

Equilibrium transport formulation

The calculation method of the CUR 157 is based on an equilibrium transport formula, which is often used for situations where no rapid changes are present. During a closure, the water accelerates a lot over a short distance and decelerates again during the outflow. The distances over which the flow accelerates and decelerates is smaller than the adaptation length of the flow. Therefore the equilibrium transport which is calculated by the formula is not necessarily reached yet.

2.7   Recent closures

Since the publication of the CUR 157 in 1992 not many sand closures were executed. Last year a couple of closures were constructed and the observed sand losses were smaller than calculated using the CUR 157 formulas. This lead to the question to develop a more reliable model for the prediction of the sand losses. The gaps that were closed last year were at the Maasvlakte 2 in the Netherlands and at the River Niger in Nigeria.

'Compartimenteringsdam'

During the extension of the Port of Rotterdam at 'Maasvlakte 2', PUMA (a consortium of Van Oord and Boskalis) build two closure dams. One relative small closure and a large closure.

An overview of 'Maasvlakte 2' is shown in figure 2.13 and the two closures are discussed more extensively in appendix C.

Figure 2.13: The 'Maasvlakte 2', with at number 1, the closure gap of the outer closure and number 2 is the closure gap of the 'compartimenteringsdam'

To get an idea of the size of a closure, the closure of the 'Compartimenteringsdam' is discussed. For the construction of the dam, first a sill is constructed till 1.5m below NAP. The final closure is performed one-sided horizontally. Table 2.3 presents the parameters of the geometry and the tidal forcing accessory to the dam, about 10 hours before closure.

parameter	value
Length of the gap	$150m$
Width of the bed	$100m$
Level of the sill below NAP	$1.5m$
Slope of the banks	$1:9$
D_{50}	$380\mu m$
Tidal amplitude	$0.9m$
Tidal period	$44700s$

Table 2.3: The values of the parameters of the closure gap 10 hours before closure of the 'Compartimenteringsdam' [PUMA,2012]

During the first closure at 'Maasvlakte 2', measurements are performed which are used to do a new calibration of the a-value of the CUR 157 formulation. This was needed to do, because the grain sizes were larger than used in the calibration of the CUR 157. The grain sizes at the 'Maasvlakte 2' had a median grain diameter of $380\mu m$. Also a strong feeling prevailed at the contractor that the CUR 157 was very conservative for large grain sizes and more reliable predictions were needed to guarantee succession of the closure operations. In the calibration, the a-values are determined again. The results of the calibration are shown in table 2.4.

	Calibration CUR 157	Calibration PUMA
Main current	0.06	0.018
Vortex street	0.34	0.0612

Table 2.4: The calibration of the a-parameter in the CUR 157 formulation

Calibration confirmed that the CUR 157 overestimates the sand losses. The new calibration provided good results for the second closure at the 'Maasvlakte 2' [PUMA,2012b]. But for each new situation a new calibration is probably needed. So still no generic tool is present to calculate the sand losses during the execution of a closure.

2.8 Conclusions

The most important processes in the determination of the sand losses are the flow through the closure gap and the erosion caused by the flow of the water. The flow is determined by the water level at sea and the response of the system to the tidal forcing. The response depends on the geometry of the closure gap and the size of the tidal basin. The interaction between the tidal fluctuations and the change of the geometry of the closure gap causes a continuous change of the flow.

The interaction between the flow and the sediment particles in the bed and banks determine the change of the geometry. The presented calculation technique of the CUR 157 calculates the sand losses using a formula based on the equilibrium transport formulation of Engelund and Hansen. This formula is based on an equilibrium flow of less than $1m/s$. In the final phase of a closure this is not necessarily the case. Thereby the range of grain sizes that are used for the calibration of the formulas is small. So the formula is not applicable to all cases.

Chapter 3 presents a calculation model for the sand losses in the closure gap. This is done based on a 1-dimensional flow equations and it uses a pick up function which is tested for flow velocities higher than $1m/s$.

Chapter 3

Analytical description of a closure gap model

The calculation method of the CUR 157 contains restrictions related to the flow velocity, grain sizes and the continuous changing flows. This chapter presents a model, which is used to analyze the behaviour of the flow in and out of a tidal basin and the interaction of this flow with the geometry of a closure gap. First a schematization is given of a tidal basin with a closure gap. Subsequently the assumptions and simplifications are given, followed by the governing equations and theory of the flow through a closure gap. Finally the description of the sedimentation and erosion of sand is presented. The erosion is described using the pick up formula of Van Rhee [Van Rhee,2007].

3.1   Schematization of the system

To calculate the erosion of a closure gap, a lot of complicated processes have to be described. To perform an analysis of the system, a simplified model of the geometry of a closure gap is used. Schematically, the tidal basin is used as presented in figure 2.1 in chapter 2. The tidal basin is connected to the sea by one inlet, which has to be closed. An overview of the tidal inlet is given in figure 3.1. The boundary condition of the model consists of the water level at sea. The water level at sea is schematized as a sinusoidal movement of the water level.
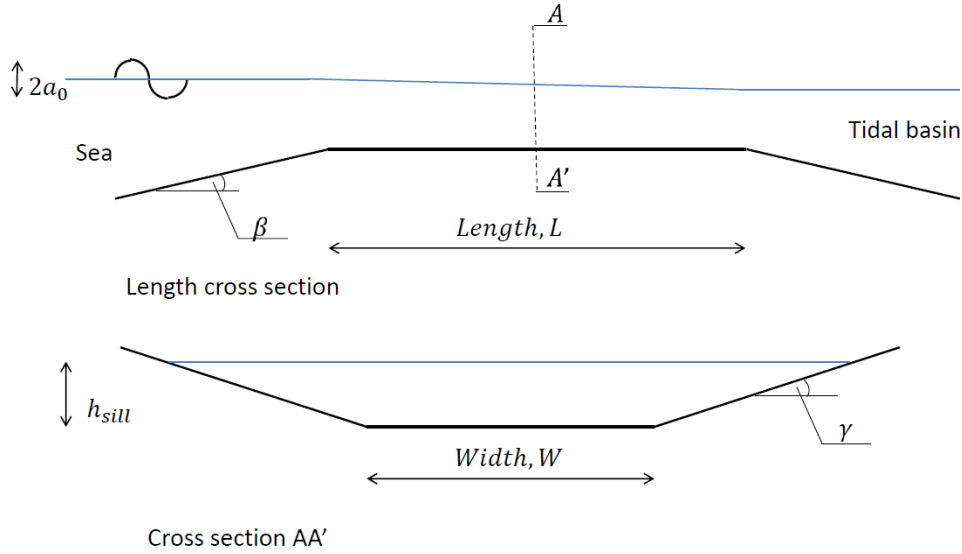
Figure 3.1: Schematic view of a tidal basin with a closure gap

3.2 Assumptions and simplifications

As described above, simplifications are made to describe the processes and calculate the sand losses during closure. The simplifications and assumptions for the model are described in this section.

As described in chapter 2, the tide is the most dominant forcing which influences the flow through the closure gap. The tidal forcing is assumed to be sinusoidal. So the influence of daily inequality and skewness are kept out of this analysis. Other water level differences caused by swell or wind waves are also neglected.

The geometry of the basin is important for the response of the system to the tidal forcing. The storage surface of the basin is assumed constant during the in or outflow of the water.

The third assumption is that the water is stagnant in the basin as well as at sea. This assumption simplifies the boundary conditions in such a way that the boundaries of the system only consist of water levels.

For the calculation of the water level, the basin storage approach is used. This starting point is allowed when the water level in the basin can be assumed to be the same everywhere. Chapter 2 presented that this is the case if the length of the basin is much smaller than the wave length. As mentioned in chapter 2, a basin of $15m$ depth has to be shorter than $25km$ for an M2-tide.

To calculate the flow through the closure gap analytically, the above mentioned basin storage approach is used together with the rigid column approach. This is only allowed when the change of the closure gap has to be very small during a tidal period. Another requirement for this method is that the geometry of the closure gap is the same over the whole length of the closure gap. In that case the resistance is the same over the whole length of the dam.

To simplify the situation, it is assumed that the sediment concentration is well mixed over the whole water column and is the same at every depth. This assumption seems to be allowed because of the turbulent nature of the flow in a closure gap.

The analysis that is carried out in this thesis neglects the inflow of a river in a tidal basin. The river discharge in a tidal basin and the associated density currents can be neglected. Often,

when the closure gap is the only connection with the sea, this assumption is allowed, because otherwise the water from the river is not discharged to the sea naturally after closure.

The final assumption is that the flow is sub-critical. When the flow becomes critical, an other flow description is necessary to describe the flow. The consequence of this assumption is that for critical flows, this analysis overestimates the discharge and the flow velocities through the closure gap.

3.3 Flow model

The tide causes a fluctuation of the water level at sea. These fluctuations, and how the system responds to them, cause a water level difference over the closure gap, which causes a flow in or out of the basin. Since the closure gap is the only opening which can supply water to or discharge water from the basin, the water level in the basin changes with in- or outflow through the closure gap. A fluctuation of the tide causes also a fluctuation in the basin. According to the continuity law of mass and volume, the water level fluctuation in the basin depends on the discharge through the gap and the size of the basin. This is shown in equation 3.1.

$$A_b \frac{dh_b}{dt} = Q \tag{3.1}$$

In which:

h_b = the water level in the basin $[m]$
t = the time $[s]$
Q = the discharge through the closure gap $[m^3]$
A_b = the area of the tidal basin $[m^2]$

The water level gradient over the closure gap causes a flow through the closure gap. The flow experiences resistance of the bed while flowing through the closure gap. So the flow depends on the gradient and the resistance over the gap. The resistance can be expressed in a friction term which consists of the bed roughness and the geometry of the closure gap. As shown in figure 3.1, the geometry consists of the slopes of the banks and the toes of a possible sill, the length and the width of the gap. The flow can be calculated using equation 3.2. This is the momentum equation for the flow in one direction.

$$\frac{\partial Q}{\partial t} + \frac{Q}{A_c} \frac{\partial Q}{\partial x} + g A_c \frac{\partial h_{sill}}{\partial x} + c_f \frac{|Q| \, Q}{A_c R} = 0 \tag{3.2}$$

In which:

A_c = the surface of the closure gap $[m^2]$
Q = the discharge through the closure gap $[m^3/s]$
h_{sill} = the water level above the sill in the closure gap $[m]$
c_f = a dimensionless friction coefficient based on a pipeline flow $[-]$
R = the hydraulic radius of the closure gap $[m]$

The two relations shown in equation 3.1 and 3.2 together form a system of equations which describe the flow through the closure gap. This system can be elaborated analytically. This is done by Battjes [Battjes,2002b], and is described in appendix B. The most important processes

which influence the flow are the friction and the tidal forcing. The friction in Battjes' method is calculated using a dimensionless friction coefficient (equation 3.3), which contains the parameters of the geometry of a closure gap. Later in chapter 5, the same system of equations is used to set up a numerical model for the flow through a closure gap.

$$\chi = \frac{1}{2} + c_f \frac{L}{R} = \frac{1}{2} + \left(\frac{1}{5.75 log \left(\frac{12R}{k_0} \right)} \right)^2 \frac{L}{R} \tag{3.3}$$

In which:

χ	=	the dimensionless friction term, used in Battjes method $[-]$
R	=	$\frac{A_c}{P}$ = the hydraulic radius $[m]$
k_0	=	the roughness of the bed of the closure gap ($= 3D_{90}$) $[m]$ [Battjes,2002a]
L	=	the length of the closure gap $[m]$
P	=	the wetted perimeter $[m]$

3.4   Erosion and sedimentation model

The change of the cross section of a closure gap depends on the amount of sedimentation and erosion. Sand can settle if a large amount of sand is supplied to the closure gap. This supply can be done by production or by nature. However the production is mostly much larger than the amount of sand brought in the dam body naturally. The sedimentation depends on the concentration of sediments in the fluid and the settling velocity. The erosion on the other hand depends on the sediment and the bed properties. The relation for the change of the closure gap over time is given equation 3.4.

$$\frac{dA_c}{dt} = \frac{(E - S)}{\rho_s(1 - n_0 - c_{nb})} P \tag{3.4}$$

In which:

$\frac{dA_c}{dt}$	=	the change of the closure gap in time $[m^2/s]$
E	=	the erosion rate per squared meter $[kg/m^2 s]$
S	=	the sedimentation rate per squared meter $[kg/m^2 s]$
ρ_s	=	the density of the sediment $[kg/m^3]$
n_0	=	the porosity of the bed $[-]$
c_{nb}	=	the near bed volumetric sediment concentration $[-]$
P	=	the wetted perimeter $[m]$

Erosion

As described in chapter 2, the soil properties become more significant for flow velocities higher than 1 m/s. The influence of the soil properties is described by Van Rhee, who investigated the erosion at high flow velocities. He formed a formula for hindered erosion based on the pick up formula of Van Rijn. First the formula of Van Rijn is discussed, followed by the addition of Van Rhee for high flow velocities.

Van Rijn's pick up formula

Van Rijn constructed a pick up function to calculate the amount of sediment which is picked up from the bed. The Van Rijn formula is tested for velocities up to $1m/s$ and a wide range of grain sizes [Van Rijn,1984]. Van Rijn uses the critical shields parameter as described in chapter 2 and his formula is given in equation 3.5.

$$\phi_p = 0.00033 D_*^{0.3} \left(\frac{\theta - \theta_{cr}}{\theta_{cr}} \right)^{1.5} \tag{3.5}$$

In which:

ϕ_p = the dimensionless pick up rate $[-]$
D_* = the dimensionless diameter, described in equation A.1 in appendix A $[-]$
θ_{cr} = the critical shields parameter which indicates the initiation of motion, see appendix A $[-]$

As shown in equation 3.5, all terms are dimensionless. To generate an erosion flux from the dimensionless pick up parameter, the formula has to be multiplied by data of the particles in the bed. So the erosion rate becomes:

$$E = \phi_p \rho_s \left(\Delta g D_{50} \right)^{0.5} \tag{3.6}$$

In which:

E = the erosion flux $[kg/m^2 s]$
ρ_s = the density of the sediment $[kg/m^3]$
Δ = the relative density $[-]$
D_{50} = the median grain size of the sand $[m]$

The pick up function of Van Rhee

For high flow velocities, the Van Rijn formula overestimates the erosion rate. This is because the Van Rijn formula is based on the single particle approach, while for large flow velocities $(u > 1m/s)$ the erosion is hindered by the soil properties and the continuum approach should be used to determine the erosion rate. To apply the continuum approach, Van Rhee used soil properties such as the permeability and the porosity to determine the initiation of motion. The addition to the critical Shields parameter is shown in equation 3.7. This formula can be used in the formula of Van Rijn to calculate the erosion rate, which is shown in equation 3.8.

$$\theta_{cr}^1 = \theta_{cr} \left(\frac{sin\left(\phi - \beta \right)}{sin\phi} + A \frac{i}{\Delta} \right) \tag{3.7}$$

$$\phi_p^1 = 0.00033 D_*^{0.3} \left(\frac{\theta - \theta_{cr}^1}{\theta_{cr}^1} \right)^{1.5} \tag{3.8}$$

In which:

θ_{cr}^1 = the critical shields parameter according to Van Rhee $[-]$
θ_{cr} = the original critical shields parameter according to Shields $[-]$
ϕ = the angle of internal friction $[rad]$

β = the slope of the bed $[rad]$

A = a parameter which is 3/4 for the single particle mode and $\frac{1}{(1-n_0)} \approx 1.7$ for the continuum mode $[-]$

i = the hydraulic gradient in the soil layer $[m/m]$

Derivation of the Van Rhee formula

To derive the new critical shields parameter, the balance of forces for a particle on a slope is considered as shown in figure 3.2. The F_s is the shear force of the flow, the G is the submerged gravity force on the particle and F_i is the force of the hydraulic gradient.
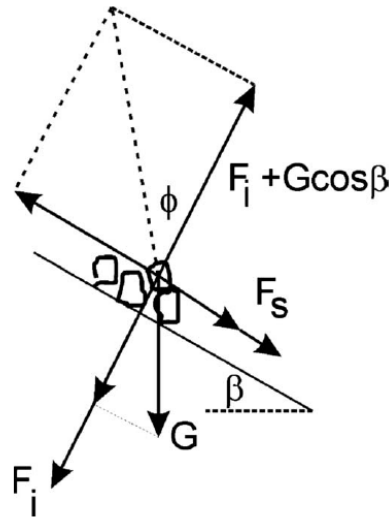
Figure 3.2: The force balance of particles on a slope [Van Rhee,2007]

In the single particle mode, the forces on a grain (F_s, F_i and G) are in balance at the initiation of motion. In the continuum mode the forces on the grain layer result in an inwardly directed hydraulic gradient (F_i). At the initiation of motion, the forces on the particle have to balance the force of the hydraulic gradient. This is shown in equation 3.9 or equation 3.10, which present the same relation.

$$F_s + Gsin\beta = (Gcos\beta + F_i)tan\phi \tag{3.9}$$

$$\frac{F_s}{G} = tan\phi \left(\frac{sin(\phi - \beta)}{sin\phi} + \frac{F_i}{G} \right) \tag{3.10}$$

Equation 3.10 is almost the same as the equation for the critical shields parameter of Van Rhee given in equation 3.7. The second term between the brackets is elaborated further to come to the definition of Van Rhee. The parameters in this term are elaborated below.

$$F_i = \rho_w gi \tag{3.11}$$

$$G = (1 - n_0)(\rho_s - \rho_w)g \tag{3.12}$$

Combining the two equations above, the following definition is given which is also stated in the addition of Van Rhee to the critical shields parameter.

$$\frac{F_i}{G} = \frac{\rho_w g i}{(1 - n_0)(\rho_s - \rho_w)g} = \frac{1}{1 - n_0}\frac{i}{\Delta} = A\frac{i}{\Delta} \tag{3.13}$$

In which:

F_i = the force exerted by the hydraulic gradient in the soil layer $[N]$
G = the force exerted by the gravity $[N]$
Δ = $\frac{\rho_s - \rho_w}{\rho_w}$ = the relative density of sediments under water $[-]$
i = the hydraulic gradient in the soil layer $[-]$

Hydraulic gradient

The hydraulic gradient given in equation 3.7, 3.11 and 3.13 is caused by dilatancy. Dilatancy is an expansion of a soil layer due to friction caused by the flow. This is shown in figure 3.3. The blue arrows represent the flow over the bed. At the left hand side, the original bed is shown and the right hand side shows the sheared soil. If dilatancy occurs, the pores between the sand grains increase and the the pressure decreases within the pores. This pressure drop causes a pressure gradient over the soil layer. The pressure gradient causes the water to flow in the soil layer. This inflow of water hinders the erosion of the soil layer and is marked with the number 1 in figure 3.3. The inflow can be calculated using equation 3.14. The hydraulic gradient becomes larger when the permeability is smaller, which results in a larger inward directed force of the water flowing in. So the hindering of the erosion is higher. The hindering of erosion due to the soil properties is called hindered erosion.
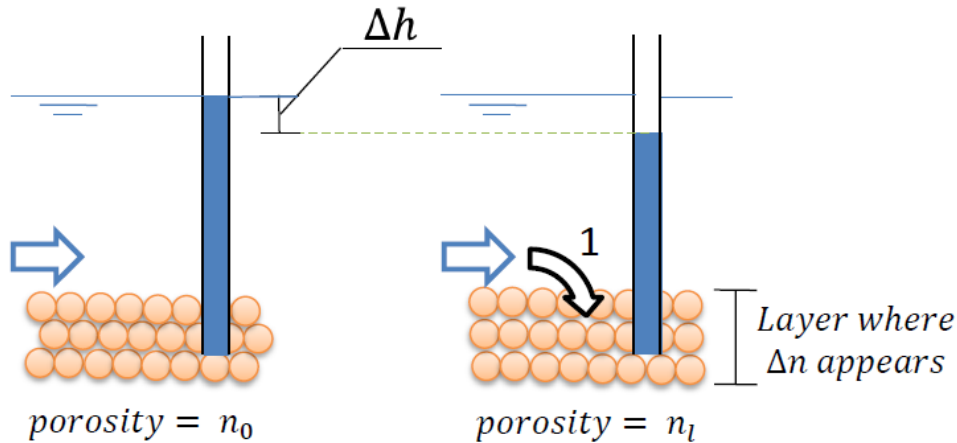
Figure 3.3: The process of dilatancy with the inflow of water

$$q = ki \tag{3.14}$$

The amount of water that flows in is equal to the difference in porosity, Δn times the layer thickness where Δn occurs. In formula this expression for the inflow, q, is given in equation 3.15.

$$q = v_e \Delta n \tag{3.15}$$

The hydraulic gradient can be found by combining equations 3.14 and 3.15. This gives the description of the hydraulic gradient, presented in equation 3.16.

$$i = \frac{v_e \Delta n}{k} \qquad (3.16)$$

In which:

q = the water that flows in the soil layer as a consequence of dilatancy $[m/s]$
k = the permeability of the soil layer, see equation 3.17 $[m/s]$
v_e = the erosion velocity of the bed $[m/s]$
Δn = $\frac{n_l - n_0}{1 - n_l}$ = the difference of the porosity after dilatancy $[-]$
n_l = the porosity of the bed after dilatancy $[-]$

$$k = \frac{g}{160\nu} D_{15}^2 \frac{n_0^3}{(1 - n_0)^2} \qquad (3.17)$$

Bed level change

The change of the bed level is calculated using the velocity of the bed. In case of erosion this is called the erosion velocity and can be calculated from the pick up rate E or the dimensionless pick up rate ϕ_p^1. This is shown in equation 3.18 for a situation without suspended sediment in the water column above the bed. In the expression for θ_{cr}^1 in equation 3.7, the erosion velocity is present as well, thus the erosion velocity has to be calculated iteratively.

$$v_e = \frac{E}{\rho_s (1 - n_0 - c_{nb})} = \frac{\phi_p^1 (\Delta g D_{50})^{0.5}}{(1 - n_0 - c_{nb})} \qquad (3.18)$$

In which:

E = the erosion flux $[kg/m^2 s]$
ρ_s = the density of the sand $[kg/m^3]$
ϕ_p^1 = the dimensionless pick up flux $[-]$
Δ = $\frac{\rho_s - \rho_w}{\rho_w}$ = the relative density $[-]$
D_{50} = the median grain diameter $[m]$
c_{nb} = the volumetric near bed sediment concentration $[-]$

Influence of slopes

In the formulation of the critical shields parameter, Van Rhee already included the influence of the longitudinal slope. For a transverse slope, the correction factor given in equation A.5 of appendix A can be used.

If θ_{cr}^1 becomes zero a slope is unstable anyhow. This only happens when the term between the brackets in equation 3.7 becomes zero. This is the case when:

$$v_e = -\frac{k_l}{\Delta n} \frac{\Delta}{A} \frac{sin(\phi - \beta)}{sin\phi} \qquad (3.19)$$

If equation 3.19 occurs, the slope collapse even if there is no flow. The velocity of which the slope propagates is called the active wall velocity and is given by equation 3.20. This formulation is

used to calculate the retreat of the banks, also if the the erosion velocity is smaller than the right hand side of equation 3.19.

$$v_{wall} = \frac{v_e}{sin\beta} = \frac{k_l}{\Delta n}\Delta cot\phi \tag{3.20}$$

Limitations of Van Rhee's pick up function

The theory of Van Rhee uses a term which is multiplied with θ_{cr}. This term takes into account the slope of the bed and the permeability. Equation 3.21 shows the boundary for which the influence of the permeability can not be ignored any more. This can be seen as the lower boundary for the high velocity regime. Below this value, the influence of the permeability can be ignored and the pick up can be calculated using the Van Rijn formula.

$$\frac{v_e}{k_l} > 3 \tag{3.21}$$

Sedimentation

As mentioned in chapter 2, the sedimentation depends on the settling velocity of sand particles. The sedimentation rate can be calculated using formula 3.22.

$$S = \rho_s w_s c_{nb} \tag{3.22}$$

In which:
  S = the sedimentation flux $[kg/m^2s]$
  ρ_s = the density of the sand $[kg/m^3]$
  w_s = the settling velocities of particles in water $[m/s]$
  c_{nb} = the volumetric near bed sediment concentration $[-]$

In the section above, the erosion rate is rewritten as an erosion velocity, which is the velocity of the bed in downward direction. The same can be done with the sedimentation velocity. This is shown in equation 3.23

$$v_{sed} = \frac{S}{\rho_s(1 - n_0 - c_{nb})} = \frac{w_s c_{nb}}{1 - n_0 - c_{nb}} \tag{3.23}$$

The total bed change, v_{bed} is composed from the erosion and sedimentation velocity. So when water flows over the bed, the change of the bed position is determined by equation 3.24

$$v_{bed} = v_e - v_{sed} = \frac{E - S}{\rho_s(1 - n_0 - c_{nb})} \tag{3.24}$$

In which:
  v_{bed} = the bed velocity (downward direction is taken positive) $[m/s]$
  v_{sed} = the sedimentation velocity $[m/s]$

3.5 Conclusions

The analytical description presented in this chapter presents a pick up formula and a method to calculate the bed change as a consequence of the local flow velocity. The transport formulation is especially developed to model erosion at high flow velocities and takes into account the hindering of the erosion. Thereby this calculation method does not use an equilibrium state of the flow, but the local friction exerted by the flow velocity. The expectation is that the Van Rhee formula provides better results for the calculation of the erosion in the final phase of the construction of a sand closure. In the next chapter the system of equation presented in this chapter is solved analytically and the results are presented to show the behaviour of the system and determine the sand losses from the closure gap qualitative.

Chapter 4

Behaviour of the analytical model

This chapter discusses the behaviour of the analytical description of the system, presented in chapter 3. The closure curve and equilibrium curve are used in this analysis to show the behaviour of a closure gap during closure. After the starting point, first the flow model is analysed. This is followed by an analysis of the change of the closure gap, in which the formulations of the CUR 157 and Van Rhee are compared. Finally the restrictions, shortcomings and conclusions of this analysis are discussed.

4.1 Starting point of the analysis

As a starting point, the example of a closure gap presented in chapter 2 is used for the analysis as a reference situation. The closure gap can be closed horizontally or vertically. During horizontal closure the height of the sill remains at 1.5m below N.A.P., while during vertical closure the width of the bed and the water level at N.A.P. remain the same. This is shown in figure 4.1. So when the flow surface is the same as presented in chapter 2, the geometries of both closure methods are the same.

Figure 4.1: The left hand panel shows the vertical closure and the right hand panel shows the horizontal closure

Determination closure curve and equilibrium curve

In chapter 2 the theory of an equilibrium state of tidal inlets and closure gaps is treated. This was based on the theory of Escoffier [Escoffier,1940]. Two curves show the stability of a closure gap, namely the closure curve and the equilibrium curve. Graphs of the two curves are used in this chapter to show the influence of different parameters and whether erosion or sedimentation occurs.

The closure curve is determined using the method of Battjes as explained in chapter 4. The equilibrium curve is determined such that over one tidal period the geometry of the closure gap

remains the same. Equation 4.1 shows this relation. For this analysis a continuous concentration of sediment is suspended in the water ($c = 0.0002$). The sedimentation is based on the grain sizes and the concentration of the water as shown in chapter 3. This means that the sedimentation rate is the same over the whole tidal period. During the high flow velocities the erosion is larger than the sedimentation and the bed will erode. During the period around slack, the sand which is suspended in the water settles.

$$\int_0^T \frac{dA_c}{dt} = 0 \rightarrow \int_0^T E dt = \int_0^T S dt \tag{4.1}$$

In which:

E = the erosion rate $[kg/ms]$
S = the sedimentation rate $[kg/ms]$
T = the period of the tide $[s]$

An example of the closure and equilibrium curve is given in 4.2. The blue line shows the closure curve for the closure gap which is closed vertically. The red line shows the closure curve for horizontal closure. It is easier to close a dam vertically since the maximum flow velocity is lower. The reason for this is explained in section 4.2. Equilibrium point B (the unstable equilibrium point, as described in chapter 2) is located at closure in this case.
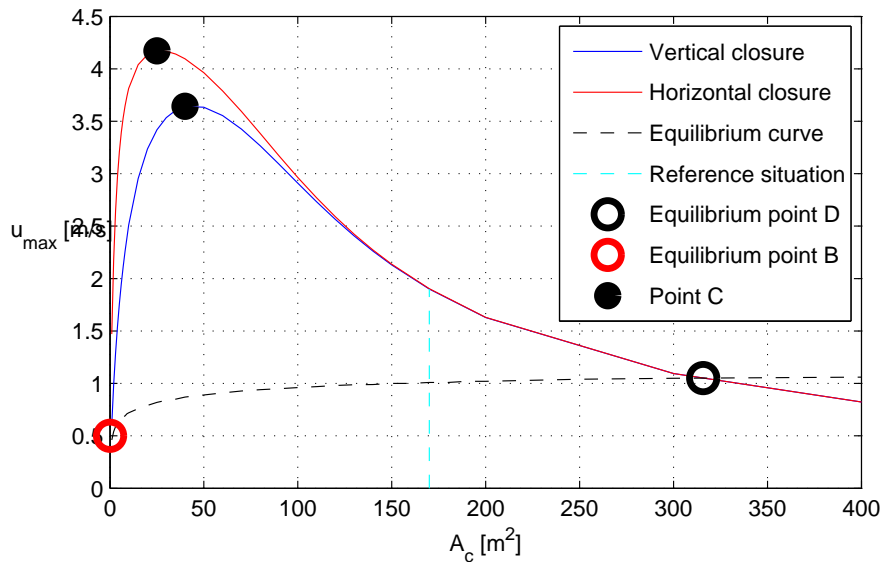
Figure 4.2: The closure curves of the reference situation

4.2 Flow analysis

Two processes are important to determine the flow through a closure gap: the resistance over the gap and the tidal forcing of the system. The resistance the water experiences while flowing through the closure gap decreases the acceleration or causes the water to decelerate. The influence of the resistance and the tidal forcing is discussed below.

Resistance of the closure gap

The resistance of the closure gap depends on the geometry of the gap. When the surface of the bed and the banks is larger or rougher, the water experiences more friction. The consequence is that the acceleration of the flow is smaller, which means that the discharge at the peak (the largest water level difference) becomes less if the friction is higher.

The resistance over the closure gap increases when the water feels more friction from the bottom. This can be reached in two ways: increase the bottom roughness or increase the friction surface (increase the length or the wetted perimeter). In the analysis of Battjes, the resistance over the dam is expressed in χ. This is shown in equation 3.3 in chapter 3.

The extend to which the friction influences the flow velocity during closure is shown in figure 4.3. The x-axis represents the ratio between the closure gap area and the surface of the basin. The y-axis represents the relative velocity with respect to the velocity which occurs at a friction coefficient, $\chi = 1$. Note that for each of the curves in figure 4.3, the friction coefficient remains the same for different closure gap geometries. In practice the hydraulic radius becomes smaller during closure, which implies an increase in the friction coefficient.
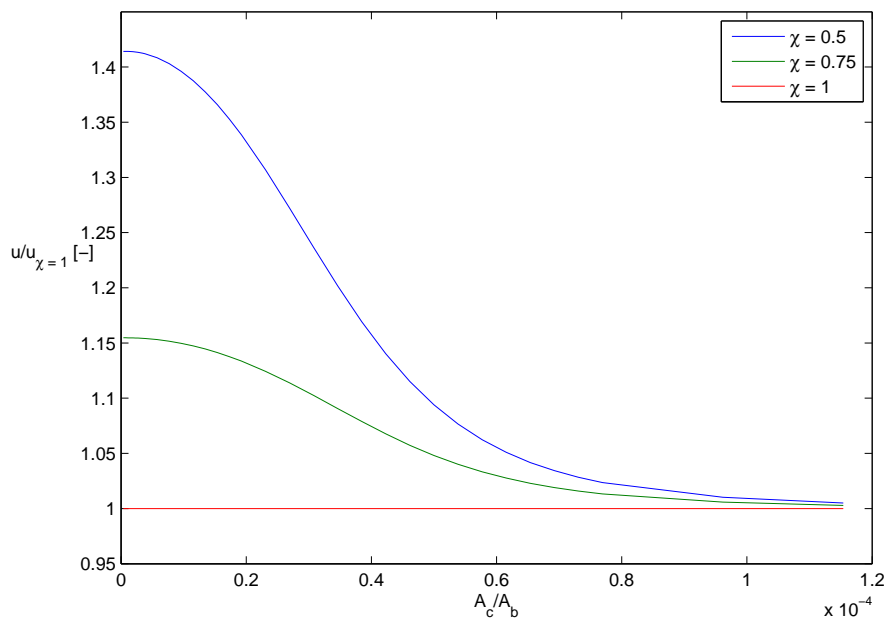
Figure 4.3: The closure curve for different values of the friction coefficient

Figure 4.3 shows that a decrease of the friction coefficient results in an increase of the velocity up to 40%. This implies that the closure of a dam is easier when the friction coefficient increases. According to equation 3.3, this can be done by increasing the length of the dam, the roughness or the wetted perimeter (which means a decrease of the hydraulic radius). The hydraulic radius depends on the slopes of the banks, the ratio between the height of the water level above the sill and the width of the gap.

During the final closure phase, the hydraulic radius changes. This causes an increase of the resistance over the dam till infinity (when the dam is finished). When the dam is closed vertically and the width of the bed is much larger than the depth, the wetted perimeter remains

larger than during horizontal closure. This causes more friction and lower flow velocities in the final phase of the closure when dam is constructed vertically. This difference is shown in figure 4.2, which presents the closure curves of the reference situation.

Tidal forcing

The tide forces the water to flow through the closure gap. So logically a larger tidal amplitude means larger flow velocities. This is shown in figure 4.4 for horizontal as well as vertical closures. The period influences the flow different than the amplitude. The maximum flow velocities are almost the same for different periods, but the difference is that for a shorter tidal period, the velocities become larger at larger closure gap sizes. So the period of large flow velocities is longer (the distance between point B and D becomes larger). This can be seen in figure 4.5.
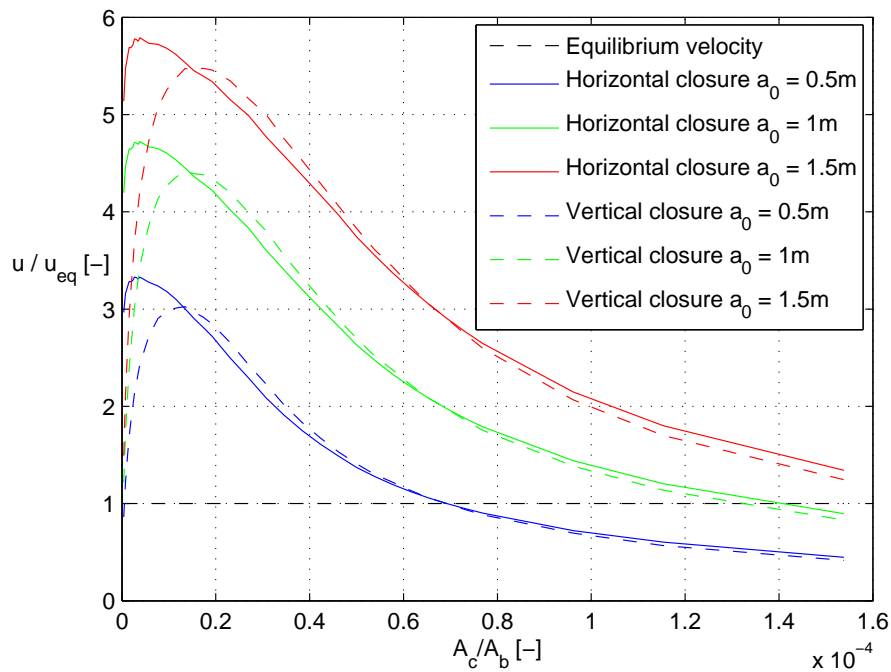
Figure 4.4: Closure curves compared to the equilibrium velocity for different tidal amplitudes
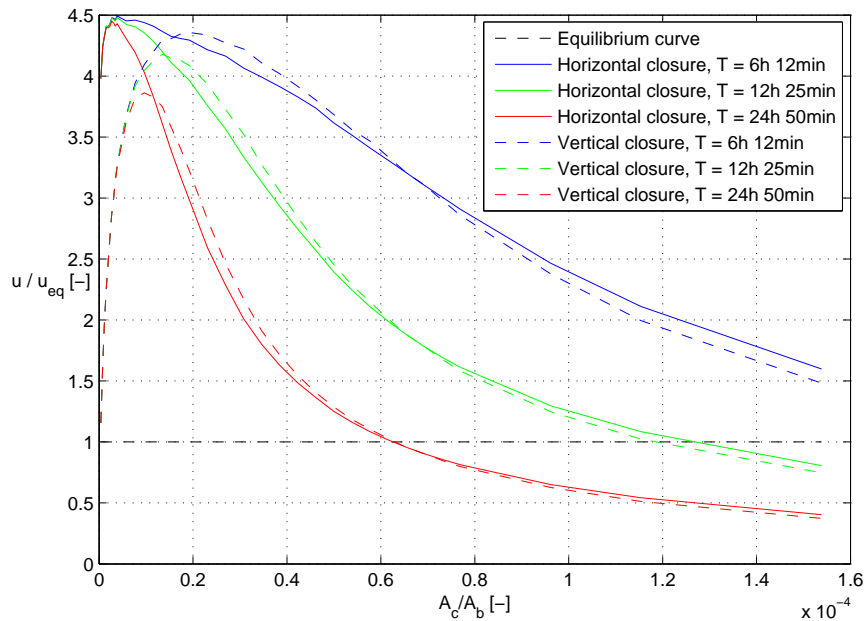
Figure 4.5: Closure curves compared to the equilibrium velocity for different tidal periods

4.3 Closure gap analysis

In this section the erosion and sedimentation over a tidal period are analysed. The total amount of erosion and sedimentation result in a change of the closure gap. Sand losses occur when the erosion becomes larger than the sedimentation. So to calculate the sand losses it is important to know how much sand erodes. Different formulas provide different amounts of erosion. So first the formula of the CUR 157 is compared with the Van Rhee formula. Subsequently the response of a closure gap is determined over a tidal period.

Comparison of erosion formulas

For a closure gap as in the reference situation, presented in chapter 2, the erosion of the bed is calculated with two formulas: the formula for the main stream of the CUR 157 and the Van Rhee formulation. This is shown in figure 4.6. The x-axis shows the flow velocity of the water and the y-axis shows the erosion velocity.
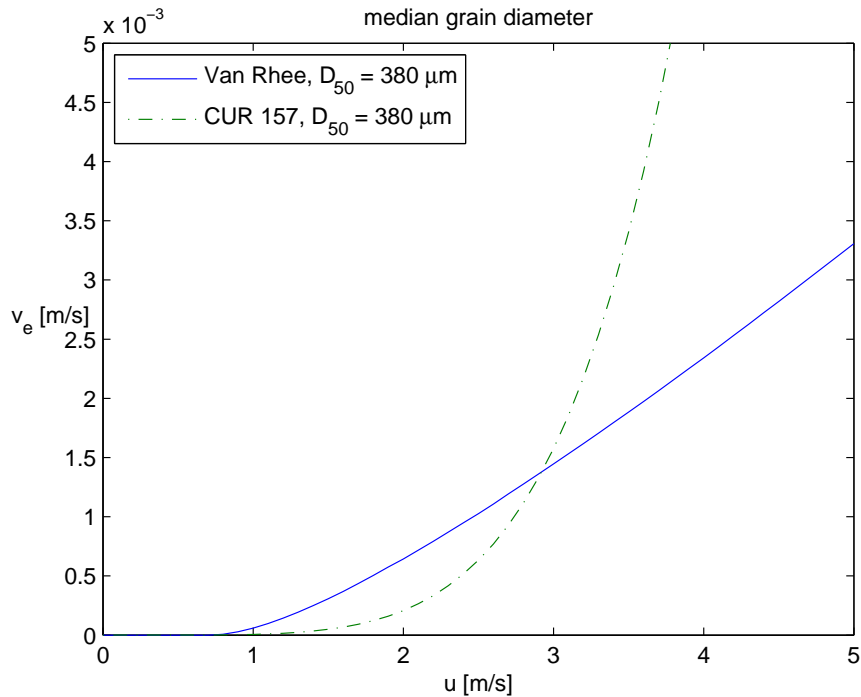
Figure 4.6: The erosion velocity of the bed

The most important difference between the two formulations is the shape of the curve. The formulation of Van Rhee provides almost a linear relation, while the formulation of the CUR 157 relates the erosion velocity to the flow velocity to the fifth power. This results in a lower erosion velocity for the CUR 157 for the flow velocities lower than $2.9m/s$. Note that at the 'Compartimenteringsdam' at 'Maasvlakte 2' the velocities weren't higher than the $2.9m/s$. When the flow velocity increases, the difference between the two formulas becomes much larger and the effect of hindered erosion becomes more important.

The erosion velocity at the banks depends on the method of closure. For a horizontal closure, the formulation of the CUR 157 takes into account the vortex street, which causes a larger erosion rate. The erosion velocity is taken perpendicular to the banks. From figure 4.7 can be seen that the correction in the CUR 157 formulation for the vortex street creates a lot more erosion. This correction is not taken into account in the Van Rhee formulation. However a correction for transverse slopes as presented in appendix A is used in the Van Rhee formulation. The effect of this correction is for large flow velocities much smaller than the approach of the CUR 157, which uses a different formulation to correct for the vortex street. Up to a velocity of $1.5m/s$, the erosion velocity of the banks is comparable for both formulations.
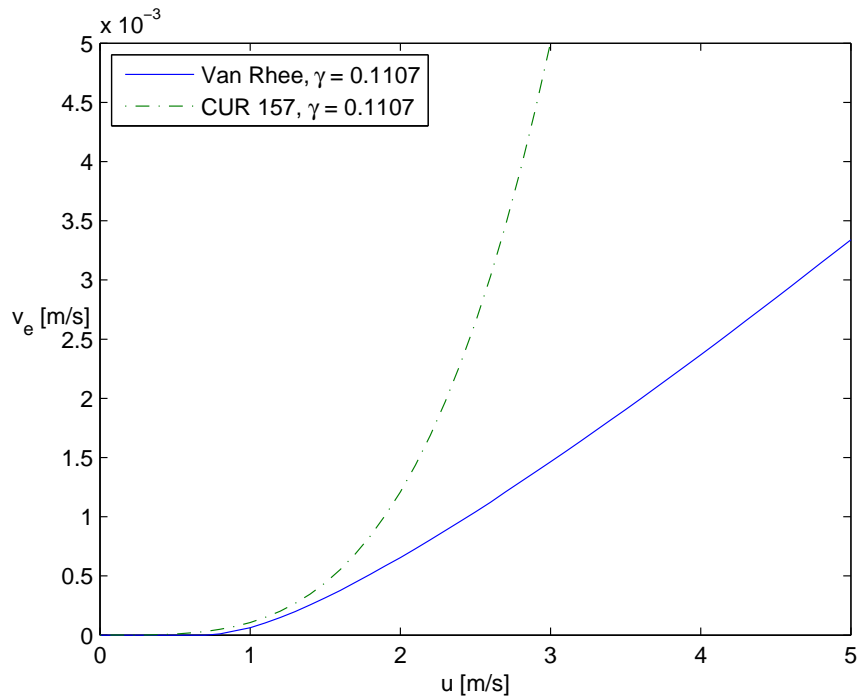
Figure 4.7: The erosion velocity of the banks

The pictures in figure 4.6 and 4.7 show differences between the two erosion formulas. However, for different parameters, the differences between the two formula's can differ a lot more. Below, the following parameters are varied to compare the two formulations: D_{15}, D_{50}, D_{90} and the porosity. As the graphs show, the Van Rhee formulation takes into account more soil properties than the formulation of the CUR 157. From figure 4.8 till 4.12, the following conclusions can be drawn:

- For a lower permeability, the erosion velocity calculated with the Van Rhee formula becomes lower, while for the CUR 157 formulation this is not the case. (the permeability is calculated using the D_{15} and the porosity, see equation 3.17)
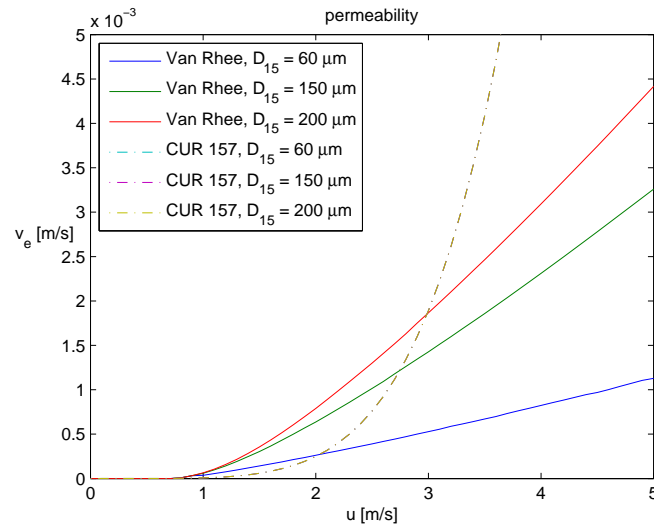
Figure 4.8: The behaviour of the CUR 157 formula and the Van Rhee formula for different values of D_{15}

- If the ratio between the D_{50} and the D_{15} remains the same, the D_{15} is more dominant than the median grain size. So a smaller grain size can lead to a smaller erosion velocity in Van Rhee's formula, while for the CUR 157 formulation, a smaller grain size means a larger erosion rate. When the D_{15} remains constant and only the median grain size changes, the largest erosion is seen at a grain size of $380\mu m$, see figure 4.10. This is remarkable, because it seems trivial that the erosion of smaller particles is larger. According to the Van Rhee formulation this is not the case. Note that the formula is tested in this analysis for erosion only without sediments suspended in the water. When sand is suspended in the water the sedimentation rate of large sand particles is larger than for small grains. Since the erosion velocities are very close to each other, the sedimentation rate of particles become significant. So for a sand closure larger grain sizes are favourable to close a dam.
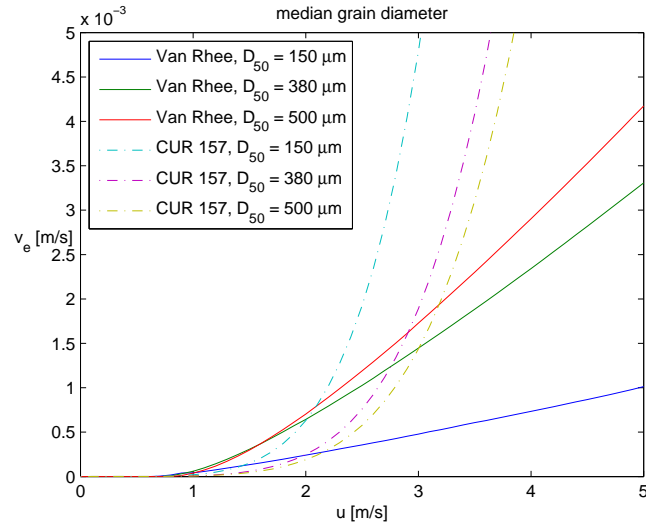
Figure 4.9: The behaviour of the CUR 157 formula and the Van Rhee formula for different values of $D_{50}*$
       Note that the D_{15} is determined as $0.4 \cdot D_{50}$, so it varies with the D_{50}
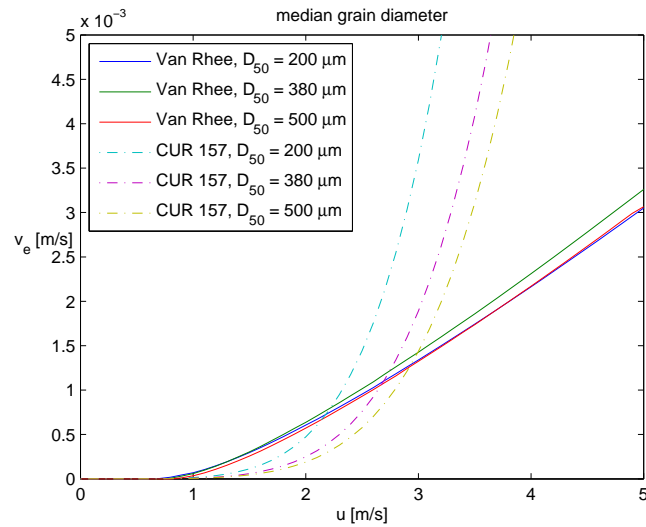
Figure 4.10: The behaviour of the CUR 157 formula and the Van Rhee formula for different values of D_{50}, with a constant D_{15}

- For a lower porosity, the erosion velocity becomes lower with the Van Rhee formulation. For the CUR 157 formulation this influence is negligible.
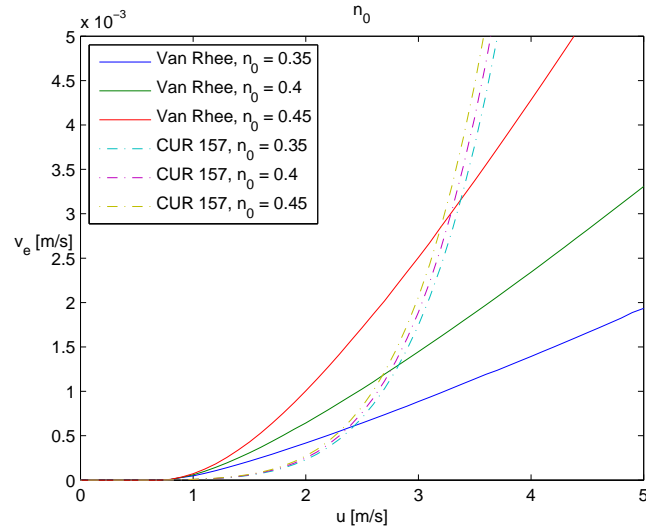
Figure 4.11: The behaviour of the CUR 157 formula and the Van Rhee formula for different values of n_0

- As shown in figure 4.12, the influence of the D_{90} on the erosion velocity is almost the same for both cases. This D_{90} influences the morphological roughness. The roughness can vary within a large range, because ripples which can be present increase the roughness. This variation can be much larger in practice than the variation in the D_{90} in this analysis. Note that the CUR 157 advices to keep the roughness at $0.1m$, but in this analysis a roughness of $3 \cdot D_{90}$ is used.
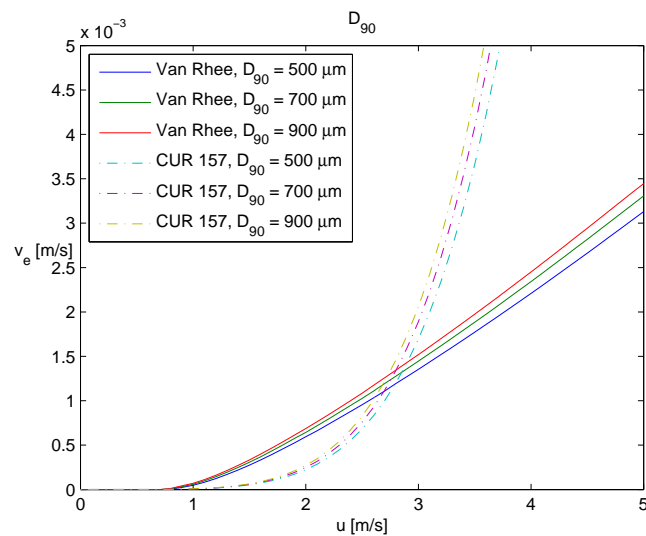
Figure 4.12: The behaviour of the CUR 157 formula and the Van Rhee formula for different values of D_{90}

- The influence of slopes is larger at the CUR 157 formulation because it uses a correction for the vortex street, see figure 4.7. However the angle of the slope is not taken into account in that formulation, while the Van Rhee formula takes the angle of the slope into account. In the end, the angle of the slope is almost negligible compared to other parameters.

Change of the closure gap

In this section the erosion in the main stream of the dam is analysed. The erosion and sedimentation together cause a change in the closure gap size. The erosion and sedimentation can be expressed in the velocities of which the bed moves up or down. If the erosion velocity and the sedimentation velocity are summed, the bed velocity is the result. This is shown in equation 4.2.

$$
\left.\begin{array}{c}
v_e = \dfrac{E}{\rho_s(1 - n_0 - c_{nb})} \\
v_{sed} = \dfrac{S}{\rho_s(1 - n_0 - c_{nb})}
\end{array}\right\} \qquad v_{bed} = \dfrac{S - E}{\rho_s(1 - n_0 - c_{nb})} \tag{4.2}
$$

In which:

E	=	the erosion rate $[kg/m^2 s]$
S	=	the sedimentation rate $[kg/m^2 s]$
ρ_s	=	the density of the sediment $[kg/m^3]$
n_0	=	the bed porosity $[-]$
c_{nb}	=	the near bed concentration of sediments in the water $[-]$

Whether erosion or sedimentation occurs can be seen from the closure curve in combination with the equilibrium curves, shown in figure 4.13. In this figure the equilibrium curves are plotted for the formula of the CUR 157 and the Van Rhee formula. As figure 4.13 shows, an equilibrium is reached at higher velocities when the CUR 157 formulation is used. This is because in the equilibrium state the flow velocities don't become very high. When the flow velocities become larger, the erosion rate, calculated with the CUR 157, becomes larger. This can be distracted from figure 4.6, where the erosion formulas are compared. Also a difference between horizontal and vertical closure is shown in figure 4.13. This difference is caused by the friction terms in the equations (the Chezy coefficient in the CUR 157 and the c_f in the Van Rhee formulation). The extend this friction term changes the flow is already treated in the flow analysis in section 4.2.
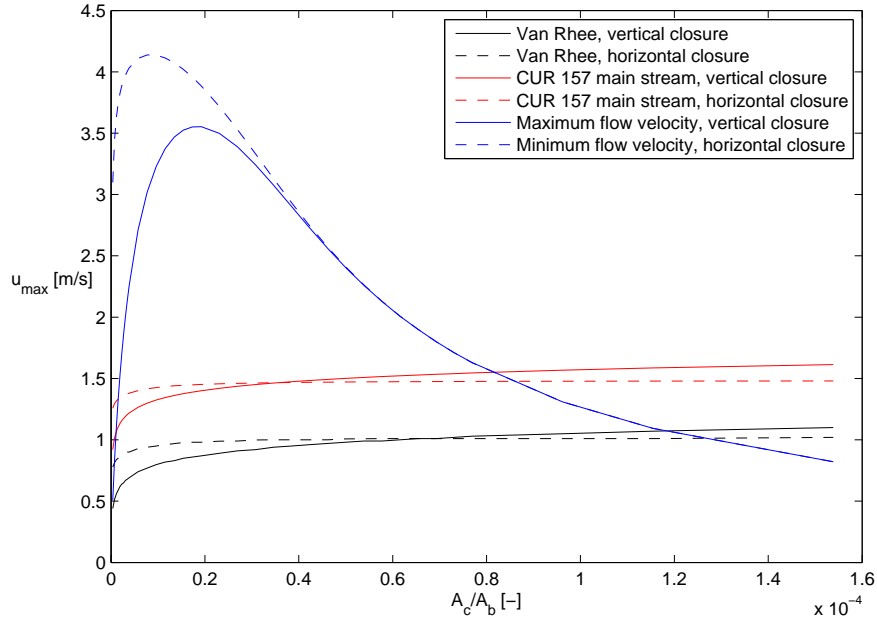
Figure 4.13: The equilibrium curves for the reference situation

Figure 4.14 shows the erosion ($\phi_e > 0$) or sedimentation ($\phi_e < 0$) during a tidal cycle for different cross sections. The pick up and sedimentation are expressed in the dimensionless pick up and sedimentation parameters (ϕ_p and ϕ_s). Equation 4.3 gives the expression of the sedimentation parameter and the expression for the pick up parameter is given in equation 3.6. The pick up or sedimentation over a tidal period is determined by equation 4.4.

$$\phi_s = \frac{S}{\rho_s \sqrt{\Delta g D_{50}}} \tag{4.3}$$

$$\phi_{e,T} = \frac{\int\limits_0^T \phi_p - \phi_s \, dt}{T} \tag{4.4}$$

In which:

ϕ_s = the dimensionless sedimentation [−]
ϕ_p = the dimensionless pick up of sediments from the bed [−]
ϕ_e = $\phi_p - \phi_s$ = the net dimensionless pick up [−]

Figure 4.14 shows indeed that for high flow velocities the pick up of sediments calculated with the CUR 157 formula is larger than with the Van Rhee formula. For lower flow velocities the Van Rhee formula gives a lower pick up of sediments. This is in agreement with the compared equilibrium curves in figure 4.13 and the comparison in figure 4.6.
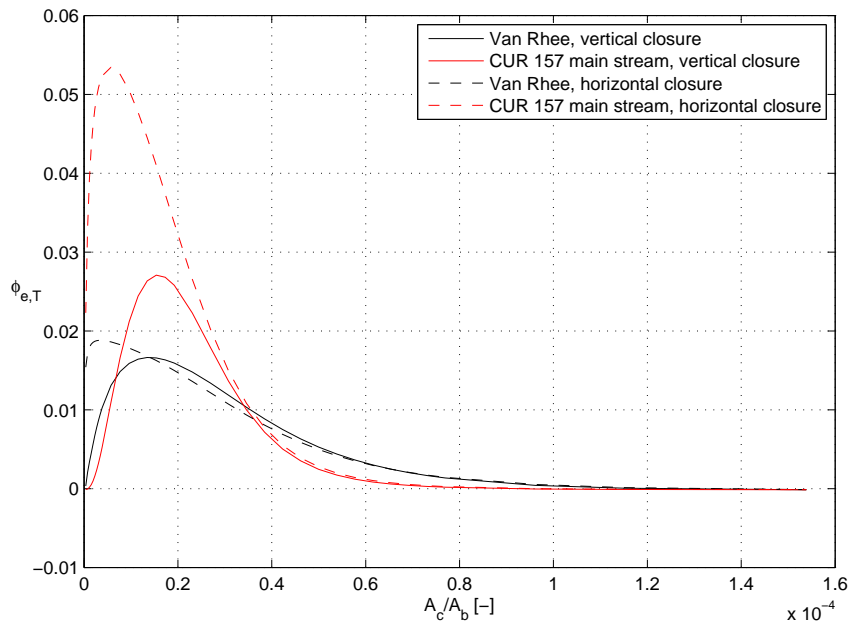
Figure 4.14: The sand losses, averaged over a tidal period for different closure gap sizes, calculated with Van Rhee and CUR 157

4.4 Restrictions of the analysis

Five major assumptions are made to analyse the system analytically. This is useful to show how the system responds to different processes and what the influence is of different parameters. For the quantification of the sand losses these assumptions are not always valid any more.

The closure gap doesn't change during a tidal period

What can be seen from figure 4.14 is that the erosion is very large within a tidal period. If a ϕ_e of 0.01 is considered, this is equals a bed change of:

$$\overline{v_e}T = \frac{\phi_e\sqrt{\Delta g D_{50}}}{1 - n_0 - c_{nb}}T = \frac{0.01 \cdot \sqrt{1.65 \cdot 9.81 \cdot 380 \cdot 10^{-6}}}{1 - 0.4 - 0.0002}T \approx 50m \quad (4.5)$$

This erosion seems to be quite large, but in practice, when the closure gap erodes $1m$, the flow decreases. For example during vertical closure with a closure gap width of $50m$, the closure gap increases with $50m^2$. This increase is a large change, which influences the flow a lot within the tidal period. This increase of the closure gap can be compared with a jump from $0.2 \cdot 10^{-4}$ to $0.4 \cdot 10^{-4}$ in figure 4.14. The change of the closure gap is thus not negligible in the final phase of a closure. In order to calculate the sand losses, a smaller time scale is needed for which the closure gap geometry remains the same.

The flow through the closure gap is sub critical

What can be seen from figure 4.2 is that in the critical phase of the construction, the flow velocities become very high; $3.5m/s$ for vertical and to $4.2m/s$ for horizontal closure. This can

result in Froude numbers above one, which means (super-)critical flows. The Battjes method is only suitable for sub-critical flows. In the final phase of the construction of a closure dam, the flow becomes critical in most cases. So a discharge relation is needed that is able to calculate with (super-)critical flows.

Discontinuous concentrations

In the analysis performed in this chapter the closure gap is considered as a cross section and the effects of the length of the dam (in flow direction) is only taken into account for the friction in the calculation of the flow velocities. The concentration of sediments in the water assumed as a constant value. In practice, when erosion takes place, sediment particles are picked up and mixed in the water column, which causes an increase of the concentration. This increase of the concentration reduces the erosion or even causes sedimentation at another location within the dam. The calculation method of the CUR 157 takes this into account by calculating the erosion based on the difference between the maximum transport capacity and zero concentration in the water column. The Van Rhee formula uses the sediment concentration near the bed. This concentration shall rise up to a maximum in the flow direction. When this maximum is reached, the sedimentation and erosion are equal for the flow velocity at that moment. In order to calculate the erosion in the dam, the local concentration has to be taken into account and the erosion has to be calculated at different locations in the closure gap.

Cross section

The erosion as discussed in this chapter is valid for a flow line with a flat bed. The wetted perimeter is an important parameter to calculate the sand losses. One can imagine that if a larger area of bed or banks are exposed to erosion, that the total erosion is larger. To calculate the sand losses which occur, the erosion over the whole cross section has to be taken into account.

Sinusoidal tide

The tide in this analysis is taken as a sinusoidal tide. In practice there is always a deviation from a perfect sinusoidal tide. This can be skewness of the tidal wave or a daily inequality. Therefore to calculate the sand losses, it is important to use the actual tide which is present at the location of the closure dam.

4.5   Conclusion

The flow is mostly dominated by the tidal forcing, the resistance over the closure gap and the ratio between the closure gap and the tidal basin. The resistance is the parameter which can be influenced during construction of a closure gap. For a vertical closure, the geometry of the closure gap leads to more resistance over the closure gap than for a horizontal closure. This means that for a vertical closure the maximum velocities are lower than for the horizontal closure.

The Van Rhee formulation contains more physical background than the formulation of the CUR 157. The process of dilatancy is an important process which is taken into account in the Van Rhee formula. The analysis shows that for a smaller permeability and porosity, the erosion calculated with the Van Rhee formulation decreases. An other consequence of the process of dilatancy is that erosion is hindered at high flow velocities. This causes a lower erosion at high flow velocities for the Van Rhee formula compared with the formula of the CUR 157. For low flow velocities ($u < 1m/s$) the dilatancy is almost negligible and the differences between the two formulas is small.

Chapter 5

1D model

At the end of chapter 4, the limitations of the analysis are presented. To quantify the sand losses, a model is needed which does not contain these limitations. This chapter presents a 1-dimensional model to calculate the sand losses. First an overview of the model is given, followed by the assumptions of the model and a description of the needed input. Subsequently the calculation steps are discussed and finally the results of a check of the behaviour of the model is presented.

5.1 Overview of the model

The one dimensional model divides the closure gap in several sections. Every section has its own geometry, which consists of three parts: the left bank, the bottom and the right bank. This is shown in figure 5.1. In this figure the upper picture shows the geometry of a section of the dam and the lower figure shows a longitudinal cross section with the dam divided in sections.
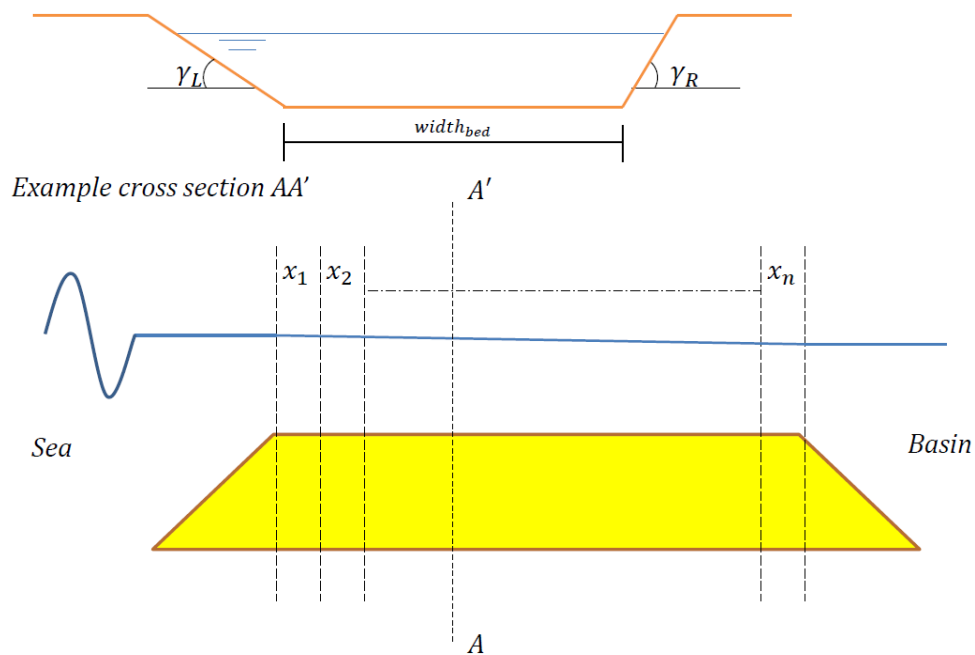
Figure 5.1: Schematic overview of closure gap in the 1-dimensional model

The model calculates the change in the closure gap geometry as a consequence of the flow through the closure gap. In order to do so, the model runs through different calculation steps. The steps are shown in figure 5.2. Different elements in the flowchart are explained in the following sections.
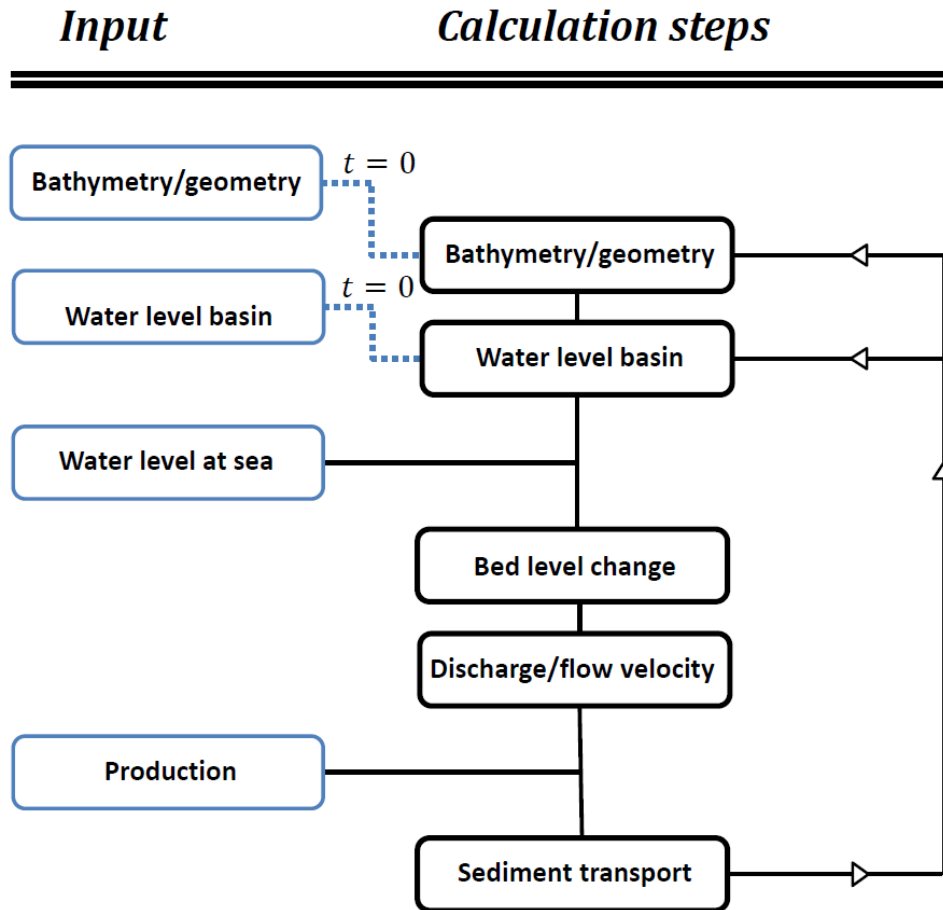
Figure 5.2: Flow chart of the calculation steps of the 1-dimensional model

5.2 Assumptions

The assumptions of the 1-dimensional model differ in five points from the assumptions as described in chapter 3 and which are also used for the analytical model. The five differences are presented below.

The first difference is that the closure gap is not symmetric any more as was regarded in the analytical model. The cross section in this model is divided in three sections, the left bank, the right bank and the bottom. This has the advantage that different slopes of the banks can be considered. An example of a cross section is given in cross section AA' of figure 5.1.

The second difference is the determination of the discharge through the closure gap. In the analytical model this is done using Battjes' method. Here a discharge relation is used, which makes the model also applicable to non sinusoidal tides and critical flows. This theory of the flow is described later in this chapter.

The third difference is that the dam is divided in different sections in the flow direction. This is more complex than the 0-dimensional analytical model, but provides advantages. By describing different cross sections, the flow velocity, the concentration of sediments and the geometry of the cross sections can be different per section. This makes the model better applicable to quantify the actual sand losses.

The fourth difference between the 1-dimensional and the analytical model is the determination of the concentration of sediments in the water. In the analytical model, the concentrations were assumed to be constant over time and place. This is not the case in the 1-dimensional model.

The fifth difference holds that the closure gap can change size within a tidal period. The tidal period is be divided in small time steps. During a time step the geometry, the concentration and the discharge remain the same. After a time step, the geometry is changed, based on the bed velocities and the production. The same holds for the sediment concentration in the water.

5.3   Input

The input of the model consists of four parameters. The geometry of the closure gap, geometry of the basin and the water level in the basin are initial conditions, while the water level at sea and the amount of production are input parameters which are needed for every time step.

Geometry and bathymetry

The bathymetry of the closure gap consists of the position of the bed in different sections. The sand bed in the model contains the following soil properties: the median grain size, the D_{15}, the D_{90}, the porosity and the density of the sand particles. The D_{90} is needed for the calculation of the hydraulic and morphological roughness of the bed. The D_{15} is used for the calculation of the permeability.

To determine the initial cross sections, bed levels, widths of the bed and the slopes of the left and the right bank are necessarily. During the model run these parameters change due to erosion, sedimentation and production.

Boundary conditions

The model has only one boundary condition, the water level at sea. With one initial water level in the basin, the flow can be calculated and the water level of the basin is determined after every time step using the basin storage approach, explained in chapter 3.

Production

The production can be added to the model in two different ways. The first one (direct deposition) is when the sand is brought in suspension directly from a hopper or a jet pontoon. The second method is by use of a land pipeline and land equipment. For direct deposition, an amount of sediment is added to the water, which increases the concentration of the sediment in the given cross section. This is shown in figure 5.3. The increase of the concentration is calculated using equation 5.1.
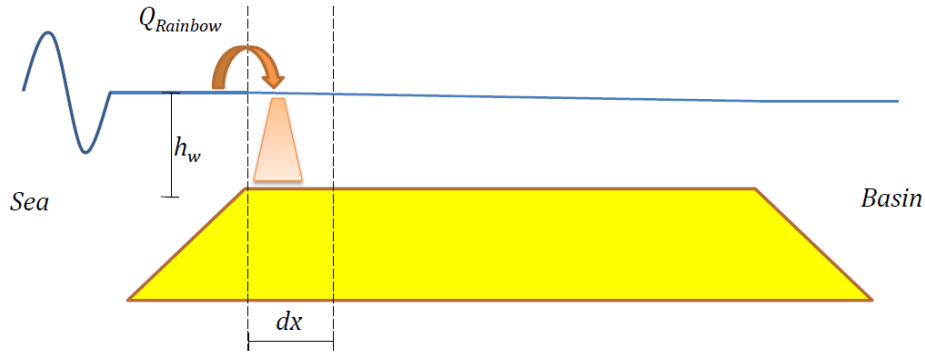
Figure 5.3: A schematization of the sand dumped directly from a hopper

$$C_{prod}^t = \frac{Q_{rainbow}^t \cdot (1 - n_m)}{A_c^t dx} dt \tag{5.1}$$

In which:

C_{prod}^t	=	the added volumetric concentration by rainbowing at time step t $[-]$
$Q_{rainbow}^t$	=	the discharge of the sand production at time step t $[m^3/s]$
A_c	=	the flow surface of the closure gap at time step t at the section of deposition $[m^2]$
dx	=	the length of a section $[m]$
dt	=	the time step $[s]$
n_m	=	the porosity of the sand water mixture that is brought in the water $[-]$

When the sand is added to the system by use of a land pipeline, bulldozers divide the sand over the whole width of the given sections. So for horizontal closure, the model extends the bank in the sections where the production takes place. A schematic view of the production is shown in figure 5.4. The extension of the bank, dy, is calculated using equation 5.2

$$dy^t = \frac{Q_{pipe}^t \cdot (1 - n_m)}{(h_w^t + h_{cr})dx(1 - n_0)} dt \tag{5.2}$$

In which:

dy^t	=	the extension of the bank at time step t$[m]$
Q_{pipe}^t	=	the discharge of the sand production at time step t $[m^3/s]$
h_w^t	=	the water level above the NAP at time step t $[m]$
h_{cr}	=	the crest level of the dam above N.A.P. $[m]$
dt	=	the time step $[s]$
n_0	=	the porosity of the sand in the bed $[-]$
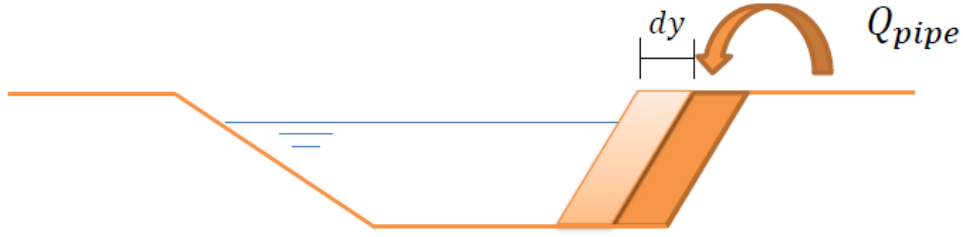
Figure 5.4: The production from the pipeline

In the final phase of the construction, the width of the bed becomes zero. The determination of the extension of the bank, dy, is not that straight forward any more as presented in equation 5.2. The complexity is shown in figure 5.5. In the left panel of the figure, the surface of A_1 does not contribute to the closure and is 'lost'. This sand needs to be placed as in the right panel.

Figure 5.5: The correction of dy when the width of the bed becomes zero

The determination of dy needs three extra calculation steps. The steps are shown in equation 5.3 till 5.5 and explained below:

- First the change of the cross sectional area of the closure gap is determined. This is equal to the old surface of the cross section minus the production fill, see equation 5.3

- The second step is the determination of the new height of the bed level as shown in equation 5.4.

- With the height of the bed and the surface of the closure gap, the width of the closure gap can be calculated. This is shown in equation 5.5. The extension of the bank is equal to the old width of the gap minus the new width.

$$A_c^{t+1} = A_c^t - \frac{Q_{pipe}^t(1 - n_m)}{dx(1 - n_0)} \tag{5.3}$$

$$h_{sill}^{t+1} = \sqrt{\frac{2A_c^{t+1}tan\gamma_R}{1 + \frac{tan\gamma_R}{tan\gamma_L}}} \tag{5.4}$$

$$W_{gap}^{t+1} = \frac{A_c^{t+1}}{0.5h_{sill}^{t+1}} \tag{5.5}$$

In which:

A_c	=	the size of the closure gap (above and below water) $[m^2]$
dx	=	the length of a section $[m]$
n_0	=	the porosity of the bed and banks $[-]$
h_{sill}	=	the height of the bed according the ground level $[m]$
$\gamma_{R,L}$	=	the angles of respectively the right and left bank $[rad]$
W_{gap}^{t+1}	=	the width of the closure gap at ground level $[m]$

5.4 Calculation steps

Discharge and flow velocity

The discharge is calculated using the steps as shown in the flowchart in figure 5.6. First the loss of energy is calculated, using the water level in the basin and the water level at sea, see equation 5.6. As presented in chapter 3, the water is stationary. So the energy level is equal to the water level at the boundaries.
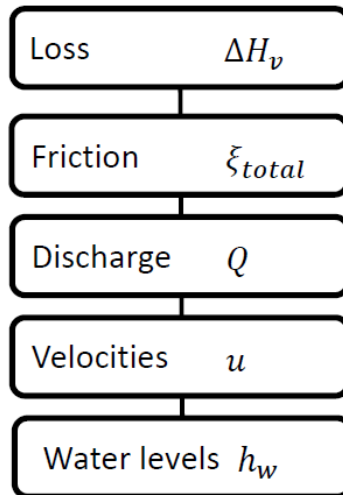
Figure 5.6: The steps to calculate the flow through the closure gap

$$\Delta H_v = abs\left(h_{sea}^{t+1} - h_{basin}^t\right) \tag{5.6}$$

The energy loss in the model takes place due to three mechanisms, inflow losses, outflow losses and friction. During the inflow, contraction occurs, which leads to a loss of energy. When an enlargement of the flow area is abrupt, outflow losses occur. The third loss is the friction of the bed and the banks over the dam. When the dam is short, this is negligible, but for a relative long dam, the influence is significant. The total energy loss can be calculated using formula 5.7.

$$\Delta H_v = \xi_{total}\frac{u_{ref}^2}{2g} \tag{5.7}$$

In which:

ΔH_v	=	energy loss over the closure gap $[m]$
ξ_{total}	=	the total friction over the gap $[-]$
u_{ref}	=	the flow velocity which is used to determine the friction $[m/s]$

The total friction consists of the following five friction terms:

$$\xi_{total} = \xi_{in} + \xi_{in_{HC}} + \xi_{out_{HC}} + \xi_{out} + \xi_{friction} \tag{5.8}$$

In which:

ξ_{total}	=	the total resistance of the dam $[-]$
ξ_{in}	=	the friction of the contraction during inflow from the sea or the basin $[-]$
$\xi_{in_{HC}}$	=	the friction of the contraction at the horizontal closure $[-]$
$\xi_{out_{HC}}$	=	the friction loss of the outflow at the horizontal closure $[-]$
ξ_{out}	=	the friction loss of the outflow in the sea or the basin $[-]$
$\xi_{friction}$	=	the friction loss of the bed and banks $[-]$

The reference velocity, u_{ref}, is used to calculate the discharge through the closure gap. The reference velocity is determined using equations 5.6 and 5.7. This velocity is the velocity in the final section at the downstream side of the dam. The reference velocity is multiplied with the associated flow surface to determine the discharge. This is shown in equation 5.9. The next step is to calculate the flow velocities using the calculated discharge and the flow surface of each section, see equation 5.10.

$$Q^{t+1} = u_{ref} A^t_{c,ref} \tag{5.9}$$

$$u_x^{t+1} = \frac{Q^{t+1}}{A^t_{c,x}} \tag{5.10}$$

In which:

u_x	=	the flow velocity in section x $[m/s]$
Q	=	the discharge through the closure gap $[m/s^3]$
$A_{c,x}$	=	the flow area of section x $[m^2]$

When the flow velocities become too large, critical flow occurs. In that case, the discharge is calculated using the formula for critical flows. For this formula a correction is made if the water level downstream of the closure gap is higher than the sill of the dam. This is based on a theory of Hager [Fritz and Hager,1998]. The reduction is given in equation 2.3 in chapter 2.

The final step is to calculate the new water levels in the dam. This is done using the energy level at every section of the dam. The energy level is calculated using the friction and the reference velocity. The water level equals the energy level minus the velocity height. This is shown in equation 5.11

$$h_{w,x}^{t+1} = (H_0 - \Delta H_{v,x}) - \frac{u_x^2}{2g} \tag{5.11}$$

In which:

H_0	=	the maximum of h_{sea} and h_{basin} $[m]$
$h_{w,x}$	=	the water level at section x $[m]$
$\Delta H_{v,x}$	=	the energy loss from the begin of the dam till section x $[-]$

Bed level change

When the flow velocities are known, the bed level change can be calculated. The bed level change is a summation of the erosion velocity and the settling velocity. This is shown in equation 5.12. The v_e is calculated using the Van Rijn formula for velocities lower than $1m/s$ and the van Rhee formula for velocities higher than $1m/s$. The formulas for the erosion and sedimentation velocity are described in chapter 3. Note that the bed velocity is taken positive when erosion occurs. The banks also erode and accrete due to erosion and sedimentation. This is calculated using equation 5.13.

$$\frac{\partial z_b}{\partial t} = v_{bed} = v_e - v_{sed} \tag{5.12}$$

In which:

z_b = the bed level $[m]$
v_{bed} = the velocity of the bed (positive in downward direction) $[m/s]$
v_e = the erosion velocity $[m/s]$
v_{sed} = the sedimentation velocity $[m/s]$

$$\frac{\partial z_{bank}}{\partial t} = v_{wall} = \frac{v_e - v_{sed}}{sin\gamma_{l,r}} \tag{5.13}$$

Sediment transport

As a consequence of the flow, the bed erodes and sediment comes in suspension. This leads to an increase of the sediment concentration in the cross section. If the flow becomes low, the sediment settles, which causes a decrease of the sediment concentration in suspension. The calculation of the settling and erosion of sediment is already discussed in chapter 4.

The sediment in suspension is transported by the flow. The advection of the concentration can be calculated with the convection equation as shown in equation 5.14 [Zijlema,2011].

$$\frac{\partial c}{\partial t} + u\frac{\partial c}{\partial x} = 0 \tag{5.14}$$

During a time step, erosion or sedimentation occurs and sand is brought into suspension or withdrawn from the water column. The sand can also be brought in suspension by production. For these additions or withdrawals extra terms are needed in the convection equation. This is shown in equation 5.15.

$$\frac{\partial c}{\partial t} + u\frac{\partial c}{\partial x} = C_{prod} + C_{ero} \tag{5.15}$$

In which:

c = the volumetric concentration of sediments in the water $[-]$
u = the flow velocity of the water $[m/s]$
C_{prod} = production term expressed in an addition of the volumetric concentration $[-]$
C_{ero} = erosion term expressed in an addition of the volumetric concentration $[-]$

In equation 5.15, the erosion term becomes negative when sedimentation occurs. Logically, the concentration of sand in the water can not become smaller than zero or larger than the maximum concentration, $(1 - n_0)$. If the maximum concentration is obtained, the dam is considered as closed.

To solve the above differential equation numerically an upwind scheme is used. This is a numerical scheme which is based on a forward in time and backward in space discretization [Zijlema,2011]. The forward in time descretization is given in equation 5.16. The backward in space discretization is given in equation 5.17.

$$\frac{\partial c}{\partial t} = \frac{c_m^{n+1} - c_m^n}{dt} \tag{5.16}$$

$$\frac{\partial c}{\partial x} = \begin{cases} \frac{c_m - c_{m-1}}{\Delta x} & \text{if } u > 0m/s \\ \frac{c_{m+1} - c_m}{\Delta x} & \text{if } u < 0m/s \end{cases} \tag{5.17}$$

If equation 5.16 and 5.17 are filled in the convection equation, the following numerical scheme is obtained. In this scheme, σ is called the Courant number. The system is numerically stable if the absolute value of the Courant number is smaller than 1. This stability condition is given in equation 5.19.

$$c_m^{n+1} = C_{prod}dt + C_{ero}dt + c_m^n - \sigma \begin{cases} c_m^n - c_{m-1}^n & \text{if } u > 0m/s \\ c_{m+1}^n - c_m^n & \text{if } u < 0m/s \end{cases} \tag{5.18}$$

In which:
c_m^n = the concentration in section m at time n $[m^3/m^3]$
σ = the Courant number, see equation 5.19 $[-]$

$$|\sigma| = \frac{|u|\Delta t}{\Delta x} \leq 1 \tag{5.19}$$

5.5 Sand losses

From the sediment transport, the sand losses can be calculated. This is done by evaluating the amount of sand which is transported out of the model area. The sand losses are calculated using equation 5.20. So during flood (flow into the basin), the sand losses are determined by the discharge and the concentration of sediment in the final cross section. During ebb the concentration in the first cross section is determinative.

$$Loss = \frac{Q \cdot dt}{1 - n_0} \cdot \begin{cases} c_{end} & \text{if } Q > 0m^3/s \\ c_1 & \text{if } Q < 0m^3/s \end{cases} \tag{5.20}$$

In which:
$Loss$ = the sand losses $[m^3/s]$
Q = the discharge through the closure gap $[m^3/s]$
c_{end} = the concentration in the last section $[m^3/m^3]$
c_1 = the concentration in the first section $[m^3/m^3]$

5.6 Verify behaviour of the model

In order to verify the behaviour of the model, the analytical calculations are compared with the 1-dimensional model. To compare the two calculation models, the closure curve and the equilibrium curve are compared. To make a comparison with the analytical model, the following assumptions are used in the 1-dimensional model:

- A sinusoidal tide is used as boundary condition

- Within the tidal period the geometry of cross sections does not change

- A constant concentration of 0.0002 is present in the water

- The cross section is for every section the same.

Points at the closure and equilibrium curve are determined for flow surfaces of: $9m^2$, $13m^2$, $20m^2$, $24m^2$, $35m^2$, $50m^2$, $100m^2$, $200m^2$ and $400m^2$. In figure 5.7 the curves of the different models are shown. The pictures below show that the flow velocities, calculated with the 1-dimensional model, are a bit lower for low small closure gap sizes. While for larger closure gap sizes, the flow velocities become a bit larger. This difference is caused by two processes. The first process is that in the model the maximum flow during a tidal period becomes critical for closure gap sizes smaller than $75m^2$. The second difference is that the 1-dimensional model takes into account more in and outflow losses, while the analytical solution only takes the friction of the bed and the banks into account. The in- and outflow losses become larger when the flow through the gap is larger. An other difference in the behaviour is observed when the dam is closed vertical. For closure gaps smaller than of $100m^2$, the sill is higher than the lowest water level. This implies that the dam is closed at that moment. So the curve could not be finished and is therefore not given in figure 5.7. The differences that are visible can be explained by the physical limitations of the analytical model. The flatter curve as can be seen in the right graph of figure 5.7 is a result of the critical flow and the extra friction that is taken into account in the 1-dimensional model.
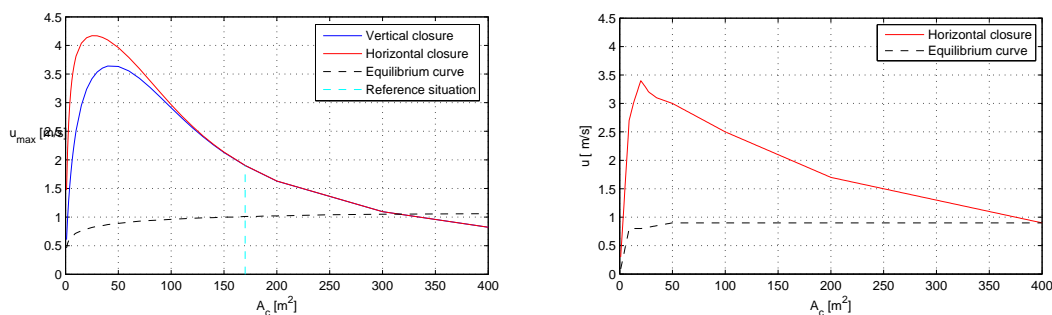
Figure 5.7: The closure and equilibrium curves of the analytical model (left) and 1-dimensional model (right)

5.7 Conclusions

This chapter presents a 1-dimensional model to calculate the sand losses. The behaviour of the model shows good results in the comparison with the analytical solution of chapter 4. The 1-dimensional model is used in the following chapter to quantify the sand losses. In order to interpret the results one has to keep in mind the simplifications of the model:

- The 2- and 3-dimensional effects are kept out of the model.

- The discharge of supercritical flows are treated according a theory of Hager, which is made for rectangular weirs, while the geometry of a closure gap has the shape of a trapezium or a triangle.

- The energy losses of the flow model are based on pipeline flows. This could cause some errors in the calculation of the flow velocities.

- During horizontal production, the slope of the banks remains the same, while in practice this is not necessarily the case. The slopes of the banks only change when the bed level changes.

Chapter 6

Calibration and sensitivity analysis

For the calibration, the case of the closure of the 'Compartimenteringsdam' at 'Maasvlakte 2' is used. This closure is described in appendix C. The calibration is done in two steps: the calibration of the flow through the closure gap and the calibration of the sand losses. Subsequently a sensitivity analysis is performed to verify the sensitivity in behaviour of the model. Finally a comparison with the calculation method of the CUR 157 is presented.

6.1   Calibration flow model

The flow through the closure gap is calibrated using the water level at the basin. This water level changes due to the in and outflow of the water through the closure gap. To perform a calibration, the geometry of the closure gap needs to be simulated over time, based on the real situation. To accomplish this, the geometry of the closure gap is determined over time using survey data of the closure. Drawings of the surveys data are given in appendix C. The geometry of the closure gap in the period between two survey drawings is interpolated linearly. By doing this, the construction of the closure is simulated.

The flow is calibrated by adapting the resistance over the closure gap. As presented in chapter 5, the losses consist of losses due to contraction during inflow, outflow losses and friction losses. For the calibration, only the friction losses are changed. The rest is kept as found in literature [Battjes,2002a]. The calculated water levels have an optimal fit to the measured water levels when the friction term, $\xi_{friction}$, is two times as large than calculated with the values according to literature. The result of the measured and calculated water levels is shown in figure 6.1.

Note that the outside water level shows fluctuations when the water levels are low. From an analysis of PUMA can be concluded that this is not caused by the change of the storage surface of the basin during closure. The fluctuations occurred also before the closure started [PUMA,2012]. The actual reason is not known in this case. What can be seen is that in the final phase the fluctuations don't have influence on the water levels in the basin.
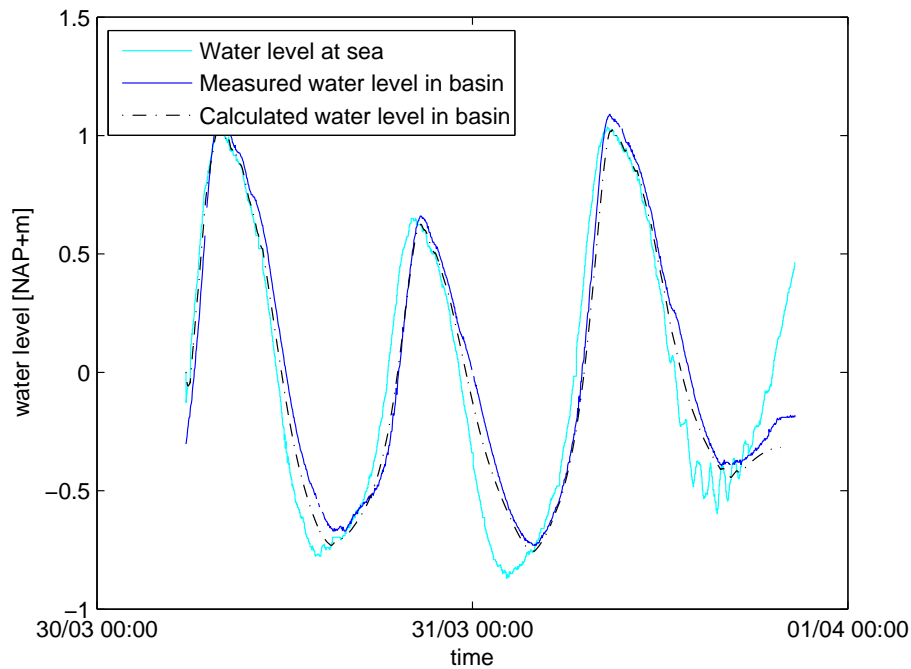
Figure 6.1: The measured and calculated water levels in the basin

6.1.1   Calibration sand loss model

To calibrate the calculated sand losses, first the sand losses which occurred in practice are determined. The sand losses at the 'Compartimenteringsdam' can be calculated from the bed levels of the survey data. The bed level is measured using a single beam echo sounder. The distance between two sailing lines of the survey boat is about $20m$, which is quite large for the amount of bed changes [PUMA,2012]. This causes errors of a couple of $1000m^3$. The dam is closed around 20:00h. The final survey before closure is performed in the morning of the same day. This was at 09:30h. Directly after closure, a survey is done only at the dam. From the difference between the two surveys, the amount of sand in the dam can be calculated. This is shown in a difference plot in figure 6.2. To calculate the sand losses, the production has to be compared with the amount of sand in the dam. The total production between 9:30h and closure is presented in table 6.1.

Ship	Time	average production	total production
Utrecht*	12:27h - 13:28h	$10296m^3/h$	$10458m^3$
Prins der Nederlanden	11:55h - 13:10h	$10548m^3/h$	$12290m^3$
Prins der Nederlanden	15:30h - 16:35h	$10800m^3/h$	$11793m^3$
Prins der Nederlanden	18:55h - 20:20h	$10656m^3/h$	$12417m^3$
		Total**	$36500m^3$

The hopper load of the Utrecht is deposed on the fore shore and does not contribute directly to the closure.
** The hopper load of the Utrecht is not taken into account for the total production.*

Table 6.1: The productions during the final day before closure.
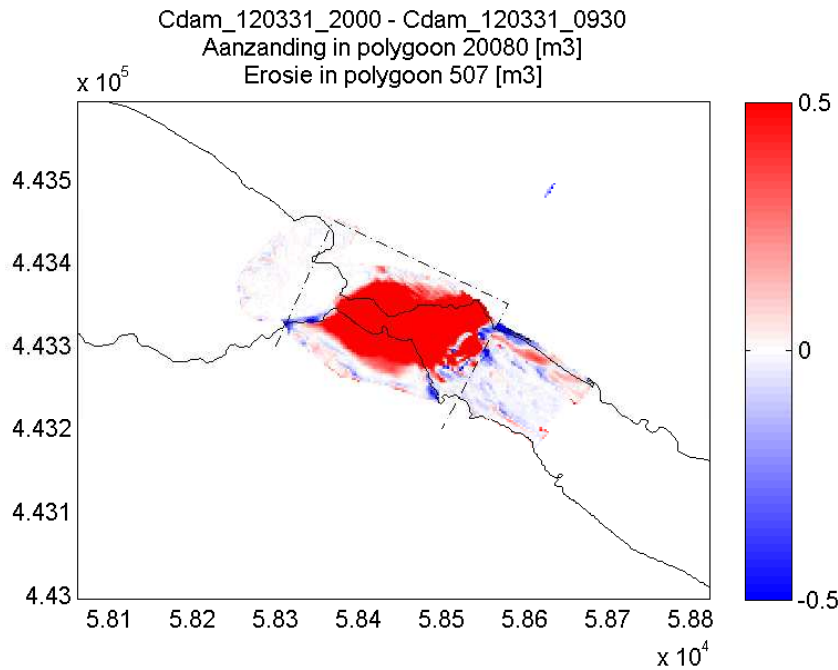
Figure 6.2: Difference plot between the morning before closure and directly after closure. The survey after closure is measured using a multibeam measurement

The total amount of sand brought in the dam during the final day is $36500m^3$. According to the survey results, the net amount of sand which is brought in the body of the dam is about $20000m^3$, see figure 6.2. This means there is a sand loss of $16500m^3$ over the final day. Because this amount is determined on basis of the survey results, this is the in situ amount of cubic meters.

As can be seen from the measured water levels, presented in figure 6.1, the direction of the flow changes around 17:00h. This causes an inflow for the final three hours of the closure. From the survey drawings can be seen that an amount of $4164m^3$ of sand is transported into the basin (figure 6.3). An amount of $1666m^3$ is lost from the basin, so the net loss from the dam towards the basin is about $2500m^3$ of sand. This results in a loss towards the sea side of the dam of $14000m^3$.
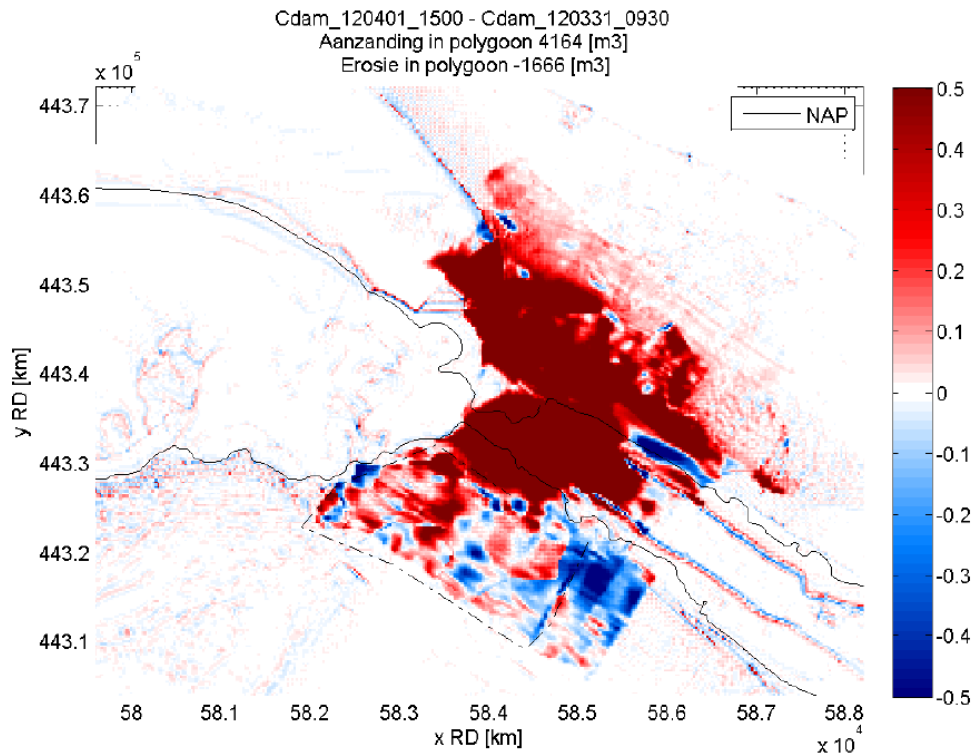
Figure 6.3: Difference plot between the morning before closure and the afternoon of the day after closure. [PUMA,2012]

Calibration sand loss model

From the available data, two checks are available to verify if the model calculates the sand losses over time correctly. The checks are the amount of sand that is lost and the closure time. Below, first the principles of the calibration are treated, followed by the boundary conditions used in the calibration and finally the results of the calibration are presented.

Principles of the calibration

For the calibration run, the following data is used as starting point to calculate the sand losses:

- The run starts at 09:30h on March 31th.

- The production from the pipeline is taken continuous and starts at 11:55h, when the 'Prins der Nederlanden' connects to the pipeline for the first time. The total production between 11:55h and 20:15h is $36500m^3$. This makes the average production $1.22m^3/s$.

- The geometry of the closure gap at the start of the simulation is:

  - Width of the bed: $100m$
  - Left slope: $1:7$
  - Right slope: $1:11$
  - Height of the sill: $1.5m$

- – Length: $150m$

- The crest level of the dam is set at NAP+1.5m.

- The data of the bed properties is given by:

  - – $D_{15} = 250\mu m$
  - – $D_{50} = 380\mu m$
  - – $D_{90} = 700\mu m$
  - – $n_0 = 0.4$
  - – $\phi = 30^o$

- The closure gap is divided in 8 sections.

- The time step is 2 seconds.

  - – The length of a section becomes $\frac{150m}{8} = 18.75m$
  - – The numerical system is stable for velocities up to $\frac{\Delta x}{\Delta t} = \frac{18.75m}{2s} = 9.3m/s$. For this velocity the Courant number is equal to 1, which means that the model is stable, see chapter 5.

- The horizontal closure is executed over two sections (section 4 and 5)

Boundary conditions

The following boundary conditions are present at the 'Compartimenteringsdam' of 'Maasvlakte 2'.

- The outside water level is measured behind the hard seawall, opposite of the closure gap. This water level is used as the forcing of the system. The water levels are shown in figure 6.1.

- The size of the basin is 260 hectare.

The calibration parameters

For the calibration is chosen to only vary the morphological roughness, $k_{s_{morph}}$. Other parameters which can be used for the calibration are the permeability and the porosity of the just settled sand. An other parameter which can be changed is a local increased friction at the banks during horizontal closure to take the losses caused by the vortex street into account. For the calibration only the morphological roughness is changed. This is done because, when the roughness is enlarged a lot, it still has a physical meaning (it indicates the presence of ripples in the bed). This while the porosity and permeability are physically bounded and therefore not totally suitable to do the calibration. Thereby the permeability and the porosity are used as input variables for other cases using other bed properties. The influence of these parameters are evaluated in the sensitivity analysis.

Closure criterion

The dam is considered to be closed when the flow is blocked by one of the sections. This means that the sill of the dam reaches the water level. This can be reached when sand settles (due to production or due to a high concentration) or by horizontal production. It is assumed that when the dam is closed during low water, the dam is raised faster than the water level raises.

Result

The initial situation with a morphological roughness provides a good amount of sand losses, but the dam is closed earlier than in practice. The results of the calibration are presented in table 6.2. Based on the sand losses, the morphological roughness should be $2.1mm$ ($3 \cdot D_{90} = 3 \cdot 700 \mu m$) and the initial situation should be used. When the model is calibrated using the closure time, the best result is provided when the morphological roughness is multiplied with 2.5. This results in a roughness of $5250 \mu m = 5.2mm$.

$k_{s,morph}$	**Sand losses in the sea**	**Sand losses in the basin**	**Closure time**
Practice	$14000m^3$	$2500m^3$	$\pm \, 20 : 00h$
$2100 \mu m$ (initial)	$17000m^3$	$500m^3$	$\pm \, 18 : 00h$
$4200 \mu m$	$22000m^3$	$3500m^3$	$\pm \, 19 : 00h$
$5250 \mu m$	$25000m^3$	$4000m^3$	$\pm \, 19 : 30h$
$6300 \mu m$	$25000m^3$	$4000m^3$	No closure

Table 6.2: The results of the calibration of the model

The larger sand losses don't necessarily have to be wrong. The surveys are performed using single beam measurements. The error of the measured sand loss is of the order of a couple of thousand cubic meters. In that case, the calculated sand losses in the basin are within the margin of the measurements. At the sea side, the Utrecht has deposited a hopper load of sand at the fore shore. This did not contribute directly to the closure, but it increased the length of the dam. When half of the load of the Utrecht lands in the dam area (shown in figure 6.2), the error of the sand losses in the sea is only $5000m^3$. This would also be within the error margin of the measurements.

Behaviour of the model

To analyse what happens during closure, the development of the water levels in the basin and at sea, the flow velocities, the closure gap development and the concentrations of sand in the water are plotted. They are shown in figure 6.4 till 6.10.

In figure 6.4 the water levels are plotted. As can be seen, between 09:30h till about 15:30h the water level in the basin is larger. So the flow is towards the sea and the sand losses in this period are towards the sea as well. From 15:30h till 17:00h, the in and outflow alternates and from 17:00h till closure, the water flows into the basin. This can be seen in figure 6.5, where the flow velocities are plotted during closure in section, 2, 5 and 8. Section 5 is where the horizontal closure takes place. Section 2 is on the sea side and section 8 is the final section on the basin side.
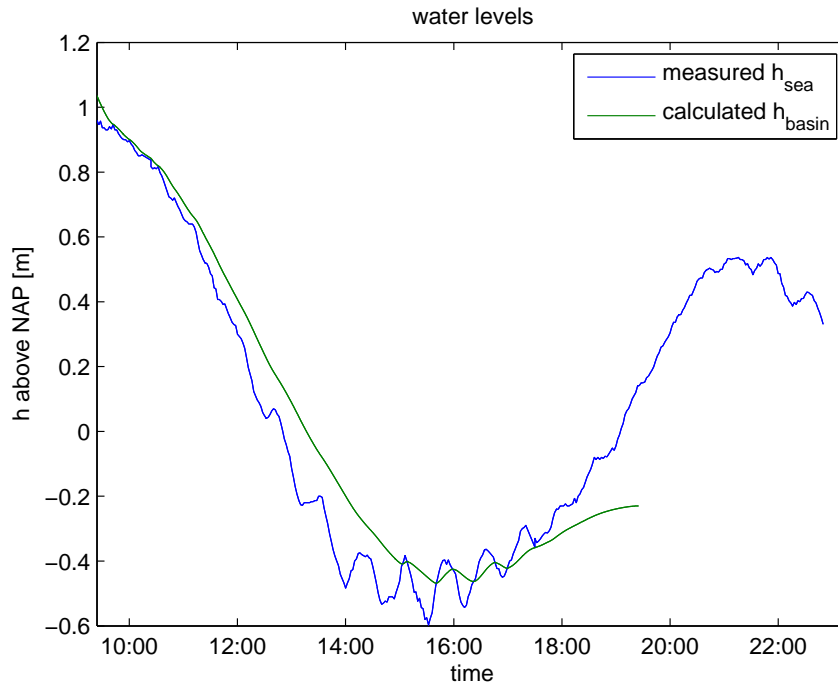
Figure 6.4: The water levels during the horizontal closure

The flow velocities are plotted in figure 6.5. From 12:00h, the production starts. From this moment the flow surface of section 5 is reduced by horizontal closure. The reduction of the closure gap size becomes noticeable from 15:00h. From that moment the flow velocities in section 5 become the largest.
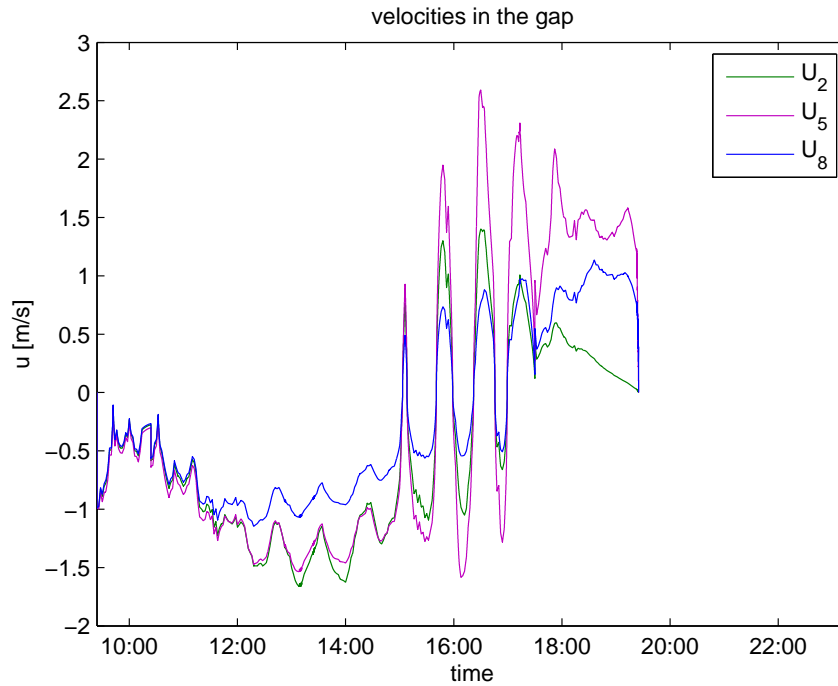
Figure 6.5: The flow velocities during closure (positive = flow towards the basin)

The flow velocities have a direct consequence for the erosion and sedimentation. Figure 6.6 shows the bed velocities. A positive bed velocity means erosion and a negative velocity represents sedimentation. The sedimentation becomes large when the concentration of sand in the water column is large. This can be seen from the formulation of the sedimentation and erosion rate, shown in chapter 3.
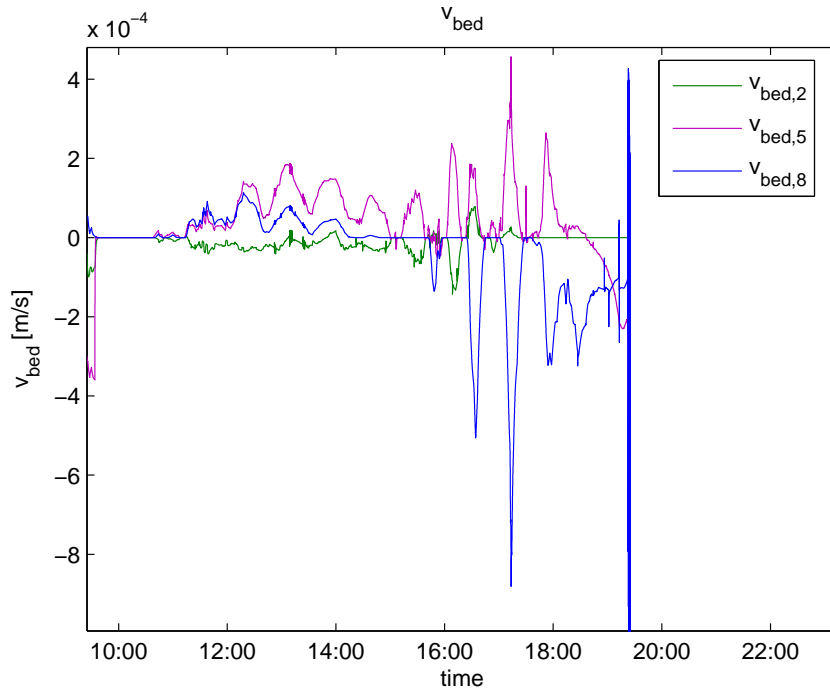
Figure 6.6: The bed velocities during closure (positive = erosion)
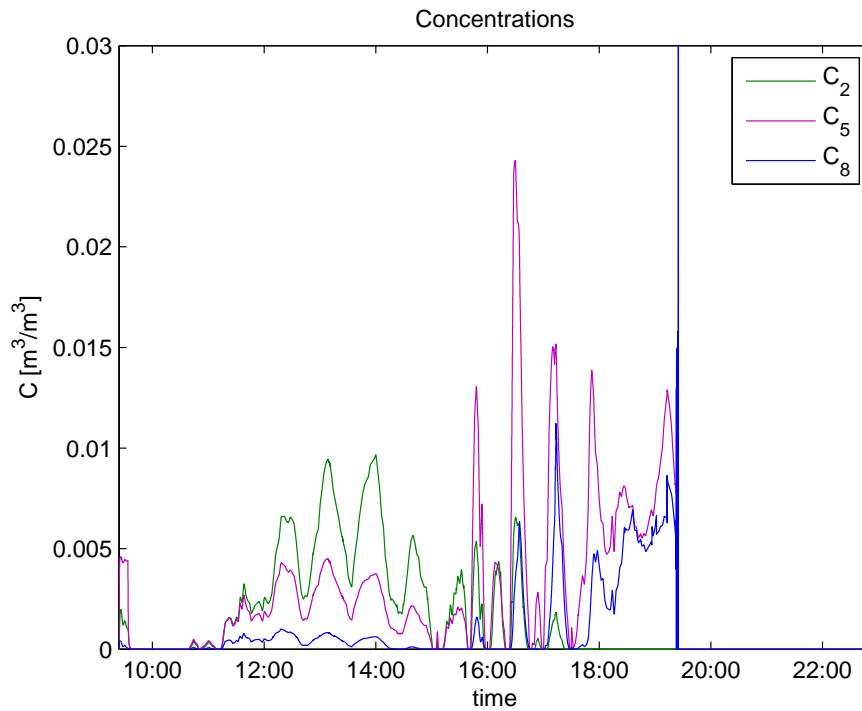
Figure 6.7: The concentrations of sand in the water (the blue peak is at closure (a concentration above 0.8, which means the dam is closed)

Figure 6.7 shows the concentrations of sand in the water column. Figure 6.6 shows that

between 16:00h and 18:30h the bed erodes relative hard. This causes a large concentration of sediment suspended in the water column. This concentration is carried by the water towards the end of the dam. Since the flow velocities in section 8 (and also in section 6 and 7) are much lower than in section 5, a lot of the eroded sand from section 5 settles in sections 6,7 and 8. This can be seen in figure 6.6 that from 17:00h the bed velocity in section 8 is negative(which means sedimentation). This results in an increase of the sill, which can be considered as vertical closure of the gap. This is shown in figure 6.9 and a decrease of the flow area in section 8 is shown in figure 6.8.

Figure 6.8 shows the flow surfaces of the closure gap in time. As shown the flow surfaces decrease from the start of the closure till 16:00h. This is the consequence of the lower water level at sea, which decreases also the water level in the closure gap. In section 2, the water level increases again after 16:00h, while there is not a lot of erosion (see figure 6.6 at that time). So this increase is due to the rise of the water level at sea. The decrease in section 5 is a consequence of the production and the decrease of the flow surface in section 8 is due to the sand that settles. This sand originates from sections upstream of section 8. The main sources for this sand are section 4 and 5, where the production takes place and the erosion is the largest.
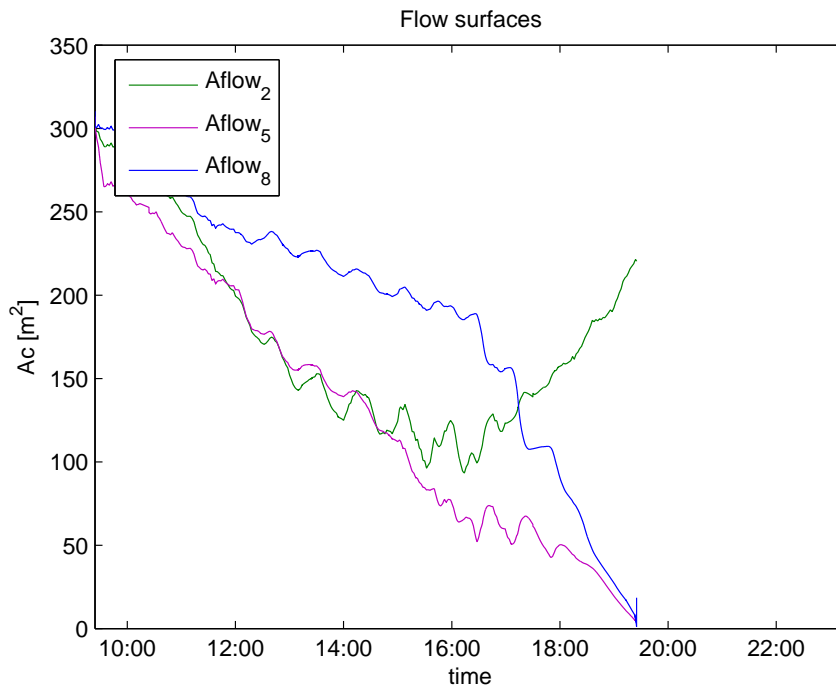
Figure 6.8: The flow surfaces during closure
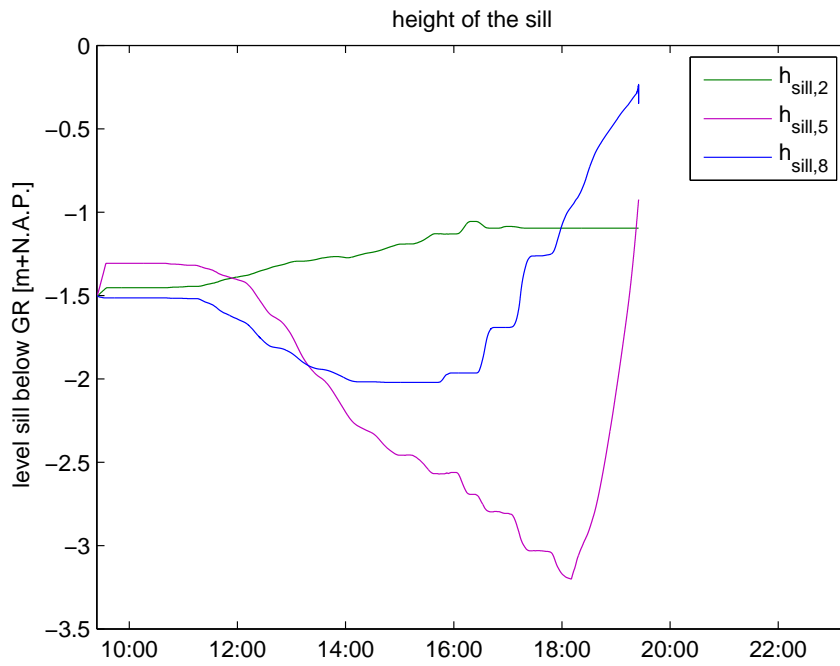
Figure 6.9: The height of the sill during closure
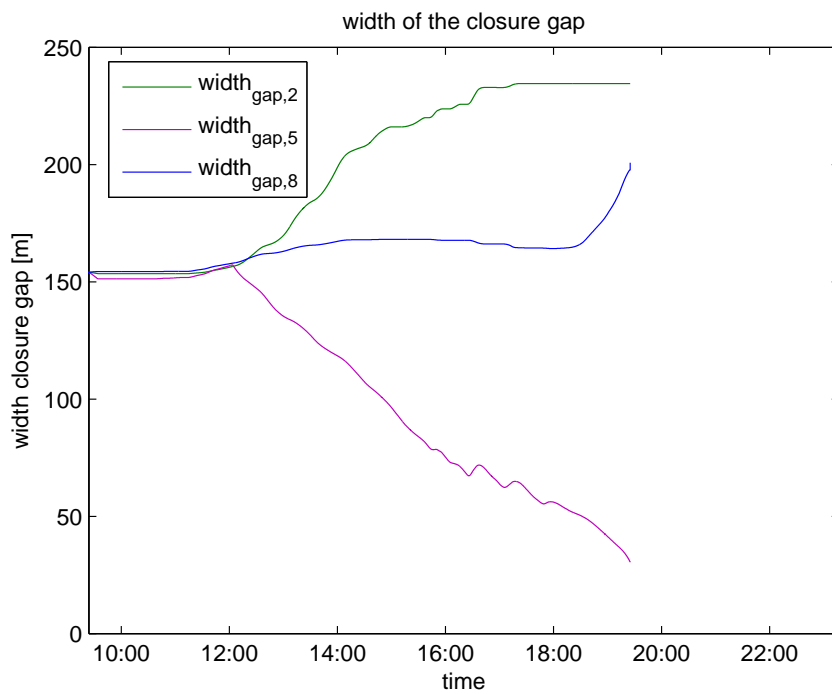
Figure 6.10: The width of the sections during closure

Figure 6.10 shows the width of the three sections. As can be seen, from 12:00h the production

reduces the width of the gap in section 5. At the rest of the sections, the width increases due to erosion.

The sand losses are determined by the discharge and the concentration of the sand in the water level. When the discharge is positive (flow towards the basin), the sand loss is towards the basin. Logically when the discharge is negative, the sand loss is towards the sea. This is shown in figure 6.11. On the left hand panel the sand losses over time are presented. The right hand panel shows the cumulative sand losses over the the simulation time.
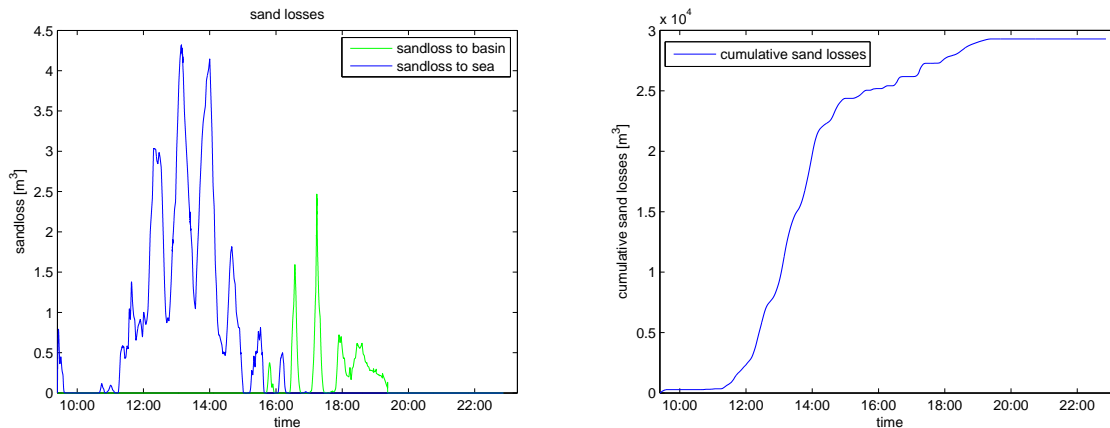
Figure 6.11: The left hand panel shows the sand losses over time. The right hand panel shows the cumulative sand losses during the simulation

Numerical errors

The large concentration at the end of the simulation (figure 6.7) is a consequence of the small flow area and erosion that takes place, (which is the case right before closure). When the flow areas become too small the model can behave a little strange. In this run, that is shown by the high concentrations and the bed velocities at closure. Since this only happens at the moment of closure, this has not much effect on the final result: the sand losses.

An other error in the model is that the flow remains sub critical. In practice the flow was critical at section 4 and 5. As in chapter 5 is presented, the discharge is calculated using the velocity in section 8. When the flow surface of section 5 is much smaller, the flow velocity is larger and can become critical in the final phase of the closure. In the 1-dimensional model, the flow surface in section 8 is not much larger in the critical phase of the closure. The differences becomes smaller when the closure comes closer (see figure 6.8). Higher flow velocities cause larger erosion rates. If the erosion is too low in this case, this has to be corrected with a calibration.

Moment of closure

Figure 6.12 shows a cross section over the length of the dam at the moment of closure. It is clearly visible that the dam is closed in section 8, downstream of the horizontal closure. In practice the dam was closed at section 4 and 5, where the end of the pipeline was located and the horizontal closure was performed. The fact that the dam is closed downstream of the location where the actual horizontal closure takes place can be explained as a shortcoming of the 1-dimensional approach.

In practice a jet is flowing out of the gap where the production takes place (as described in chapter 2). This jet causes erosion and a channel arises at the cross sections downstream of the sections where the horizontal closure takes place. At the 'sheltered' area behind the dam a sort of a flood plain can arise. However, this one dimensional model can not take flow differences within a cross section into account; the flow is the same over the whole cross section. Because the flow area is larger downstream of the horizontal closure sections, the flow velocity is lower. Since the concentration is large (because the flow velocities are large in section 4 and 5 and thereby the erosion as well, see figure 6.5 and 6.6) and the velocity is low, a lot of sand settles. From figure 6.9, 6.10 and 6.12, can be concluded that the model closes the dam using a vertical closure in section 8. When the moment of closure is reached, the flow surface is also small in the final section. But since a vertical closure is performed more easily than a horizontal closure, will the dam be closed more easy in the section where the gap is wider and shallower.
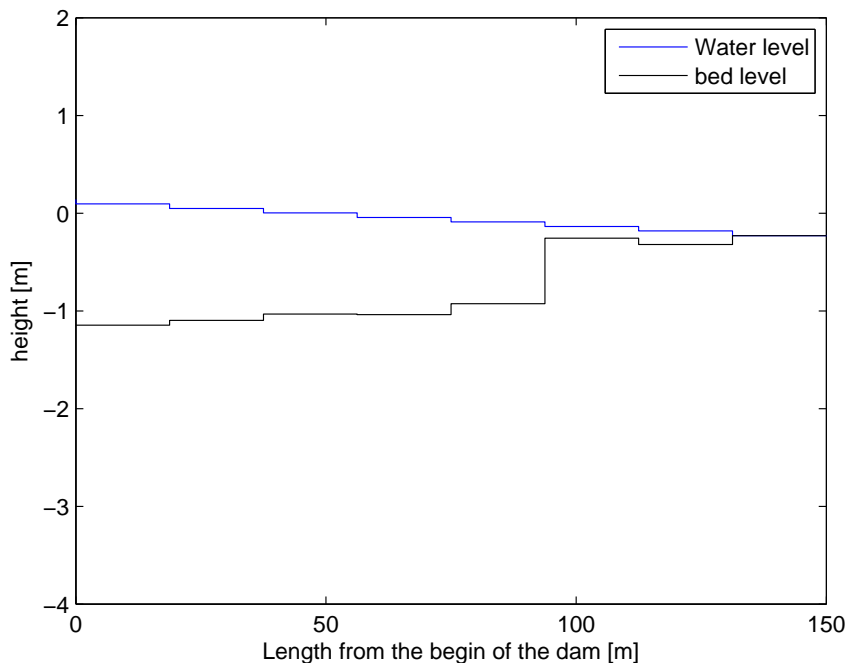
Figure 6.12: Longitudinal cross section of the dam at closure. The left side is the sea side and the right side is the basin side.

6.2   Sensitivity analysis

For the input of the model, assumptions are made for different parameters. Whether the outcome of the model is sensitive for these assumptions is verified in this section. The following properties of the bed are investigated:

- Porosity

- Permeability

- Grain size

Besides these bed properties, the possibility to take into account the vortex street is investigated. This is done by a local increase of the friction on the bank during horizontal closure. Thereafter the input of the geometry is verified together with differences in the production. The results are presented below.

Porosity

A higher porosity means that the soil is packed more loosely. This results in a higher value of the erosion according to the Van Rhee formulation. Also the permeability becomes larger, which also leads to more erosion. On the other hand, with a more loosely packed dam, less sand is needed to fill a certain amount of volume. A porosity of 0.4 is generally used for settled sand under water. According to the CUR 152, Artificial build sand bodies in water, the porosity of just produced sand is between 0.45 and 0.49 [CUR152]. Table 6.3 shows the results for different values of the porosity. As can be seen in the table, the sand losses are larger when a higher porosity is used. The influence on the closure time is almost nothing. In chapter 4 is shown that the porosity has a large influence and a more sand losses are expected when the porosity is larger. The influence on the sand losses can be seen. The fact that the closure time remains the almost the same, can be explained by the fact that less sand is necessary to fill the body of the dam.

Porosity	Sand losses in the sea	Sand losses in the basin	Closure time
0.4 (initial)	$25000m^3$	$4000m^3$	$\pm\ 19:30h$
0.45	$25000m^3$	$5200m^3$	$\pm\ 19:30h$
0.49	$27000m^3$	$5000m^3$	$\pm\ 19:45h$

Table 6.3: Sensitivity for the porosity

Permeability

As shown in chapter 4, the erosion decreases for a smaller permeability. The permeability depends on the porosity of the bed and the grain size distribution. Table 6.4 shows the results for different permeabilities. The values of the permeability in table 6.4 represent the range of possible permeabilities calculated with the formula shown in equation 3.17 in chapter 3. Within the possible range of permeabilities, the dam is closed earliest at 17:00h and in the most extreme case, no closure is reached before 23:00h. This behaviour is consistent with the analysis in chapter 4, where one of the conclusions was that the erosion is lower for a lower permeability.

Permeability	Sand losses in the sea	Sand losses in the basin	Closure time
$0.0001m/s$	$14000m^3$	$0m^3$	$\pm\ 17:00h$
$0.0007m/s$ (initial)	$25000m^3$	$4000m^3$	$\pm\ 19:30h$
$0.0017m/s$	$29000m^3$	$17000m^3$	No closure

Table 6.4: Sensitivity for the permeability

The median grain diameter

In this analysis the only parameter which is varied is the D_{50}. The D_{15} and the D_{90} remain the same. The influence of the grain size distribution is treated in the sensitivity for the permeability and the calibration by means of the roughness($=3 \cdot D_{90}$). Table 6.5 shows the results for different

median grain sizes. For smaller grain sizes the dam does not close according to the calibrated model. Note that often, for smaller grain sizes, the D_{15} and thereby the permeability becomes smaller, which means less erosion, see also in chapter 4, where the Van Rhee formula is compared with the CUR 157.

Median grain size	Sand losses in the sea	Sand losses in the basin	Closure time
$320\mu m$	$27000m^3$	$12000m^3$	No closure
$380\mu m$ (initial)	$25000m^3$	$4000m^3$	$\pm 19:30h$
$440\mu m$	$20000m^3$	$600m^3$	$\pm 18:00h$

Table 6.5: Sensitivity for the median grain size

Vortex street

In the calculations of the 'CUR 157, Sand Closures', a distinction is made between the main current and the vortex street. The difference is made in the power above the flow velocity in the formulation and in the calibration factor for the cubic loss. In this model the influence of a vortex street can be taken into account by increasing the friction on the banks, which means that more erosion occurs. The influence of the vortex street is investigated using a friction factor. This friction coefficient c_f is multiplied with the friction coefficient. This increased friction should represent the extra turbulence which is present in the vortex street. The friction factor is only applied when the width of the dam at the section where the dam is closed horizontally is smaller than 0.8 times the width of the dam of the section downstream of the horizontal closure. The results are shown in table 6.6. The result is remarkably, because the time till closure becomes less.

Friction factor	Sand losses in the sea	Sand losses in the basin	Closure time
1 (initial)	$23000m^3$	$4000m^3$	$\pm 19:30h$
2	$25000m^3$	$4500m^3$	$\pm 19:15h$
3	$25000m^3$	$4000m^3$	$\pm 19:00h$
4	$25000m^3$	$1400m^3$	$\pm 17:30h$

Table 6.6: Sensitivity for the friction of the vortex street

The influence of the increased friction on the banks leads to a wider closure gap in section 4 an 5 (where the horizontal closure takes place). Because the decrease of the gap is less (due to the higher erosion), the flow velocities are smaller as well. Besides the lower velocity, the eroded sand from the banks is suspended in the water column. This increases the concentration of sand in the water. The increased concentration and lower velocities lead to less erosion on the bed and a larger concentration in the sections downstream of the closure gap. The closure gap is closed in the sections behind the horizontal closure again, as we have seen in the calibration.

Input

As input, the width of the bed, the crest height above NAP, the height of the sill and the production can be varied. The sensitivity of those parameters on the sand losses in the model is analysed below.

Production

The results for different productions are shown in table 6.7. The influence is the largest on the closure time. As the results show, closure is at 23:00h for a production of $0.8m^3/s$ and there is a large difference between continuous production and discontinuous. When the closure gap becomes small and the production stops, a lot of erosion is observed. All the sand that erodes has to be added extra to the system on a later time step. The larger the time of no between the productions is, the more sand erodes. At the 'Compartimenteringsdam', the time was over 2 hours (see figure 6.13), because a hopper had a breakdown.

Production	Sand losses in the sea	Sand losses in the basin	Closure time
$0.8m^3/s$	$25000m^3$	$12000m^3$	$\pm\, 23:00h$
$1.22m^3/s$ (initial)	$25000m^3$	$4000m^3$	$\pm\, 19:30h$
$2m^3/s$	$24000m^3$	$0m^3$	$\pm\, 15:30h$
Discontinuous	$23000m^3$	$20000m^3$	$\pm\, 22:00h$

Table 6.7: Sensitivity for the production of a closure dam

The discontinuous production is shown in figure 6.13. This is the production in cubic meters of sand. For this case, the assumption is made that the mixture contains 60% of sand, so the discharge of the mixture is larger. The production after 20:00 (the closure in real life) is assumed to be the same as was just before the closure to verify how much longer it takes before the dam is closed when the simulation is not able to close the dam within the time it took in practice.
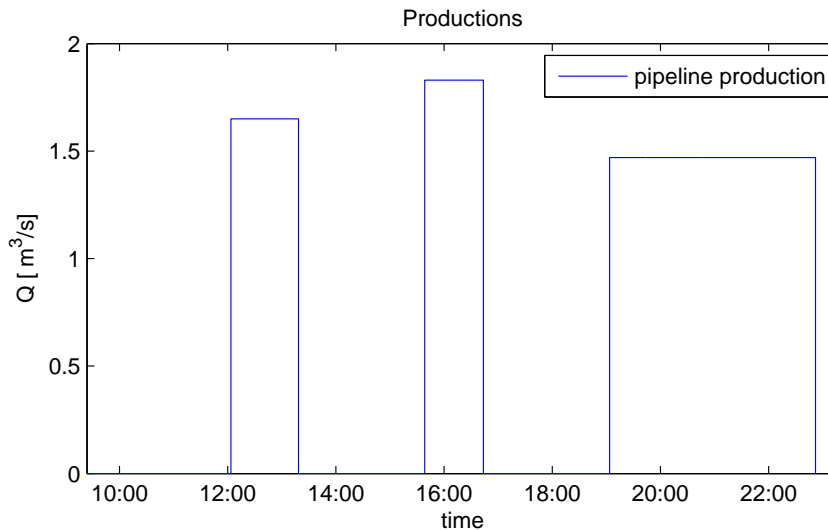
Figure 6.13: The sand productions over time as at the 'Compartimenteringsdam' of 'Maasvlakte 2'.

Height of the sill

Table 6.8 shows the results for different heights of the sill before the horizontal phase of the closure starts. As can be seen, the closure times are directly correlated with the height of the sill. For a lower sill (1.8m below N.A.P.), the erosion in the first phase of the closure is lower. The reason for this, is a larger flow surfaces and thus lower flow velocities. The closure time is

later, because more sand is needed. For a higher sill ($1.2m$), the dam is closed earlier and the total sand losses are lower as well.

Level of the sill below NAP	Sand losses in the sea	Sand losses in the basin	Closure time
$1.2m$	$21000m^3$	$0m^3$	$\pm\,15:30h$
$1.5m$ (initial)	$25000m^3$	$4000m^3$	$\pm\,19:30h$
$1.8m$	$16000m^3$	$14000m^3$	$\pm\,22:00h$

Table 6.8: Sensitivity for the height of the sill

Width of the dam

For a smaller width of the dam, the flow velocities are larger and the erosion in the first phase is much larger than for a situation with a wider gap. Because a lot of sand is lost in the first phase, more sand is needed in a later stage. This leads to a later closure time and more sand losses. This makes clear that the model is very sensitive to the geometry of the gap and thereby the moment of production. For a larger width, it is clear that the losses in the first phase are smaller, but in the final phase the behaviour of the model is the same as when the initial width is ($100m$) is used as input.

Width	Sand losses in the sea	Sand losses in the basin	Closure time
$80m$	$33000m^3$	$5800m^3$	$\pm\,20:00h$
$100m$ (initial)	$25000m^3$	$4000m^3$	$\pm\,19:30h$
$120m$	$20000m^3$	$4000m^3$	$\pm\,22:00h$

Table 6.9: Sensitivity for the width of the closure gap

Crest height

The results for different crest heights is shown in table 6.10. A lower crest means that the horizontal extension of the banks during production is larger, but the amount of sand that erodes if the bank retreats is lower. The lower amount of sand that erodes, causes lower concentrations of sediment suspended in the water column. As the results show, higher crests cause less losses in the first phase, but in the end, the time till closure is longer.

Crest height	Sand losses in the sea	Sand losses in the basin	Closure time
$1.2m$	$30000m^3$	$250m^3$	$\pm\,18:00h$
$1.5m$ (initial)	$25000m^3$	$4000m^3$	$\pm\,19:30h$
$1.8m$	$17000m^3$	$8800m^3$	$\pm\,20:30h$

Table 6.10: Sensitivity for the height of the crest of the dam

6.3   Comparison with the CUR 157

The results of the 1-dimensional model is compared with the results of the calculation method of the CUR 157. In chapter 2 the results of two calibrations are described. One calibration is made by the CUR 157 and one by PUMA. To compare the 1-dimensional model with the CUR 157, simulations are done with both calibration parameters.

The result is presented, using the cumulative sand losses from the start of the simulation. Figure 6.14 shows the results of the different simulations. For all simulations the same flow model is used.
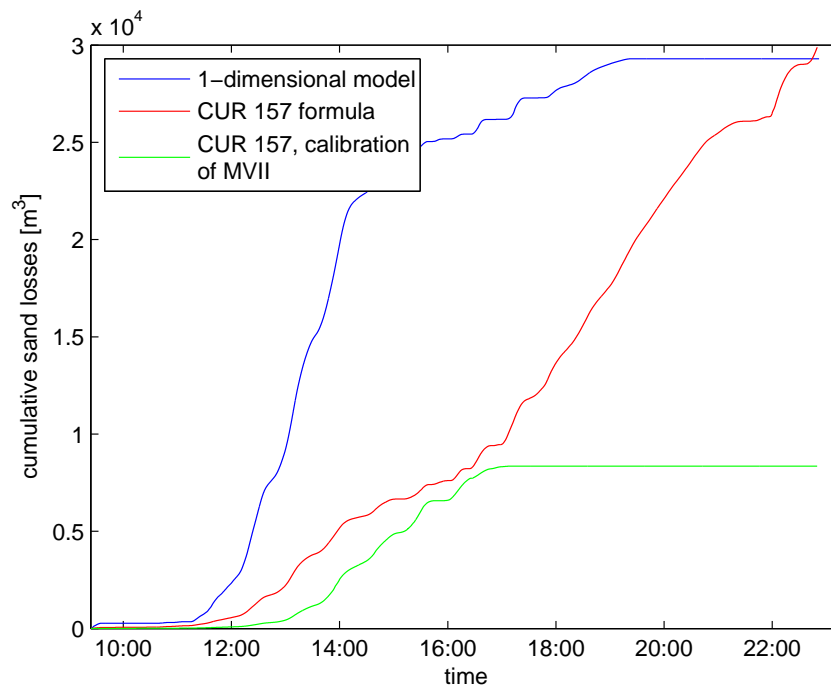
Figure 6.14: The cumulative sand losses for different calculation techniques

The calibration of the 'Maasvlakte 2' results in much lower sand losses. This is strange since this calibration is performed on the closure of the 'compartimenteringsdam'. After investigation of the used data, is found that in that this calibration is based on a production of 2 hopper loads, while the actual production consists of three hopper loads. This causes an error of about $10000m^3$. Further can be concluded that the sand losses using the CUR 157 are a bit lower than calculated with the 1 dimensional model. However the model closes the dam, while according to the CUR 157 calculation no closure occurs. That the CUR 157 calculates less erosion seems to be logic, since the flow velocities don't become very large in the first part of the simulation and as shown in chapter 4, the CUR 157 calculates lower erosion rates for velocities lower than $2.9m/s$. The reason that the CUR 157 does not close the dam is because the high erosion rates when the flow surface becomes smaller. This is in agreement with the analysis of chapter 4, that the CUR 157 calculates larger erosion rates at higher flow velocities (which occur in the final phase before closure).

From the results shown in figure 6.14, can be concluded that the 1-dimensional approaches the closure time the best. The sand losses are too large, but when the hopper load of the Utrecht

(see table 6.1) is deposited on the foreshore of the dam, but within the area of the survey drawing at figure 6.2, the sand losses are rather close to the actual sand losses.

6.4 Conclusions

The model is calibrated on the construction of the 'Compartimenteringsdam' at 'Maasvlakte 2'. The optimal fit is found with a morphological roughness of $5.25mm$. The closure time is approached within half an hour. The sand losses are higher than measured from the survey, but they are within the fault margin of the measured sand losses.

A lack of functioning of the model is found because 2-dimensional processes are not taken into account. This is shown in the behaviour of the model. Two numerical errors are present in the model. The strange behaviour of the model at closure has not much influence and the error in the flow model is corrected with a calibration.

The sensitivity analysis shows that the model is very sensitive to different parameters. The grain size and permeability are the most important soil parameters. The vortex street, as used in the CUR, has only a small influence on the sand losses in the model and is therefore kept out of the further investigation. In real life the vortex street contributes significantly to the total sand loss. In the model, a potential error as a result of ignoring the vortex street is corrected with the calibration.

The production is a very important parameter in the determination of the closure time and the sand losses. For higher productions the dam closes easier. The closure time is very sensitive to the continuity of the production. At the 'Compartimenteringsdam', the discontinuous production leads to a closure time, which is 2 hours later than with continuous production and the sand losses are significantly higher.

Chapter 7

Verification on other cases

This chapter tests the model that is calibrated in chapter 6. The 1-dimensional model is tested on three different cases. First the large closure at 'Maasvlakte 2' is used for a verification. This is followed by two cases, which are used in the calibration of the formulas in the CUR 157. The used cases are the closure of 'Tholense Gat' and the final phase of the 'Krammer' closure.

7.1 'Maasvlakte 2'

In chapter 6, the 'Compartimenteringsdam' of 'Maasvlakte 2' is used to calibrate the sand losses. The second dam is used here as a verification case. The dam is closed at July 11$^{\text{th}}$ around 15:15h. First the input for the model run are described, followed by productions and the sand losses that occurred during the closure.

Starting points

The following data is used as input for the model.

- The size of the tidal basin is: $5100000m^2$.

- The tidal forcing is based on measurements of the water level at the outer side of the dam.

- The following soil properties are used in the model run:

  - $D_{15} = 200\mu m$
  - $D_{50} = 380\mu m$
  - $D_{90} = 700\mu m$

- The final phase of the closure is a 2-sided horizontal closure.

- The width of the closure gap at the start of the simulation is: $150m$.

- The length of the sill is $250m$.

- The level of the sill is $1.5m$ below N.A.P.

- The crest level of the dam is at $1.5m$ above N.A.P.

- The dam is divided in 8 sections.

Production

The final phase of the construction is performed with a two sided horizontal closure. On the north side, the Edax (Cutter Suction Dredger) pumped sand in the body of the dam and on the south side, two hoppers take turns and pump sand through a pipeline towards the dam. The productions during the final day of the closure are presented in table 7.1.

Ship	Time	average production	total production	in situ production
Edax	345 min	$2651m^3/h$	$15243m^3$	$14025m^3$
Vox Maxima	09:00h - 10:28h	$9700m^3/h$	$13229m^3$	$12171m^3$
Vox Maxima	14:04h - 15:47h	$13500m^3/h$	$23154m^3$	$21302m^3$
Prins der Nederlanden	16:15h - 17:30h	$1080m^3/h$	$13492m^3$	$14025m^3$
		Total	**$65118m^3$**	**$59954m^3$**

Table 7.1: Productions during construction of the closure at the outer sea wall

Sand losses in practice

The sand losses are calculated from the results of the surveys in the area in front of the dam and in the basin behind the dam. In contrast with the 'Compartimenteringsdam', the surveys are performed, using multi-beam soundings. The final survey before closure was at 09:15 at the day of closure. Six hours later, the dam is closed. After closure, the production continues and the first survey after the closure is at 17:15h.

The net amount of sand that is brought in the dam is shown in figure 7.1 and is equal to: $53242 - 2973 \approx 50000m^3$. The sand loss on the sea side is shown in figure 7.2 and is equal to $11749m^3$. A remarkable erosion gap is found at the sea side of the closure gap. The presence of the gap is kept out of this analysis.
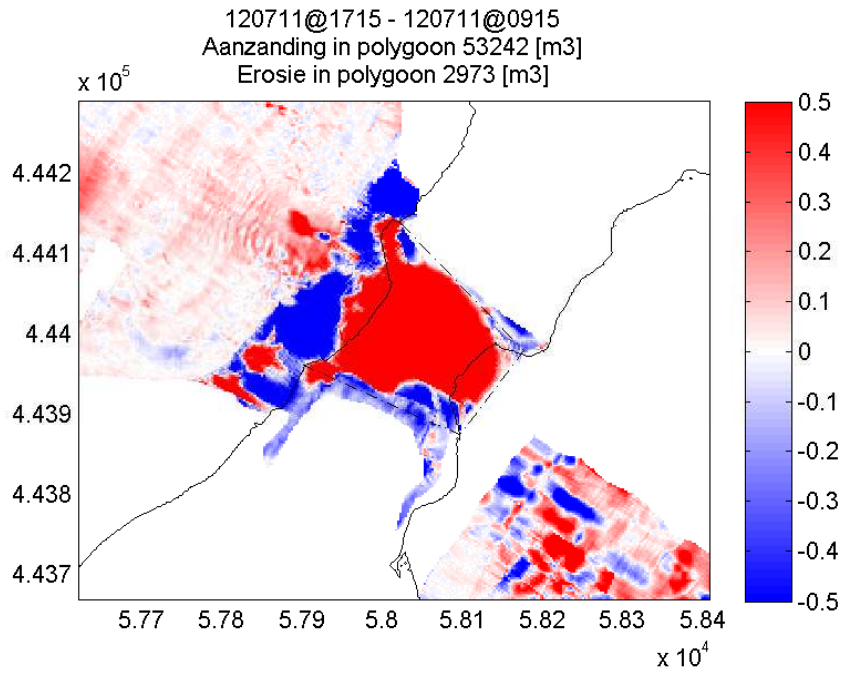
Figure 7.1: Dam area and the change of volume in the dam
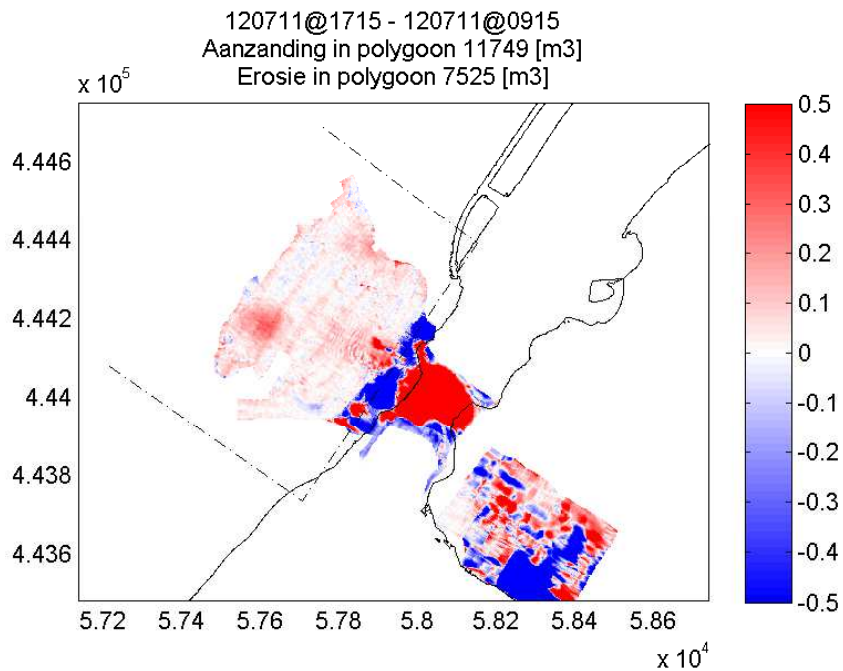
Figure 7.2: Sand deposition off shore

Results of the simulation

During a simulation with the roughness, which is obtained from the calibration in chapter 6, no closure is obtained during the simulation time. To obtain a result, the initial morphological roughness ($2.1mm$) is used. Now the model closes the dam at 15:30h. This is almost the time of the actual closure. However, the calculated erosion is much larger than the actual erosion. The erosion towards the sea is about $60000m^3$, which is six times the amount of sand that is found in front of the dam, based on the difference plot in figure 7.2. The sand loss towards the basin is about $20000m^3$, which makes the total sand loss during the simulation equal to $80000m^3$. This is more than the amount of sand that is produced. This means that a lot of erosion took place at other sections than where the dam is closed.

The cumulative sand losses of the model are presented in figure 7.3. In this figure the sand losses which are calculated with the CUR 157 are drawn as well. This figure shows that the CUR 157 formula calculates lower sand losses, but the dam is closed later when the CUR 157 is used. The total amount of sand losses is calculated correctly with the CUR 157. So in this closure, the CUR 157 achieves a better result than the 1 dimensional model.
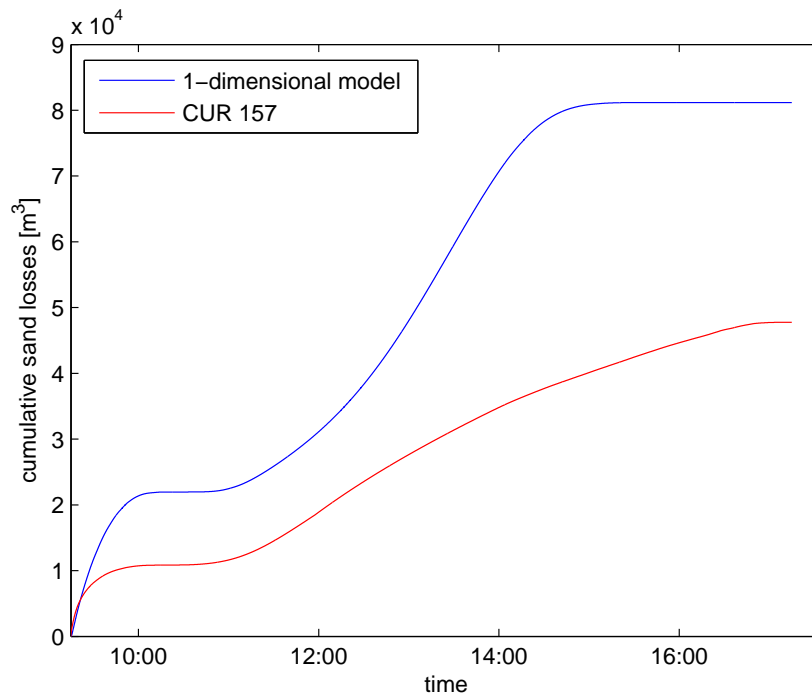
Figure 7.3: The cumulative sand losses, calculated with the 1-dimensional model and the CUR 157

To analyse what happens in the model, the water levels are plotted. As shown in figure 7.4, the water level in the basin is a bit lower than the actual water level. This can be caused by the fact that calculated sand losses are larger than the actual losses. This makes the flow area of the dam larger and more outflow of water is possible, which causes a lower water level in the basin between 11:00h and closure. This water level difference causes lower flow velocities in final part of the closure, because the gradient of the water level over the dam is smaller. The velocities are shown in figure 7.5.
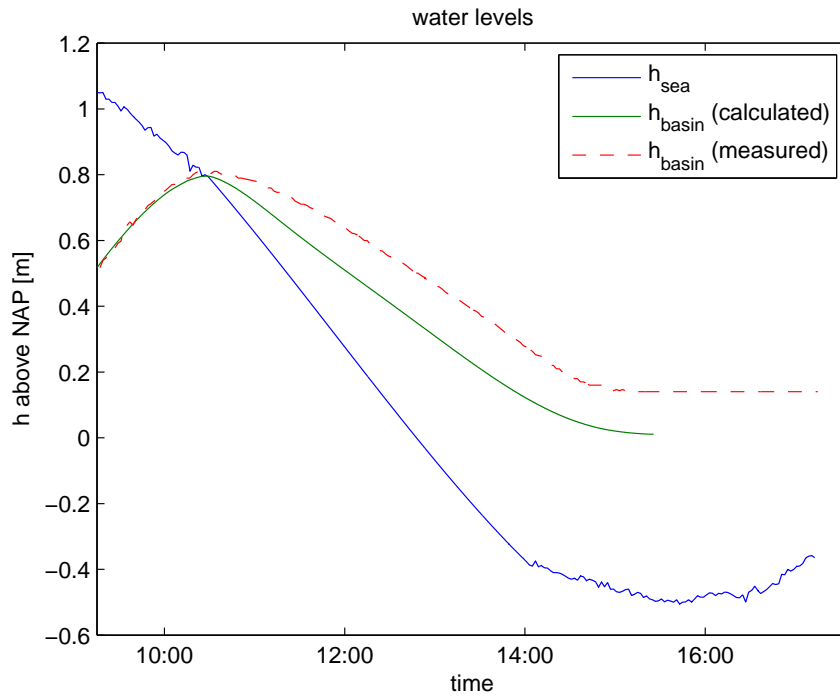
Figure 7.4: The water levels in the simulation of the closure at the outer contour of 'Maasvlakte 2'
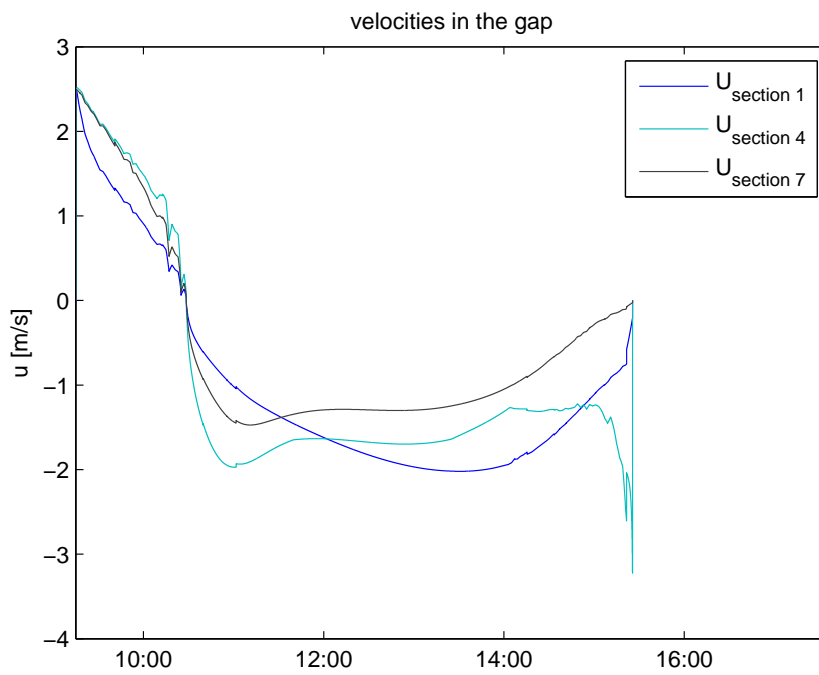
Figure 7.5: The flow velocities in the closure gap (positive = inflow)
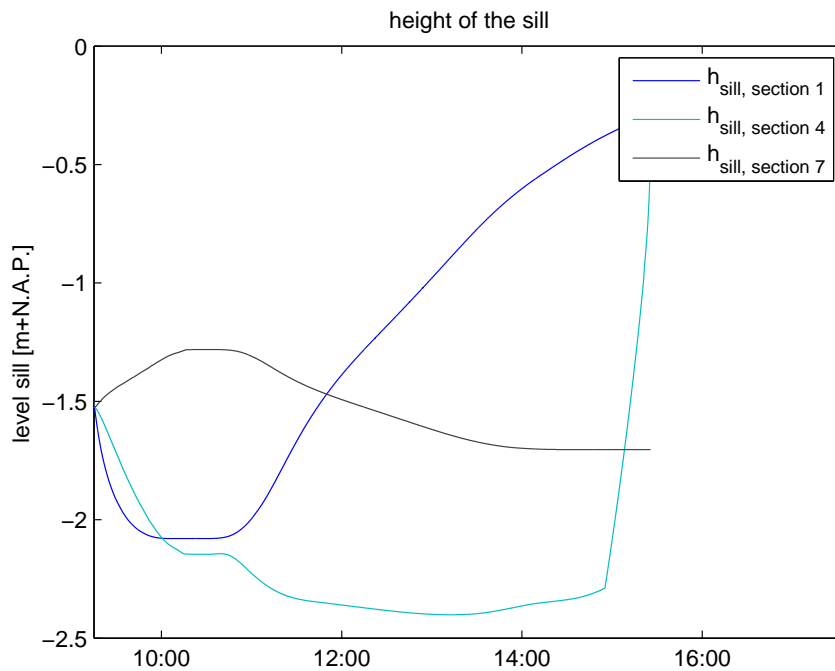
Figure 7.6: The height of the bed level during closure

The development of the closure gap is shown in figure 7.6 and 7.7. From 10:30h the flow is directed towards the sea. From that moment sand settles downstream of the sections where horizontal closure takes place. The gap becomes wider and a vertical closure takes place. This is the same effect as was found during the runs of the calibration in chapter 6. The effect of this increasing sill at the end of the dam is also shown in figure 7.8, where the concentrations in the first section are large and thereby the settlement as well.
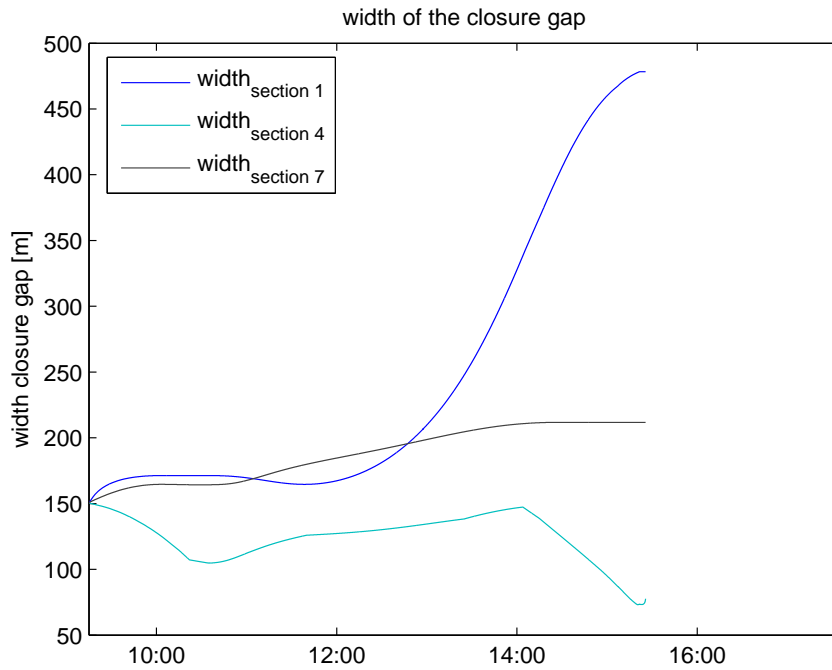
Figure 7.7: The width of the closure gap (at water level) during closure
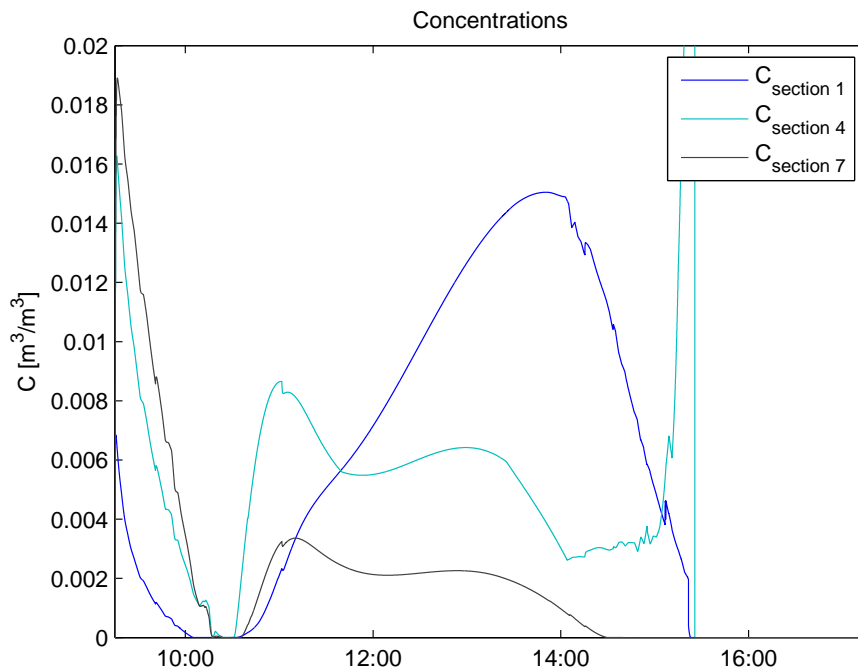
Figure 7.8: The concentrations of sand in the water

The reason for the large differences between this result and the result of the calibration is

because of the large flow velocities. The flow velocities become large because the storage volume of the basin is large and the gradient over the dam becomes larger. This makes clear that the 1-dimensional model is not jet suitable to calculate sand losses for different situations than that of the 'Compartimenteringsdam'.

7.2 'Krammer' part 2 and 'Tholense Gat'

For the 'Krammer and 'Tholense Gat', the closure is performed in two phases. First a sill is constructed. The second phase is a horizontal closure. This section first discusses the available data and subsequently the model runs are described.

Available data

There are a lot of uncertainties in the data of the closures. The CUR 157 presents the data given in table 7.2. To model the sand losses in the final phase of the closure, the water levels have to be known. However, only the flow velocities are known and the water levels are not available.

	'Krammer Dam'	'Tholense Gat'
Closure gap width	$1100m$	$355m$
Height of the sill	$8m$	$5m$
Closure gap area	$5580m^2$	$1350m^2$
type of closure	2-sided horizontal	2-sided horizontal
Mean production	$14700m^3/h$	$5300m^3/h$
Dam volume direct after construction	$1840000m^3$	$280000m^3$
duration of closure	6.5 days	3.2 days
Grain size	$180/200\mu m$	$160/180\mu m$

Table 7.2: The data of the horizontal phase of the 'Krammer' closure and the 'Tholense Gat' [CUR157]

Water levels

To simulate the flow velocities, a sinusoidal tide is imposed to the model. Since both 'Krammer' as well as 'Tholense Gat' are partial closures, there is not a storage volume where the water level is only influenced by the flow through the closure gap. To simulate the flow, the water level in the 'basin' is taken to be zero all the time in the model. Off course an error is made in this assumption, but with the available data, this approach provides acceptable flow velocities. The results of the measurements for the 'Krammer' dam at the day of the closure are shown in figure 7.9. The flow is measured in front of the closure gap. Figure 7.10 shows the calculated flow velocities in the closure gap. Note that in figure 7.9 the inward directed flow ('vloed') is at the negative side of the y-axis, so the two pictures are mirrored over the y-axis.
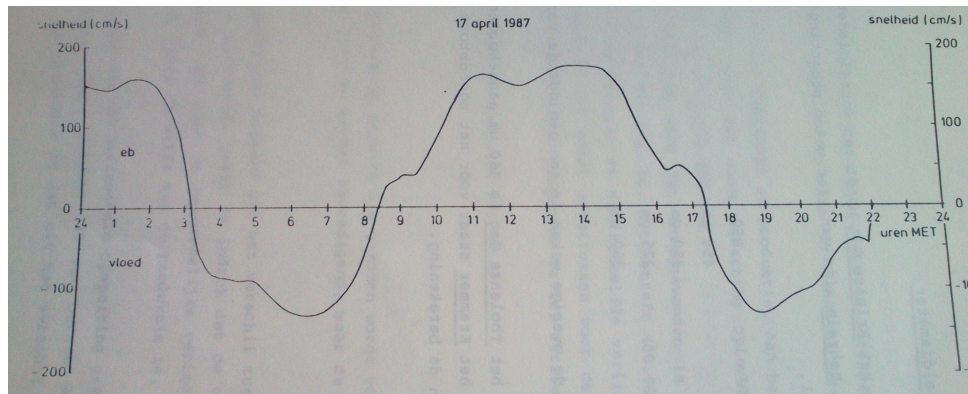
Figure 7.9: The flow velocities for the 'Krammer' closure [Rijkswaterstaat,1987]
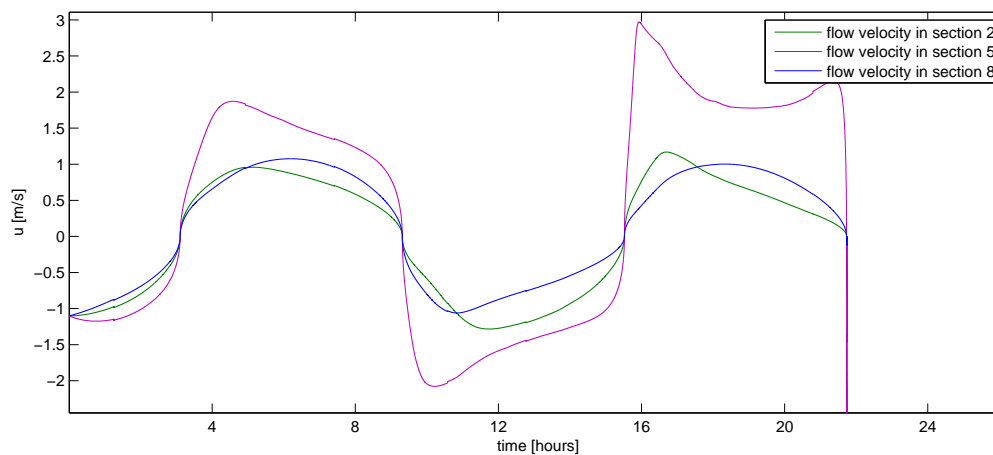
Figure 7.10: The velocities through the closure gaps

Sand losses

At the 'Tholense Gat' and 'Krammer', the sand losses are estimated using the production and the volume of sand in the dam. The measurements are not very accurate as shown in table 7.3.

	Sand losses	Uncertainty	Measurement period
'Krammer'	$257000m^3$	$95000m^3$	± 2.5 days
'Tholense Gat'	$83000m^3$	$48000m^3$	$\pm$ 4 days

Table 7.3: The data of the sand losses of the two closures [Rijkswaterstaat,1987]

'Krammer'

The final phase of the 'Krammer' dam is constructed in 2.5 days. The dam is closed at April 17th at 22:00h. What is known is that the width of the gap is between $250m$ at the April 16th and $500m$ at the April 14th. What the exact geometry of the gap was at the start of the simulation is not known. In order to verify the behaviour of the model, two runs are performed. One with an initial width of $275m$ and one of $325m$.
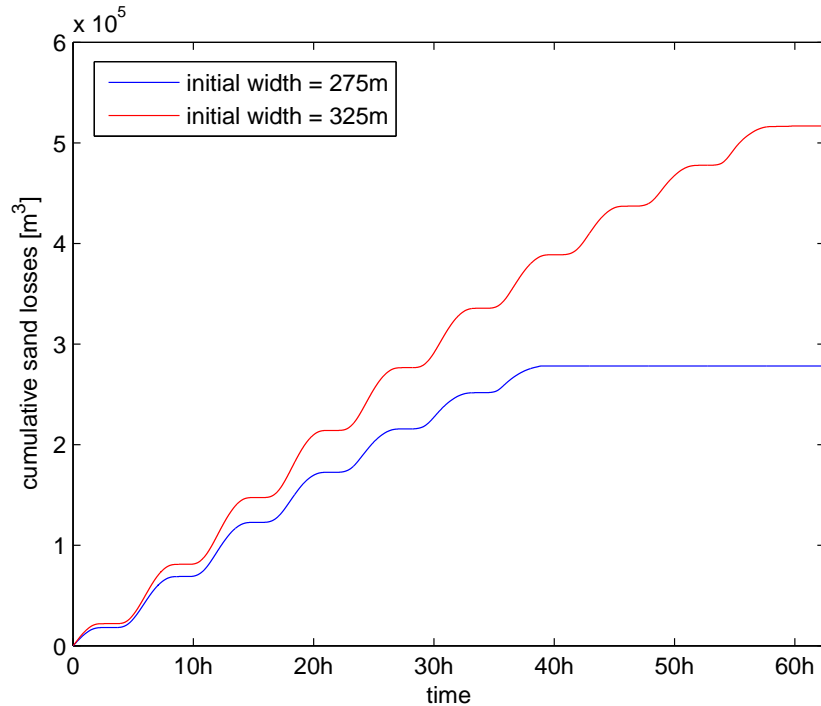
Figure 7.11: The cumulative sand losses of the model runs

- Width of the gap: $275m/325m$

- Height of the sill: $5m$

- Length of the sill: $400m$

- Grain sizes:

    - $D_{15} = 130\mu m$
    - $D_{50} = 200\mu m$
    - $D_{90} = 370\mu m$

- Amplitude tide: $0.1m$

- Production is applied over a width of $100m$

The cumulative sand losses are presented in figure 7.11. What can be seen is that for the width of $325m$ the dam closes in exactly 2.5 days. However the sand losses are too large. The sand losses calculated with a closure gap of $275m$ are about the amount of the sand losses which are measured. From this analysis can be seen that the model predicts the sand losses quite well, assumed that the initial width of the closure gap is somewhere between the two values which are chosen.

'Tholense Gat'

From figure 7.11, can be seen that the sand losses over time are almost constant. For that reason, the closure of the 'Tholense Gat' is modelled for a shorter time and subsequently are the sand losses extrapolated. This leads to shorter model runs and makes it possible to verify the sensitivity of the input of the model. The closure of the 'Tholense gat' is simulated from 14.5 hours before closure till closure. The total horizontal closure took about 80 hours. So almost the final quarter of this closure is simulated. The input for the model is presented below:

- Width of the gap: $80m$

- Height of the sill: $5m$

- Length of the sill: $400m$

- Grain sizes:

    - $D_{15} = 110\mu m$
    - $D_{50} = 160\mu m$
    - $D_{90} = 300\mu m$

- Amplitude tide: $0.08m$

- Production is applied over a width of $100m$

Results

Because the input of the tidal amplitude, the grain size and the width of the closure gap contain the largest uncertainties, these parameters are varied. The results are shown in table 7.4.

	Sand losses	**Moment of closure**
width = 60	$8000m^3$	$\pm 12h$
Width = 80 (initial)	$14000m^3$	$\pm 19h$
Width = 100	$20000m^3$	$\pm 25h$
Amplitude = 0.06	$5000m^3$	$\pm 13h$
Amplitude = 0.08(initial)	$14000m^3$	$\pm 19h$
Amplitude = 0.1	$22000m^3$	$\pm 19h$
Grain size = $160\mu m$	$14000m^3$	$\pm 19h$
Grain size = $180\mu m$(initial)	$14000m^3$	$\pm 19h$

Table 7.4: The data of the model runs for 'Tholense Gat'

To analyse the results of this closure, again the sand losses are assumed to be the same over time. For the initial situation, with a width of $80m$, the total sand loss becomes $56000m^3$. This is within the margin of the of the measured data. When the larger amplitude is considered, the measured sand loss is almost obtained with a sand loss of $4 \cdot 22000 = 88000m^3$. The small difference in the grain size barely influence the closure time and the sand losses.

comparison with the CUR 157

The CUR 157 also presented the sand losses for the closures of 'Krammer' and 'Tholense Gat'. The results are shown in table 7.5. Despite the uncertainty, the 1-dimensional model does a pretty good job in calculating the sand losses.

Closure	Measured sand loss	CUR 157	1-dimensional model
'Krammer'	$257000m^3 \pm 95000m^3$	$90000m^3$	$300000m^3$
'Tholense Gat'	$83000m^3 \pm 48000m^3$	$68000m^3$	$56000m^3$

Table 7.5: The sand losses compared with the CUR 157

7.3 Conclusions

Because of the high inaccuracy in the measurements and data of the 'Krammer' closure and the 'Tholense Gat', it is not possible to say that the model is applicable for a wide range of grain sizes. What can be concluded is that the results of the model are comparable with than the calculated sand losses using the CUR 157.

The closure of the outer contour at 'Maasvlakte 2' shows that for every case a new calibration is required, even when the properties of the sand are about the same. Higher velocities of the water causes much more erosion than observed from the survey drawings and the calibrated morphological roughness is too large for the closure of the outer contour.

Chapter 8

Conclusions and recommendations

The research question of this investigation is as stated in the introduction: "How can the processes during construction of a sand closure be described and modelled to improve the prediction of the sand losses over time?" The goal of this research is divided in two parts: the first part is to analyse the processes that influence the sand losses which occur during the construction of sand closures. This is done using the theory of Van Rhee which describes the processes of sedimentation and erosion as a consequence of the flow over the bed. The second goal is to implement the processes in a tool to calculate the sand losses over time. The results of this tool are finally compared with the calculation method of the CUR 157. In this way the hypothesis that the sand losses can be calculated more accurate for a wide range of grain sizes when the interaction between the bed and the continuous varying flow is taken into account, can be tested.

8.1 Conclusions

Processes

The theory of Van Rhee is a promising method to describe the processes of the interaction between the flow and the bed and calculate the sand losses. The analysis shows that the flow velocity is an important parameter in the determination of the sand losses. The velocity depends on the tidal forcing, the size of the tidal basin and the geometry of the closure gap. The analysis shows that a larger resistance over the closure gap reduces the flow velocities through the closure gap. In order to increase the resistance it is favourable to close the gap vertically instead of using a horizontal closure method.

Further it is stated that the interaction between the flow and the bed is determined by the the soil properties and the flow velocity. When flow velocities become large ($u > 1m/s$), the process of dilatancy becomes significant for the determination of the erosion rate. Dilatancy causes an inward flow into the bed. This flow hinders the erosion and the hindering becomes larger if the porosity and the permeability of the bed are smaller.

Model

To implement the interaction between the flowing water and the bed, the formula of Van Rhee is used in a 1-dimensional model. This model is build especially to investigate the processes during the construction of a sand closure and to calculate the sand losses. In order to calculate the erosion, the model takes into account the physical properties of the bed and therewith takes

into account more physical processes that occur during the closure of a dam, compared with the formulation of the CUR 157.

The model is a replenishment to, but not a replacement of the calculation method of the CUR 157. The model contains shortcomings and this leads to a general conclusion that the processes which occur during a sand closure are too complex to describe in a 1-dimensional model. The first shortcoming is that the model closes the gap in a section downstream of the section where the production takes place (and where the actual closure took place). This is a consequence of the fact that the model is 1-dimensional. High concentrations and relative low flow velocities in the sections downstream cause a vertical closure in these sections instead of the horizontal closure at the sections where production takes place. The second shortcoming is that the model shows unstable behaviour when the flows become supercritical. This leads to numerical errors and sometimes even to a closure at the wrong moment.

Therefore the hypothesis can't be tested, because the 1-dimensional model can't calculate sand losses during a closure more accurate than the CUR 157. However, the analyses and the way these processes are used in the model provides more knowledge about the processes that occur during the construction of a sand closure as well as about the knowledge that has to be improved. To build a new more dimensional and specific model we need for instance more knowledge about the development of the bed and banks during the closure operation.

8.2 Recommendations

In the analysis performed in this research, the only reference to compare the model with the actual situation are the survey drawings and the water levels. The survey drawings are snapshots, but to what extend the processes described by Van Rhee actually occur in the time between the two surveys is not known exactly. To verify the behaviour of a model it is important to gain knowledge about the development of the bed level and the banks in the time between two survey drawings. To gain this knowledge it is recommended to perform tests with a physical closure gap model.

The model which is used in this investigations is only tested using four cases. The different sub routines which are in the model such as the the erosion model, the sedimentation model and the transport of suspended sediments are not tested. It is recommended to test the sub routines separately to investigate if the model works correctly. Laboratory experiments can help with these tests as well.

As concluded, the model contains two shortcomings. The first one is that the model shows unstable behaviour when the flow becomes critical. Before the model can be used a new flow model is necessary, which is stable for all flow regimes. This can possibly be obtained by solving the continuity and momentum equation numerically.

The second shortcoming of the model is that it clearly shows the consequence of the deficiency of not taking into account the 2- or 3-dimensional effects. To obtain a more reliable result of the sand losses, it is recommended to develop a module of the Van Rhee formula in a 2-dimensional model and if necessary expand this model with a 3-dimensional model for an even better accuracy.

If the possibility of a more dimensional model is not available or takes too much time, it can be a solution to simplify the 1-dimensional model to one section instead of the eight which are used in this research. Using only one section where the production takes place, the more dimensional processes downstream of the dam are avoided. To do so an assumption has to be made for the concentration of sand in the water column during inflow, because erosion processes

upstream of the section are neglected, when only one section is considered.

In this analysis the production during horizontal closure is considered as a displacement of the bank. In practice a sand water mixture flows over the bank. This can result in a change of the slope and sand losses can occur. It is interesting to investigate the consequences of these processes for the development of the banks and the sand losses.

In the model runs, the sediment concentrations became high as a consequence of erosion or production (deposit sand directly in the water). The interaction between the flow and high sediment concentrations as a result of production and erosion can be important for the flow through the closure gap. For future research, it is important to investigate the influence of high concentrations.

In the model an assumption is made that the sediment is evenly concentrated over the depth. This is an important parameter, which determines the settlement. So for future research it is recommended to correct for this assumption and calculate the sedimentation with the near bed concentration.

Bibliography

[Battjes,2002a] Battjes, J.A., Collegehandleiding vloeistofmechanica, Delft University of Technology, 2002.

[Battjes,2002b] Battjes, J.A., Collegehandleiding Stroming in Waterlopen, Delft University of Technology, 2002.

[Bosboom and Stive,2011] Bosboom, J, and Stive, M.J.F., Lecture notes Coastal Dynamics I, version 0.2, Delft University of Technology, 2011.

[CUR152] van 'T Hoff, J, CUR 152, Kunstmatig in zand opgebouwde zandlichamen, 1991

[CUR157] Struik, P., CUR 157, Sand Closures, Centre for Civil Engineering Research and Codes, 1992

[Escoffier,1940] Escoffier, Francis, F., The stability of tidal inlets, Shore and Beach, volume VIII, October 1940.

[Escoffier,1977] Escoffier, Francis F., Hydraulics and Stability of Tidal Inlets, U.S. Army Coastal Engineering Research Center, GITI Report 13, 1977.

[Fritz and Hager,1998] Fritz, H.M. and Hager, W.H., Hydraulics of Embankment Weirs, Journal of Hydraulic Engineering, vol. 124 No.9, 1998

[Hager,1994] Hager, W.H., Broad-Crested Weir, Journal of Irrigation and Drainage Engineering, Vol. 120, No. 1, 1994

[Holthuijsen,2007] Holthuijsen, Leo, H., Waves in Oceanic and Coastal Waters, Cambridge University Press, 2007.

[Keulegan,1967] Keulegan, G. H., Tidal flow in entrances water-level fluctuations of basins in communication with seas, U.S. Army Corps of Engineering, 1967

[Miedema and Vlasblom,1996] Miedema,S.A. and Vlasblom,W.J., Theory for Hopper Sedimentation, 29th Annual Texas A and M Dredging Seminar. New Orleans, 1996.

[Myers,2010] Myers, J.D., Lecture Solar System and Tidal forces, Department of Geology and Geophysics, University of Wyoming, 2010.

[PUMA,2012] Kroon, A., Projectorganisatie Uitbreiding Maasvlakte 2: Kalibratie zandverliesmodel zandsluiting compartimenteringsdam, PUMA, 2012.

[PUMA,2012b] Kroon, A., Projectorganisatie Uitbreiding Maasvlakte 2: Prognose zandverliezen sluiting ZZ, PUMA, 2012.

[Van Rhee,2007] Van Rhee, C, Erosion of granular sediments at high flow velocity, Hydrotransport 17th. The 17th International Conference on the Hydraulic Transport of Solids, The Southern African Institute of Mining and Metallurgy and the BHR Group, 2007.

[Van Rhee,2010] Van Rhee, C, Sediment Entrainment at High Flow Velocity, Journal of Hydraulic Engineering, 2010.

[Van Rhee and Talmon,2010] Van Rhee, C and Talmon, A.M., Sedimentation and erosion of sediments at high solids concenctration, BHR Group, 2010

[Rijkswaterstaat,1987] Deelnota XIII zandverliezen bij zandsluitingen, GWAO-87.376, 1987.

[Rijkswaterstaat,1987] Deelnota XIV Zandtransportberekeningen sluitgaten compartimenteringswerken Oosterschelde sluitgat Krammer, P. Termes, 1987

[Van Rijn,1984] Van Rijn, L.C., Sediment Pick-Up Functions, Journal of Hydraulic Engineering, volume 110, no. 10, 1984.

[Van Rijn,1993] Van Rijn, L.C., Principles of Sediment Transport in Rivers, Estuaries and Coastal Seas, Aqua Publications, 1993.

[Schmocker and Hager,2010] Schmocker, L. and Hager, W.H., Overtopping and breaching of dikes - Breach profile and breach flow, Bundesanstalt fr Wasserbau, 2010

[Van der Schrieck,2012] Van der Schrieck, G.L.M., Lecture notes Dredging Technology, Delft University of Technology, 2012.

[Shields,1936] Shields, A, Application of Similarity Principles and Turbulence Research to Bedload Movement, Hydrodynamics laboratory, California Institute of Technology, Pasadena, publication no. 167, 1936.

[Tran,2012] Tran, Thanh-Tung, Cross-sectional stability of tidal inlets: A comparisson between numerical and emperical approaches, Elsevier journal of Coastal Engineering, volume 60, 2012

[De Vriend,2011] De Vriend, H.J., Lecture notes River Engineering, Delft University of Technology, 2011.

[Zijlema,2011] Zijlema, M., Lecture notes computational modelling of flow and transport, Delft University of Technology, 2011.

Appendix A

Initiation of motion

This appendix treats a method to calculate the initiation of motion and the settling velocity. First the initiation of motion is discussed.

A.1 Initiation of motion

If the shields parameter, described in chapter 2 is below a certain value, no motion of particles occurs. The particles start to move at the so called threshold of motion and is called the critical shields parameter, θ_{cr}. The critical shields parameter is determined by use of the so called particle Reynolds number, given in figure A.1. With this particle Reynolds number the critical shields parameter can be determined graphically using figure A.1. The critical shields parameter can also be determined numerically, using the dimensionless diameter of a particle, see equation A.1. According to the numerical method the θ_{cr} is determined by equation A.2 [Van Rijn,1993].

$$D_* = D_{50} \left[\frac{\Delta g}{\nu^2} \right]^{1/3} \tag{A.1}$$

In which:
$\quad D_*$ = the dimensionless diameter $[-]$
$\quad \nu$ = the kinematic viscosity $[m^2/s]$

$$\theta_{cr} = \begin{cases} \frac{0.24}{D_*} & \text{for } 1 < D_* \leq 4 \\ \frac{0.14}{D_*^{0.64}} & \text{for } 4 < D_* \leq 10 \\ \frac{0.04}{D_*^{0.1}} & \text{for } 10 < D_* \leq 20 \\ 0.013 D_*^{0.29} & \text{for } 20 < D_* \leq 150 \\ 0.055 & \text{for } D_* > 150 \end{cases} \tag{A.2}$$
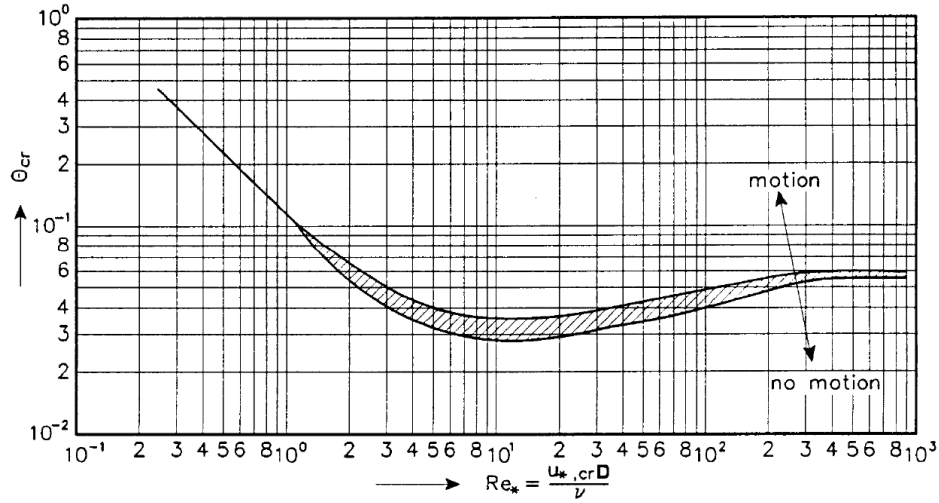
Figure A.1: Determination of the critical shields curve by use of the particle Reynoldsnumber Re_* [De Vriend,2011]

influence of slopes

When a particle is on a slope the gravity exerts a force in the direction of the slope (downhill). For flows along the slope or in the downhill direction is the initiation of motion reached at lower flow velocities. So a correction to the critical shields parameter can be used to express the initiation of motion correctly, see equation A.3. Van Rijn made a distinction between the flow over a longitudinal slope of the flow along a transverse slope [Van Rijn,1993].

For longitudinal slopes, Van Rijn expressed the correction factor as k_β. This factor can be calculated using equation A.4.

$$\theta_{cr,\beta,\gamma} = \theta_{cr,0} k_\beta k_\gamma \tag{A.3}$$

$$k_\beta = \begin{cases} \frac{sin(\phi-\beta)}{sin\phi} & \text{for downsloping flow } (k_\beta > 1) \\ \frac{sin(\phi+\beta)}{sin\phi} & \text{for upsloping flow } (k_\beta < 1) \end{cases} \tag{A.4}$$

To calculate the initiation of motion on a slope, the critical shields parameter needs to be multiplied by the k_β as shown in equation A.3.

For a transverse slope the correction factor which is a bit different from the longitudinal slope. The correction factor is calculated by equation A.5. This value gives imaginary numbers for values of $\gamma > \phi$. So this term is only applied for mild slopes that are smaller than the angle of internal friction. For values of $\gamma > \phi$, the slope is unstable and collapses anyhow.

$$k_\gamma = cos\gamma \sqrt{1 - \frac{tan^2\gamma}{tan^2\phi}} \tag{A.5}$$

In which:
g = the gravitational acceleration on earth $[m/s^2]$
d = the size of the particle $[m]$
ν = the kinematic viscosity of the water $[m^2/s]$

Appendix B

Battjes method

The flow through a closure gap can be described by the shallow water equations. This section treats a method to solve the shallow water equations analytically for a tidal basin, which is connected to the sea by an inlet, the closure gap. To do so, two simplifications are made, namely the Basin storage approach and the rigid column approach.

basin storage approach

The basin storage approach assumes the water level in the basin is the same everywhere and is only influenced by the tidal flow through the closure gap. This simplification is allowed if the wave length of the tide is much larger than the length of the basin. This assumption simplifies the continuity equation to equation 3.1, which is repeated here [Battjes,2002b].

$$A_b \frac{dh_b}{dt} = Q \tag{3.1}$$

In which:
A_b = the surface of the basin $[m^2]$
dh = the difference in water level over time step dt $[m]$
Q = the discharge through the closure gap $[m^3/s]$
dt = a time step $[s]$

Rigid column approach

The rigid column approach assumes that there is no storage in the closure gap. This implies that the discharge which flows through the closure gap is the same over the length of the closure gap $\left(\frac{dQ}{dx} = 0\right)$. The same assumption is made for the flow area which remains constant over the gap. So the advective term of the momentum equation can be neglected. This simplifies the momentum equation in equation 3.2, which is repeated here.

$$\frac{\partial Q}{\partial t} + gA_c \frac{\partial h}{\partial x} + c_f \frac{|Q|Q}{A_c R} = 0 \tag{3.2}$$

In which:
B = the width of a channel $[m]$
h = the water depth $[m]$

Q = the discharge $[m^3/s]$
A_c = the flow area $[m^2]$
c_f = a dimensionless friction coefficient $[-]$

Limitations

The basin storage approach and the rigid column approach are applicable as long as the time scale of which the closure gap size changes significantly (by influence of production or erosion), is larger than the time scale of a tidal cycle. An other limitation to this method is that the flow has to be sub-critical. So in the critical phase this approach is not valid any more and a numerical solution has to be used with a description for the supercritical flow.

Analytical elaboration

The goal of the this analysis is to calculate the flow velocities which later on can be used to determine the erosion of the bed and banks in the closure gap. To calculate the velocity it is important to know the decay of the water level over the dam. This is provided if equation 3.2 is integrated over x. This results in equation B.1. Integrate over x and rewrite:

$$h_0 - h_b = \frac{l}{gA_c}\frac{dQ}{dt} + W \tag{B.1}$$

In which:
h_0 = the water level at sea $[m]$
h_b = the water level in the basin $[m]$
W = the total loss over the dam expressed in a decay of the water level $[m^3/s]$

In equation 3.2 the friction term gives the resistance over the dam, which is given in equation B.2. To give an expression of the total losses over the closure dam, the in- and outflow losses should be included in the expression for the losses, which is expressed by W. The value for the in- and outflow losses is given in equation B.3. This is why the friction term is expressed as W in equation B.1.

$$\Delta H_w = c_f \frac{l}{R}\frac{|U|U}{g} \tag{B.2}$$

$$\Delta H_v = \frac{|U|U}{2g} \tag{B.3}$$

$$W = \Delta H_v + \Delta H_w = \chi\frac{|U|U}{g} = \chi\frac{|Q|Q}{gA_s^2} \tag{B.4}$$

In which:
ΔH_v= the decay caused by the resistance of the bottom $[m]$
ΔH_w= the decay caused by entrance and exit losses $[m]$
χ = $c_f\frac{l}{R} + \frac{1}{2}$ = a dimensionless loss coefficient $[-]$
c_f = $\left(\frac{1}{5.75log\left(12\frac{R}{k}\right)}\right)^2$
k = $3D_{90}$ [Battjes,2002a]

Equation B.1 and 3.1 form a system of two differential equations. If all the Q's in equation B.1 are substituted by the term for Q in equation 3.1, a second order differential equation is obtained (equation B.5).

$$\frac{l}{g}\frac{A_b}{A_c}\frac{d^2 h_b}{dt^2} + \frac{\chi}{g}\left(\frac{A_b}{A_c}\right)^2 \left|\frac{dh_b}{dt}\right|\frac{dh_b}{dt} + h_b = h_0 \tag{B.5}$$

In which:
l = the length of the closure dam $[m]$

Linearisation of the differential equation

The second term on the left hand side gives the damping in the system. The modulus in this term makes it a non linear differential equation. To solve this analytically the differential equation has to be linearised. To do so, the friction term is linearised in such a way that the total energy loss by friction over a tidal cycle is equal to the non linearised friction.

$$W = \lambda_1 |Q| Q \tag{B.6}$$

$$W = \lambda_2 Q \tag{B.7}$$

In which:
λ_1 = $\frac{\chi}{gA_c}$
Q = $\hat{Q}cos\omega t$
$\hat{Q}$ = the amplitude of the discharge in the closure gap $[m^3/s]$

By equate equation B.6 and B.7, equation B.8 is found. This equation can be solved for a tidal period and an expression for λ_2 is the solution, which is presented in equation B.9.

$$\int_0^T W Q dt = \int_0^T \lambda_1 |Q| Q^2 dt = \int_0^T \lambda_2 Q^2 dt \tag{B.8}$$

$$\frac{\lambda_2}{\lambda_1} = \frac{\int_0^T |cos\omega t| cos^2 \omega t dt}{\int_0^T cos^2 \omega t dt}\hat{Q} = \frac{\int_0^{T/4} cos^3 \omega t dt}{\int_0^{T/4} cos^2 \omega t dt}\hat{Q} = \frac{8}{3\pi}\hat{Q} \tag{B.9}$$

This expression for the linearised friction can replace the non-linear friction term in equation B.5. This results in equation B.10, presented below.

$$\frac{l}{g}\frac{A_b}{A_c}\frac{d^2 h_b}{dt^2} + \tau\frac{dh_b}{dt} + h_b = h_0 \tag{B.10}$$

This differential equation can be expressed in deviations of the mean sea level. The deviations are named ζ_b and ζ_0 for respectively the basin and the sea.

$$\frac{l}{g}\frac{A_b}{A_c}\frac{d^2 \zeta_b}{dt^2} + \tau\frac{d\zeta_b}{dt} + \zeta_b = \zeta_0 \tag{B.11}$$

In which:

$\tau \quad = \quad \frac{8}{3\pi}\chi\frac{A_b}{gA_c^2}\hat{Q}$, which is the relaxation time of the system $[s]$

$\zeta_b \quad = \quad \hat{\zeta}_b cos(\omega t - \theta)$

$\zeta_0 \quad = \quad \hat{\zeta}_0 cos(\omega t)$ the amplitude of the water level at sea $[m]$

$\hat{\zeta}_b \quad = \quad$ the amplitude of the water level in the basin $[m]$

$\hat{\zeta}_0 \quad = \quad$ the amplitude of the water level at sea $[m]$

$\theta \quad = \quad$ the phase difference between the tide and the oscillation in the basin

Solution of the differential equation

The intended result is the velocity in the closure gap, which can be calculated from the water level differences between the basin and the sea. The water level difference can be calculated with the parameters θ and r.

$$r = cos\theta \tag{B.12}$$

In which:

$r \quad = \quad$ the relation between the amplitudes in the basin and at sea $= \frac{\hat{\zeta}_b}{\hat{\zeta}_0}$

Equation B.11 is a standard differential equation for a linear, damped mass spring system, with a damping factor τ and eigenfrequency ω_0. The solution of this differential equation for r and θ is:

$$r = \frac{1}{\sqrt{\left(1 - \frac{\omega^2}{\omega_0^2}\right)^2 + (\omega\tau)^2}} \tag{B.13}$$

$$tan\theta = \frac{\omega\tau}{1 - \frac{\omega^2}{\omega_0^2}} \tag{B.14}$$

τ contains the unknown parameter $\hat{Q}$, r and θ are unknown. This implicit system can be made explicit by use of a dimensionless parameter Γ, see equation B.15. The Γ contains all the parameters of the geometry of the closure gap and the tidal forcing. With this parameter the ratio between the amplitude at sea and in the basin is given in equation B.16 and the phase difference is given by equation B.17

$$\Gamma = \frac{\omega\tau}{r} = \frac{8}{3\pi}\chi\left(\frac{A_b}{A_c}\right)^2\frac{\omega^2\hat{\zeta}_0}{g} \tag{B.15}$$

$$r = \frac{\hat{\zeta}_b}{\hat{\zeta}_s} = \frac{1}{\sqrt{2}\Gamma}\sqrt{-\left(1 - \frac{\omega^2}{\omega_0^2}\right)^2 + \sqrt{\left(1 - \frac{\omega^2}{\omega_0^2}\right)^4 + 4\Gamma^2}} \tag{B.16}$$

$$tan\theta = \frac{\omega\tau}{1 - \frac{\omega^2}{\omega_0^2}} = \frac{\Gamma r}{1 - \frac{\omega^2}{\omega_0^2}} \tag{B.17}$$

In which:

Γ = a dimensionless coefficient which contains all the parameters which determine the geometry of the closure gap and the tidal forcing.

ω_0 = $\sqrt{\frac{gA_c}{lA_b}}$ = the eigenfrequency of the system $[s^{-1}]$

Note that for a closure gap with a length of the dam of $500m$ or less, the eigenfrequency is much larger than the wave number. Which makes the term $1 - \frac{\omega^2}{\omega_o^2}$ go to 1 and the expression for r can be written as equation B.18:

$$r = \frac{1}{\sqrt{2}\Gamma}\sqrt{-1 + \sqrt{1 + 4\Gamma^2}} \tag{B.18}$$

The amplitude of the discharge becomes:

$$\hat{Q} = A_b\omega\hat{\zeta}_k \tag{B.19}$$

For a $\Gamma \approx 10$ or larger, equation B.18 changes to: $r = \frac{1}{\sqrt{\Gamma}}$. For small closure gaps, the Γ is larger thatn 10 and the amplitude of the discharge does not depend on the ω. As can be seen in figure 4.5, when theta becomes a little smaller than 10, the omega has some influence on the amplitude of the discharge, namely for a shorter period, the amplitude becomes higher.

Appendix C

Case study: 'Compartimenteringsdam'

During the construction of the 'Maasvlakte 2' two closures are constructed. This appendix gives an overview of the construction of the the closure that is used in the calibration in chapter 6. The closures at 'Maasvlakte 2' are constructed in 2012. The first one, the 'Compartimenteringsdam' is performed to reduce the basin behind the closure and to learn about the processes which occur to perform the second larger closure, called the 'Zachte Zeewering'. Figure C.1 gives an overview of the 'Maasvlakte 2', with the two locations where the closure dams are constructed.

Figure C.1: Picture of the 'Maasvlakte 2', taken at March[th] 2012 [PUMA,2012]

In the figure above the 1 and 2 indicate respectively the closure at the 'zachte zeewering' and the 'Compartimenteringsdam. The YH indicates the Yangtze harbor, the ZZ the sandy shore and the HZ indicates the hard seawall constructed to protect the 'Maasvlakte 2'.

The 'Compartimenteringsdam' is constructed is constructed in 5 days, starting at March 27th. The closure was at March 31th, 20:00h. The dam is closed using a vertical closure combined with a one sided horizontal closure. First a sill is build up till 1.5m below water level. The final phase is of the dam is constructed as a horizontal closure. The horizontal closure is performed using a hopper connected to a land pipeline. At the end of the pipeline, bulldozers divide the sand over the width of the dam and construct the extension of the dam evenly.

Water levels

The water levels are measured behind the hard sea wall and inside the basin. This water levels are used in the 1D model described in chapter 5. Figure C.2 shows the water level over the time during the final phase of the first closure.
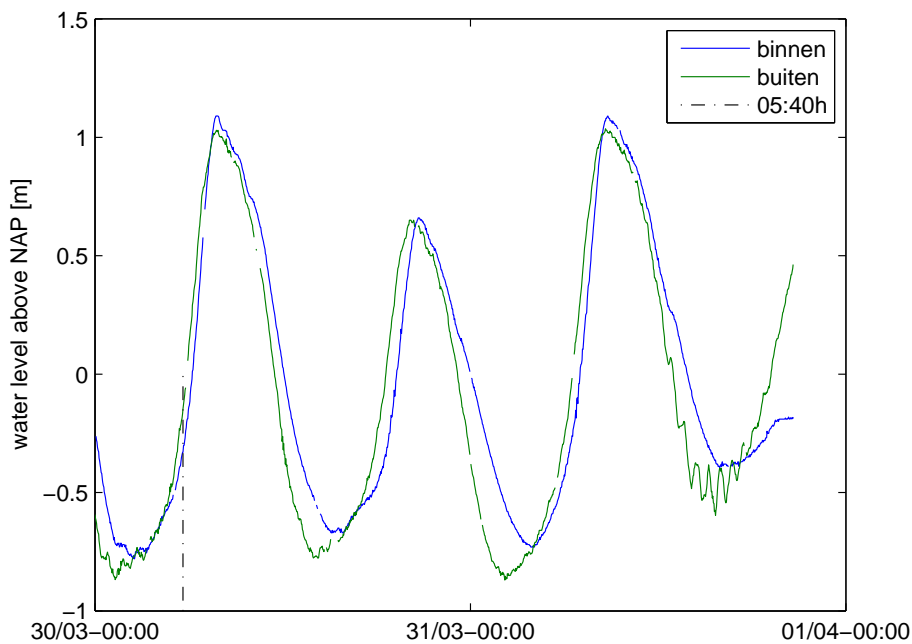
Figure C.2: The water levels in and outside the basin during the final stage of the closure

Progress

March 27th the construction of the 'Compartimenteringsdam'started. The initial situation is given in figure C.3. The upper part of the dam is connected to the sea and at the bottom of the picture the basin is shown.
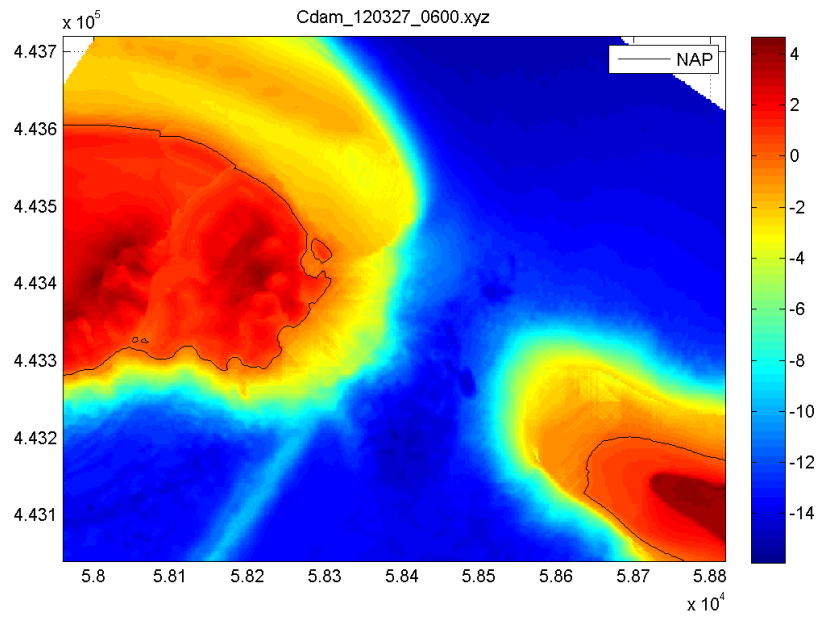
Figure C.3: The situation just before the start of the construction of the 'Compartimenterings-dam'

In the following days the sill is built up using hoppers up to the 1.5m below water level is reached. In figure C.4, pictures are shown of the surveys.
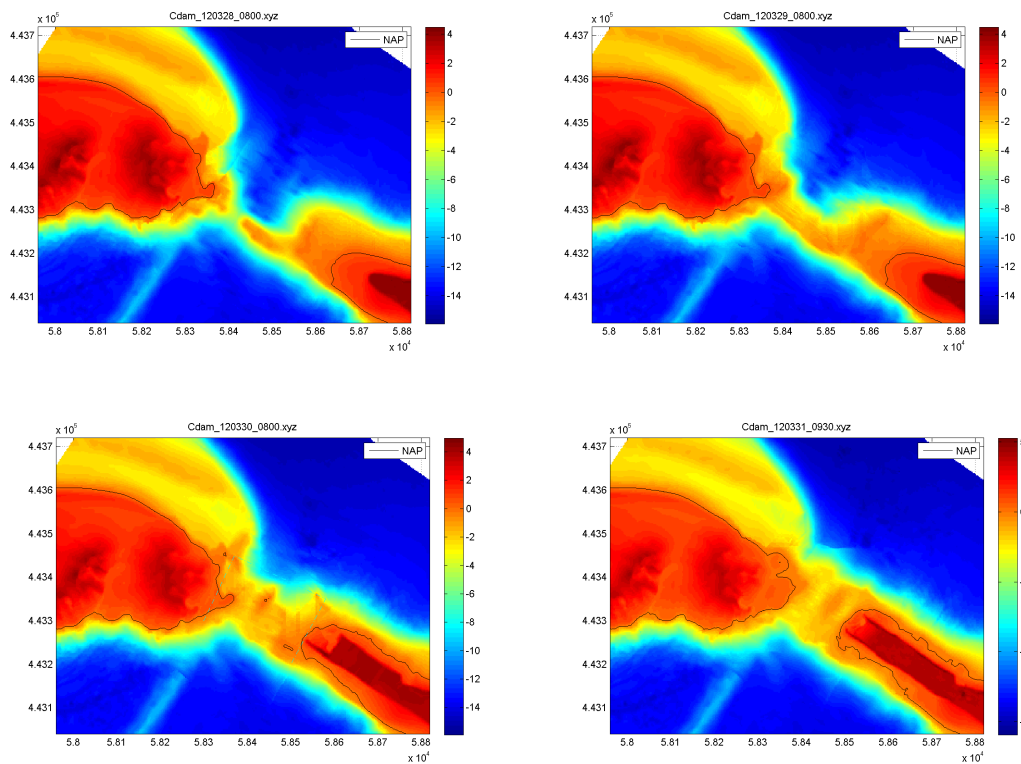
Figure C.4: Process of the vertical construction of the 'Compartimenteringsdam'

The lower right panel of figure C.4 shows the situation at the morning before closure. At this time the cross section of the closure gap is comparable with the reference situation used in chapter 4. From this moment one hopper is unloaded on the foreshore of the sill and three hoppers are unloaded from the pipeline to close the dam by a one sided horizontal closure. At 20:00h the dam was closed. This is shown in a survey drawing at figure C.5.
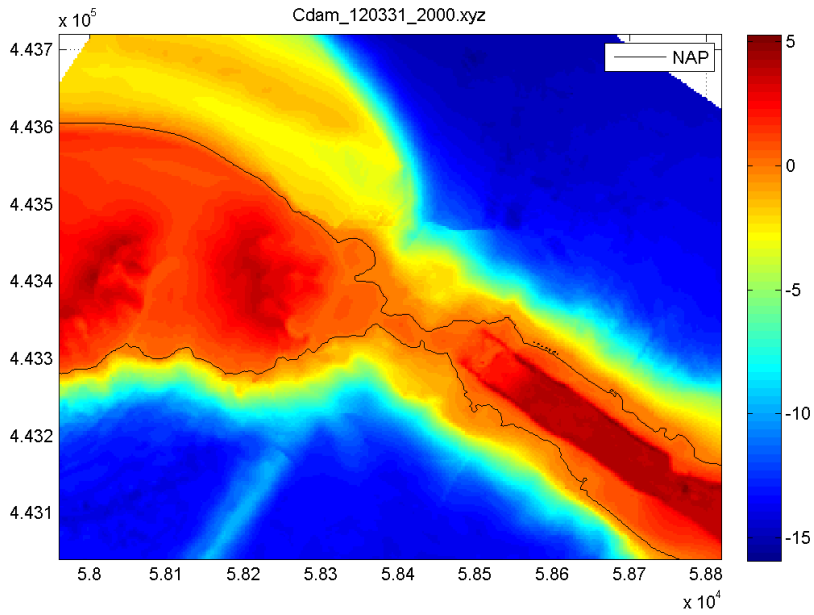
Figure C.5: Overview of the bed level right after closure

Appendix D

Source code 1-dimensional model

The model consists of a master file, which uses function files for different routines. First the master file is shown, followed by the function files. To understand the code a bit better, first some terms are explained.

The geometry of the closure gap is determined by four points. X1, X2, X3 and X4. These positions are as shown in figure D.1. The x-coordinates of the points are defined by their points in the code. The y-coordinate is of X1 and X4 is always equal to GR (crest level of the dam). The y-coordinate of X2 and X3 is determined by hsill (level of the sill below N.A.P.)
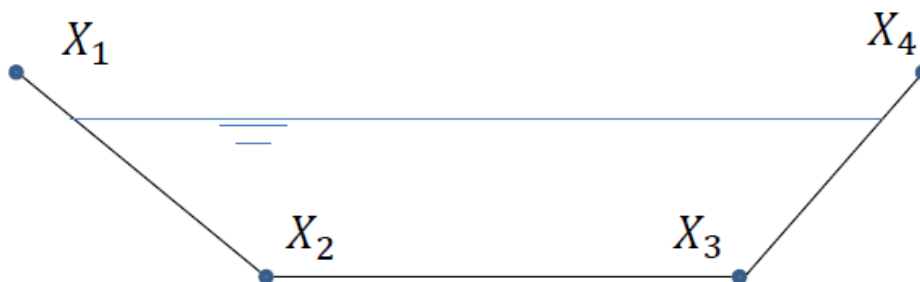
Figure D.1: The points X1, X2, X3 and X4 in the mondel

In every time step, first the erosion and sedimentation of the bed and banks is calculated. This leads to a replacement of the points. The new temporarily values of parameters is determined with the addition $_{ero}$ behind the parameter. The following action is to calculate the displacement of the points as a consequence of the construction. Finally the new values for X1, X2, X3, X4, hsill and so on... is determined.

Master file

```
clear all; clc; close all;

%% Input
addpath funfiles
% standard data
g = 9.81;
rho_W = 1025;
rho_S = 2650;
Delta = ( rho_S - rho_W ) / rho_W;
visc = 1 * 10^-6;
% Basin parameters
Ab = 2600000;
% production
damisconstructed = 0; % 1 if yes

%% sediment/bed properties
D15 = 250*10^-6;
D50 = 380*10^-6;
D90 = 700*10^-6;
morph_fac = 2.5;     % multiplication factor for ks for erosion
ks = 3*D90;          %3*D90 (vloeistofmechanice p. 215)
n0 = 0.40;           % 0.45-0.49 voor direct geproduceerd zand ( CUR 152, p. 108)
ni = 0.50;           % the loose porosity
phi = ( 30 / 360 ) * 2 * pi;    % angle of internal friction
k = g / ( 160 * visc ) * D15^2 * ( n0^3 / ( ( 1-n0 )^2 )); % Permeability

%% numerical data
L0 = 150;            % Length of the closure gap

sections = 8;        % Number of sections
dx = L0 / sections;
dt = 2;

CFL_test = 5 * dt / dx;
if CFL_test > 1
    error([ 'CFL condition not passed, \sigma = ' num2str(sigma_test) ])
end

%% Water level at sea
datdir1 = 'D:\Dropbox\Afstuderen\Maasvlakte data\Cdam\';
cd(datdir1)
load tijdreeks_LoswalA_Cdam

xbegin = 98206;      % at 09:30 morning of closure day - 97370;
xend = 98610;
buiten = hh(xbegin+1:xend,1)';  % outside water level
binnen = hh(xbegin+1:xend,2)';  % outside water level
t = tt(xbegin+1:xend);

STARTMODEL = t(1);               % start time of the model
datdir2 = 'D:\Dropbox\Afstuderen\calculations\Tool\Calibratie\';
cd(datdir2)
addpath funfiles
```

```matlab
%% Interploation of the water level from h_sea
begintime = 1;
endTime = ( xend − xbegin ) * 2 * 60;
plottime = 1;
STEPS = 120 * (1:endTime/120);
h_sea = interp1(STEPS  , buiten, 1:endTime) ;

%% production input
starttime = 147800 − endTime;          % start time of the model run for production
[ Q_prod, CMS_prod ] = funproduction( endTime, dt, sections, starttime );

%% prealocation files
h_basin = NaN((endTime)/dt,1); Ac = NaN((endTime)/dt,sections);
h_sill  = NaN((endTime)/dt,sections);
width_GR = NaN((endTime)/dt,sections); width_bed = NaN((endTime)/dt,sections);
L = NaN((endTime)/dt,1);
Q = zeros((endTime)/dt,1); P = NaN(1,sections); R = NaN(1,sections); cf = NaN(1,sections);
ve_bot = NaN((endTime)/dt,sections); ve_side = NaN((endTime)/dt,sections);
v_bed = NaN((endTime)/dt,sections); v_wal = NaN((endTime)/dt,sections);
vsed = NaN((endTime)/dt,sections);
C = zeros((endTime)/dt,sections); beta = NaN((endTime)/dt,sections);
h_sea_calc = NaN((endTime)/dt,1);
gammaL = NaN((endTime)/dt,sections); gammaR = NaN((endTime)/dt,sections);
dxdt = NaN((endTime)/dt,sections); dx_prod = NaN((endTime)/dt,sections);
ve_sideL = NaN((endTime)/dt,sections); ve_sideR = NaN((endTime)/dt,sections);
v_walL = NaN((endTime)/dt,sections); v_walR = NaN((endTime)/dt,sections);
X1_ero = NaN((endTime)/dt,sections); X2_ero = NaN((endTime)/dt,sections);
X3_ero = NaN((endTime)/dt,sections); X4_ero = NaN((endTime)/dt,sections);
width_bed_ero = NaN((endTime)/dt,sections); width_GR_ero = NaN((endTime)/dt,sections);
Ac_ero = NaN((endTime)/dt,sections); Eroded = NaN((endTime)/dt,sections);
sandlossBasin = zeros((endTime)/dt,1); sandlossSea = zeros((endTime)/dt,1);
hw = NaN((endTime)/dt,sections); U = NaN((endTime)/dt,sections);
A_flow = NaN((endTime)/dt,sections);
width_water = NaN((endTime)/dt,sections); depth = NaN((endTime)/dt,sections);
Fr = zeros(1,8);

%% Initial conditions (30/03 09:30)
h_basin(1) = 1.0359;
GR = 1.5;            %Crest level of the dam above NAP
x1_inp = 50; x2_inp = 60; x3_inp = 160; x4_inp = 177; h_sill_inp = 1.5;
% Input of geometry

X1(1,:) = x1_inp * ones(1,sections) − abs(x2_inp − x1_inp) * GR / h_sill_inp;
X2(1,:) = x2_inp * ones(1,sections);
X3(1,:) = x3_inp * ones(1,sections);
X4(1,:) = x4_inp * ones(1,sections) + abs(x4_inp − x3_inp) * GR / h_sill_inp;
width_GR(1,:) = X4 − X1;
width_bed(1,:) = X3 − X2;
h_sill(1,:) = h_sill_inp * ones(1,sections);%[ 1.5 1.5 1.5 1.5 1.5 1.5 1.5 1.5];
Ac(1,:) = 0.5 .* (h_sill(1,:) + GR) .* ( width_GR(1,:) + width_bed(1,:));

for i = 1:sections
    gammaL(1,i) = atan( ( h_sill(1,i) + GR) / abs(X2(1,i) − X1(1,i)));
    gammaR(1,i) = atan( ( h_sill(1,i) + GR) / abs(X4(1,i) − X3(1,i)));
    hw(1,i) = h_sea(120) + (i+1) / (sections + 2) * ( h_basin(1) − h_sea(120) );
    depth(1,i) = h_sill(1,i) + hw(1,i);
    width_water(1,i) = width_bed(1,i) + depth(1,i) * (1/tan(gammaL(1,i))...
    + 1/tan(gammaR(1,i)));
```

```matlab
    A_flow(1,i) = 0.5 * depth(1,i) * ( width_bed(1,i) + width_water(1,i) );
    P(i) = width_bed(1,i) + depth(1,i) / sin( gammaL(1,i)) ...
    + depth(1,i) / sin(gammaR(1,i) ) ;
    R(1,i) = A_flow(1,i) / P(i);
    cf(i) = (1 / (5.75 * log( 12 * R(i) / ks ) ) )^2;
    cf_morph(i) = (1 / (5.75 * log( 12 * R(i) / (ks*morph_fac) ) ) )^2;
    U(1,i) = 0;
    Q(1) = 0;
    EL(1,i) = max(h_basin(1), h_sea_calc(1));
end
xi_outflow_dam(1) = 0;
for zz = 1:sections
        if zz ==1
            beta(1,zz) = atan( ( h_sill(1,zz+1) - h_sill(1,zz) ) / (2 * dx) );
            %dummycel has the value of the first cell
        elseif zz == sections
            beta(1,zz) = atan( (h_sill(1,zz) - h_sill(1,zz-1) ) / (2 * dx) );
            %dummycel has the value of the final cell

        else
            beta(1,zz) = atan( 0.5 * ( h_sill(1,zz+1) - h_sill(1,zz-1) ) / (2 * dx) );
        end
end
C(1,:) = zeros(1,sections);

%% determination of the water levels at sea
for tt = 1:endTime/dt
        if tt*dt + 120 < length(h_sea)
            if dt < 1
                h_sea_calc(tt) = h_sea(fix(tt*dt) + 120)
                + (tt * dt - fix(tt*dt)) * abs ( h_sea(fix(tt*dt) + 120)
                - h_sea(fix(tt*dt) + 121) );
            else
                h_sea_calc(tt) = h_sea(tt*dt + 120);
            end
        else
            break
        end
        test = isnan(h_sea_calc(tt));
        if test == 1
            h_sea_calc(tt) = h_sea_calc(tt-1) + (h_sea_calc(tt-1) - h_sea_calc(tt-2));
        end
end


for tt = 1:(endTime/dt) %7493
%% numerical flow calculation
        test_end = tt * dt;
test5 = isreal(Q);
if test5 == 0
   error('imaginaire nummers')
end
            if test_end < endTime
                h_basin(tt+1) = h_basin(tt) + Q(tt) / Ab * dt;
            end

            if h_sea_calc(tt) > h_basin(tt)
                display('instroom')
```

```matlab
                begin = 1;
                finish = sections;
                step = 1;
            else
                display('uitstroom')
                begin = sections;
                finish = 1;
                step = -1;
            end
    for zz = begin: step: finish
%% determination of the settling velocity
        [ws0, ws] = funSettlingVelocity( D50, C(tt,zz), g, visc, rho_S, rho_W );

%% Displacement dam as a consequence of production
        dxdt(tt,zz) = Q_prod(tt,zz) / ( (1-n0) * dx * (GR + h_sill(tt,zz)) ); %m/s
        dx_prod(tt,zz) = dxdt(tt,zz) * dt ; % m/timestep

%% sediment erosion
if xi_outflow_dam(tt) > 0.1
    if zz == 4 || zz == 5
        VF = 1;          % possible increase of the local friction for
    else                 % correction of the vortex street
        VF = 1;
    end
else
    VF = 1;
end
        if tt > 1
            [ ve_bot(tt,zz), vsed(tt,zz) ] = funero...
            ( n0, ni, rho_W, rho_S, g, visc, abs(U(tt,zz)), Ac(tt,zz),  cf_morph(tt,zz),...
             D50, k, phi, 0, beta(tt,zz), ws, C(tt,zz), ve_bot(tt-1,zz) );
            [ ve_sideL(tt,zz), vsed(tt,zz) ] = funero...
            ( n0, ni, rho_W, rho_S, g, visc, abs(U(tt,zz)), Ac(tt,zz), VF * cf_morph(tt,zz), ...
            D50, k, phi, gammaL(tt,zz), beta(tt,zz), ws, C(tt,zz), ve_sideL(tt-1,zz) );
            [ ve_sideR(tt,zz), vsed(tt,zz) ] = funero...
            ( n0, ni, rho_W, rho_S, g, visc, abs(U(tt,zz)), Ac(tt,zz), VF * cf_morph(tt,zz), ...
            D50, k, phi, gammaR(tt,zz), beta(tt,zz), ws, C(tt,zz), ve_sideR(tt-1,zz) );
        else
          [ ve_bot(tt,zz), vsed(tt,zz) ] = funero ...
          ( n0, ni, rho_W, rho_S, g, visc, abs(U(tt,zz)), Ac(tt,zz),  cf_morph(tt,zz),...
         D50, k, phi, 0, beta(tt,zz), ws, C(tt,zz), 0.0001 );
            [ ve_sideL(tt,zz), vsed(tt,zz) ] = funero ...
            ( n0, ni, rho_W, rho_S, g, visc, abs(U(tt,zz)), Ac(tt,zz),  VF * cf_morph(tt,zz), ...
            D50, k, phi, gammaL(tt,zz), beta(tt,zz), ws, C(tt,zz), 0.0001 );
            [ ve_sideR(tt,zz), vsed(tt,zz) ] = funero ...
            ( n0, ni, rho_W, rho_S, g, visc, abs(U(tt,zz)), Ac(tt,zz),  VF * cf_morph(tt,zz), ...
            D50, k, phi, gammaR(tt,zz), beta(tt,zz), ws, C(tt,zz), 0.0001 );
        end

%% Calculation of the bed and bank velocities
        v_bed(tt,zz) = ve_bot(tt,zz) - vsed(tt,zz);
        v_walL(tt,zz) = ( ve_sideL(tt,zz) ...
        - (depth(tt,zz) / (h_sill(tt,zz) +GR))*vsed(tt,zz) ) / abs(sin(gammaL(tt,zz)));
        v_walR(tt,zz) = ( ve_sideR(tt,zz) ...
        - (depth(tt,zz) / (h_sill(tt,zz) +GR))*vsed(tt,zz) ) / abs(sin(gammaR(tt,zz)));

%% Determine the new flow area after erosion/sedimentation, without production
        h_sill(tt+1,zz) = (h_sill(tt,zz) + v_bed(tt,zz) * dt) ;
```

```
        X1_ero(tt+1,zz) = X1(tt,zz) − v_walL(tt,zz) * dt;
        X2_ero(tt+1,zz) = X2(tt,zz) − v_walL(tt,zz) * dt;
        X3_ero(tt+1,zz) = X3(tt,zz) + v_walR(tt,zz) * dt;
        X4_ero(tt+1,zz) = X4(tt,zz) + v_walR(tt,zz) * dt;

%% Correction for too steep slopes
        gammaL(tt+1,zz) = atan( ( h_sill(tt+1,zz) + GR ) / abs(X2_ero(tt+1,zz) ...
        − X1_ero(tt+1,zz) ) );
        gammaR(tt+1,zz) = atan( ( h_sill(tt+1,zz) + GR ) / abs(X4_ero(tt+1,zz) ...
        − X3_ero(tt+1,zz) ) );
        if gammaL(tt+1,zz) > phi
            X1_ero(tt+1,zz) = X1_ero(tt+1,zz) − ( h_sill(tt+1,zz) + GR ) ...
            * ( tan(gammaL(tt+1,zz) − tan(phi)) );
            X2_ero(tt+1,zz) = X2_ero(tt+1,zz) + ( h_sill(tt+1,zz) + GR ) ...
            * ( tan(gammaL(tt+1,zz) − tan(phi)) );
            gammaL(tt+1,zz) = phi;
        end

        if gammaR(tt+1,zz) > phi
            X3(tt+1,zz) = X3_ero(tt+1,zz) − ( h_sill(tt+1,zz) + GR ) ...
            * ( tan(gammaL(tt+1,zz) − tan(phi)) );
            X4(tt+1,zz) = X4_ero(tt+1,zz) + ( h_sill(tt+1,zz) + GR ) ...
            * ( tan(gammaL(tt+1,zz) − tan(phi)) );
            gammaR(tt+1,zz) = phi;
        end

%% Determination of the amount of sand that erodes/settles
        width_bed_ero(tt+1,zz) = max(0, X3_ero(tt+1,zz) − X2_ero(tt+1,zz));
        width_GR_ero(tt+1,zz) = max(0, X4_ero(tt+1,zz) − X1_ero(tt+1,zz));

        if width_bed_ero(tt+1,zz) == 0
           WGL_ero = width_GR_ero(tt+1,zz) * (tan(gammaR(tt+1,zz)) / tan(gammaL(tt+1,zz))) ...
           / ( 1 + (tan(gammaR(tt+1,zz)) / tan(gammaL(tt+1,zz))) ) ;
            h_sill(tt+1,zz) =  WGL_ero * tan(gammaL(tt+1,zz)) − GR;
            X2_ero(tt+1,zz) = X1_ero(tt+1,zz) + WGL_ero;
            X3_ero(tt+1,zz) = X2_ero(tt+1,zz);
        end
        Ac_ero(tt+1,zz) = max(0, (h_sill(tt+1,zz) + GR) * 0.5 * ...
        ( width_bed_ero(tt+1,zz) + width_GR_ero(tt+1,zz) ) );

        if (Ac(tt,zz) − Ac_ero(tt+1,zz)) * ( 1 − n0 ) > C(tt,zz) * A_flow(tt,zz)
        % if more sedimentation than sand in water column
            sedimented = C(tt,zz) * A_flow(tt,zz) / (1−n0);
            Ac_ero(tt+1,zz) = Ac(tt,zz) − sedimented;
            width_bed_ero(tt+1,zz) = (2* Ac_ero(tt+1,zz) − (h_sill(tt+1,zz) + GR) ...
            * width_GR_ero(tt+1,zz) ) / (h_sill(tt+1,zz) + GR);
            extrwidth = width_bed_ero(tt+1,zz) − (X3_ero(tt+1,zz) −X2_ero(tt+1,zz));
            X2_ero(tt+1,zz) = X2_ero(tt+1,zz) − 0.5 * extrwidth;
            X3_ero(tt+1,zz) = X3_ero(tt+1,zz) + 0.5 * extrwidth;
        end

        if X3_ero(tt+1,zz) < X2_ero(tt+1,zz) || X4_ero(tt+1,zz) < X3_ero(tt+1,zz)
            X4_ero(tt+1,zz) = X3_ero(tt+1,zz)
%            KR2
        end
%% Determination new position of banks after production
        X4(tt+1,zz) = X4_ero(tt+1,zz);
    if X3_ero(tt+1,zz) − X2_ero(tt+1,zz) > dx_prod(tt,zz)
```

```
    % in dit geval wordt: width_bed = 0
        X1(tt+1,zz) = X1_ero(tt+1,zz) + dx_prod(tt,zz);
        X2(tt+1,zz) = X2_ero(tt+1,zz) + dx_prod(tt,zz);
        X3(tt+1,zz) = X3_ero(tt+1,zz);
        width_GR(tt+1,zz) = max(0, X4(tt+1,zz) - X1(tt+1,zz));
    else
        Ac(tt+1,zz) = Ac_ero(tt+1,zz) - Q_prod(tt,zz) * dt / ( (1-n0) * dx );
        h_sill(tt+1,zz) = sqrt( (2* Ac(tt+1,zz) * tan(gammaR(tt,zz)) )
        / ( 1 + (tan(gammaR(tt,zz)) / tan(gammaL(tt,zz)) ) ) ) - GR;
        width_GR(tt+1,zz) = Ac(tt+1,zz) / ( 0.5 * (h_sill(tt+1,zz)+GR) );
        X1(tt+1,zz) = X4(tt+1,zz) - width_GR(tt+1,zz);
        X2(tt+1,zz) = X1(tt+1,zz) + (GR + h_sill(tt+1,zz)) / tan(gammaL(tt,zz));
        X3(tt+1,zz) = X2(tt+1,zz);
    end
        if X3(tt+1,zz) < X2(tt+1,zz) || X4(tt+1,zz) < X3(tt+1,zz)
            KR2
        end


        width_bed(tt+1,zz) = max(0, X3(tt+1,zz) - X2(tt+1,zz));
        if width_bed(tt+1,zz) == 0
            WGL = width_GR(tt+1,zz) * (tan(gammaR(tt+1,zz)) / tan(gammaL(tt+1,zz))) ...
            / ( 1 + (tan(gammaR(tt+1,zz)) / tan(gammaL(tt+1,zz))) ) ;
            h_sill(tt+1,zz) =  WGL * tan(gammaL(tt+1,zz)) - GR;
        else
            Ac(tt+1,zz) = max(0, ( h_sill(tt+1,zz) + GR ) * 0.5 * ...
            ( width_bed(tt+1,zz) + width_GR(tt+1,zz) ) );
        end
    end
%% Flow model
        BHP = 4; % first section of horizontal production
        EHP = 5; % last section of horizontal production
         [ Q(tt+1), Fr(tt+1,:), EL(tt+1,:), hw(tt+1,:), U(tt+1,:), A_flow(tt+1,:), ...
          width_water(tt+1,:), xi_outflow_dam(tt+1) ] = funflow2...
            ( g, cf(tt,:), L0, R(tt,:), h_sea_calc(tt+1), h_basin(tt+1), h_sill(tt+1,:), ...
             A_flow(tt,:), U(tt,:), width_bed(tt+1,:), ...
            gammaR(tt+1,:), gammaL(tt+1,:), BHP, EHP, sections, Fr(tt,:) );
        depth(tt+1,:) = hw(tt+1,:) + h_sill(tt+1,:);


    for zz = begin: step: finish
%% friction again, after the closure calculations
        P(tt+1,zz) = width_bed(tt+1,zz) + depth(tt+1,zz) / sin( gammaL(tt+1,zz)) ...
         + depth(tt+1,zz) / sin(gammaR(tt+1,zz) ) ;
        R(tt+1,zz) = A_flow(tt+1,zz) / P(tt+1,zz);
        cf(tt+1,zz) = (1 / (5.75 * log10( 12 * R(tt+1,zz) / ks ) ) )^2;
        cf_morph(tt+1,zz) = (1 / (5.75 * log( 12 * R(tt+1,zz) / (ks*morph_fac) ) ) )^2;

%% Concentratie van zand in het water
        Eroded(tt,zz) = ( Ac_ero(tt+1,zz) - Ac(tt,zz) ) * ( 1 - n0 ) / A_flow(tt+1,zz);
if Eroded < C(tt+1,zz) * A_flow(tt+1,zz)
    KR_ERO
end

        sigma = U(tt,zz) * dt / dx;
        if sigma > 0
            if zz > 1
                C(tt+1,zz) = C(tt,zz) - sigma * ( C(tt,zz) - C(tt,zz-1) );
```

```matlab
        else
            C(tt+1,zz) = C(tt,zz) − sigma * ( C(tt,zz) − 0 );
        end
    else
        if zz < sections
            C(tt+1,zz) = C(tt,zz) − sigma * ( C(tt,zz+1) − C(tt,zz) );
        else
            C(tt+1,zz) = C(tt,zz) − sigma * ( 0 − C(tt,zz) );
        end
    end
        C(tt+1,zz) =  C(tt+1,zz) * A_flow(tt,zz) / A_flow(tt+1,zz) + Eroded(tt,zz)...
         + CMS_prod(tt,zz) * dt / ( A_flow(tt+1,zz) * dx);
% Check for negative concentrations, Winst should be zero at the end of the simulation
    if C(tt+1,zz) < 0
        Winst(tt,zz) = C(tt+1,zz) * A_flow(tt+1,zz) * dx;
        C(tt+1,zz) = 0;
    end


%% moment of closure
    if A_flow(tt+1,zz) <= 0 || depth(tt+1,zz) <= 0 || width_water(tt+1,zz) <= 0 || ...
     C(tt+1,zz) > (1−n0)
        hours = floor(tt * dt /3600);        % duration of the simulation in real life
        min = floor( (tt * dt /3600 − hours) * 60);
        sec = ((tt * dt /3600 − hours) * 60 − min) * 60;
        closingtime = datevec(STARTMODEL + tt/dt * 60);
        disp(['The dam is closed after: ' num2str(hours) 'h, ' num2str(min) ...
         'min and ' num2str(sec) 'sec'])
        damisconstructed = 1;
    end
%% Determination of the bed slope
if Q(tt+1) > 0
        if zz ==1
            beta(tt+1,zz) =  atan( ( h_sill(tt+1,zz) − h_sill(tt+1,zz+1) ) / (2 * dx) );
            %dummycel has the value of the first cell
        elseif zz == sections
            beta(tt+1,zz) = atan( (h_sill(tt+1,zz−1) − h_sill(tt+1,zz) ) / (2 * dx) );
            %dummycel has the value of the final cell
        else
            beta(tt+1,zz) = atan( ( h_sill(tt+1,zz−1) − h_sill(tt+1,zz+1) ) / (2 * dx) );
        end
else
        if zz ==1
            beta(tt+1,zz) =  atan( ( h_sill(tt+1,zz+1) − h_sill(tt+1,zz) ) / (2 * dx) );
            %dummycel has the value of the first cell
        elseif zz == sections
            beta(tt+1,zz) = atan( (h_sill(tt+1,zez) − h_sill(tt+1,zz−1) ) / (2 * dx) );
            %dummycel has the value of the final cell
        else
            beta(tt+1,zz) = atan( ( h_sill(tt+1,zz+1) − h_sill(tt+1,zz−1) ) / (2 * dx) );
        end
end


    end


if damisconstructed == 1
```

```matlab
        break
    end
end

%% sand losses
for q = 1:length(Q)
    if Q(q) > 0
        sandlossBasin(q) = dt * abs(C(q,sections) * Q(q)) / 0.6;
    else
        sandlossSea(q) = dt * abs(C(q,1) * Q(q)) /0.6;
    end
    if q == 1
        CumSandloss(q) = max(sandlossBasin(q), sandlossSea(q) );
    else
        CumSandloss(q) = CumSandloss(q-1) + sandlossBasin(q) + sandlossSea(q);
    end
end
```

funproduction

```
function [ Q_prod, CMS_prod ] = funproduction( endTime, dt, sections, starttime )
%% 30/03 vanaf 05:40

Q_prod = zeros(endTime/dt, sections);
CMS_prod = zeros(endTime/dt, sections);

k = sections / 8;
S = k * [1 2 3 4 5 6 7 8];
finishtime = (starttime+endTime)/dt;

for tt = 1+starttime/dt:finishtime
    for zz = 1:sections
        if tt >= 4140 / dt && tt < 7980 / dt % 1h 9 min Rit 2471 Utrecht
            if zz > S(4-1) && zz <= S(5)
                CMS_prod(tt-starttime/dt,zz) = CMS_prod(tt-starttime/dt,zz) + 2.73...
                    * 0.6 * ( 4 / sections ); % 10507/3840
            end
        end

        if tt >= 14880 / dt  && tt < 18720 / dt % rit 2472 Utrecht
            if zz > S(3-1) && zz <= S(4)
                CMS_prod(tt-starttime/dt,zz) = CMS_prod(tt-starttime/dt,zz) +  2.67...
                    * 0.6 * ( 4 / sections );
            end
        end

        if tt >= 26640 / dt && tt < 30720 / dt % ritnummer 2473 Utrecht
            if zz > S(5-1)  && zz <= S(8)
                CMS_prod(tt-starttime/dt,zz) = CMS_prod(tt-starttime/dt,zz) + 2.60...
                    * 0.6 * ( 2 / sections );
            end
        end

        if tt >= 38400 / dt && tt < 42060 / dt % ritnummer 2474 Utrecht
            if zz > S(5-1) && zz <= S(6)
                CMS_prod(tt-starttime/dt,zz) = CMS_prod(tt-starttime/dt,zz) + 2.87...
                    * 0.6 * ( 4 / sections );
            end
        end

        if tt >= 48600 / dt && tt < 52200 / dt % ritnummer 2499 Prins
            if zz > S(1-1) && zz <= S(2)
                CMS_prod(tt-starttime/dt,zz) = CMS_prod(tt-starttime/dt,zz) + 3.36...
                    * 0.6 * ( 4 / sections );
            end
        end

        if tt >= 61200 / dt && tt < 64800 / dt   % ritnummer 2500 prins
            if zz > S(1-1) && zz <= S(4)
                CMS_prod(tt-starttime/dt,zz) = CMS_prod(tt-starttime/dt,zz) + 3.26...
                    * 0.6 * ( 2 / sections );
            end
        end
```

```matlab
        %% 31/03 tot sluiting
        if tt >= 74100 / dt && tt < 77700 / dt    % ritnummer 2501 prins
            if zz > S(1-1) && zz <= S(2)
                CMS_prod(tt-starttime/dt,zz) = CMS_prod(tt-starttime/dt,zz) + 3.21...
                 * 0.6 * ( 4 / sections );
            end
        end

        if tt >= 85500 / dt && tt < 88800 / dt    % ritnummer 2502 prins
            if zz > S(3-1) && zz <= S(4)
                CMS_prod(tt-starttime/dt,zz) = CMS_prod(tt-starttime/dt,zz) + 3.60...
                 * 0.6 * ( 4 / sections );
            end
        end

        if tt >= 108900 / dt && tt < 113400 / dt % ritnummer 2504 Prins
            if zz > S(4-1) && zz <= S(5)
                Q_prod(tt-starttime/dt,zz) = Q_prod(tt-starttime/dt,zz) + 2.75...
                 * 0.6 * ( 4 / sections );

            end
        end

        if tt >= 121800 / dt && tt < 125700 / dt  % ritnummer 2505 Prins
            if zz > S(4-1) && zz <= S(5)
                Q_prod(tt-starttime/dt,zz) = Q_prod(tt-starttime/dt,zz) + 3.05...
                 * 0.6 * ( 4 / sections );

            end
        end

        if tt >= 134100 / dt && tt < 147800 / dt  % ritnummer 2506 Prins
            if zz > S(4-1) && zz <= S(5)
                Q_prod(tt-starttime/dt,zz) = Q_prod(tt-starttime/dt,zz) + 2.45...
                 * 0.6 * ( 4 / sections );
            end
        end
    end
end

end
```

funSettlingVelocity

```
function [ws0, ws] = funSettlingVelocity( D50, cb, g, visc, rho_S, rho_W )


Delta = ( rho_S - rho_W ) / rho_W;  % relative density

% determination of the settling velocity according to Van Rijn (1993) p
% 3.13

if D50 < 100*10^-6
    ws0 = Delta * g * D50^2 / (18 * visc);
elseif D50 < 1000*10^-6
    ws0 = 10 * visc / D50 * ( sqrt( 1 + ( 0.01 * Delta * g * D50^3 )/(visc^2) ) - 1);
else
    ws0 = 1.1 * sqrt( Delta * g * D50 );
end

% Determination hindered settling velocity


 Re_p = ws0 * D50 * visc;              % particle raynolds number

if Re_p < 0.2
   beta = 4.65 ;
elseif Re_p < 1
    beta = 4.35 * Re_p^-0.03;
elseif Re_p <200
    beta = 4.45 * Re_p^-0.1;
else
    beta = 2.39;
end

ws = ws0 * (1 - cb)^beta;            % hindered settling velocity

% disp(['Settling velocity calculated by [Willems 2013] ' char(169)] )
end
```

funero

```
function [ ve, vsed] = funero( n0, ni, rho_W, rho_S, g, visc, U, Ac, cf, D50, k, phi,...
 gamma, beta, ws, cnb, ve_initial )

Delta = ( rho_S − rho_W ) / rho_W;
A = 1 / (1−n0);
D_star = D50 * ( (Delta*g)/visc^2)^(1/3);


%% Determination of The critical shields parameter
if D_star <= 4
    thetaCR = 0.24 * D_star^(−1);
elseif D_star <= 10
    thetaCR = 0.14 * D_star^(−0.64);
elseif D_star <= 20
    thetaCR = 0.04 * D_star^(−0.1);
elseif D_star <= 150
    thetaCR = 0.013 * D_star^(0.29);
elseif D_star > 150
    thetaCR = 0.055;
end


k_beta = sin(phi−beta) / sin(phi);  %niet gebruikt in Van Rhee, zit al in de
Van Rhee formulering
if gamma < phi
    k_gamma = cos(gamma) * sqrt( 1 − ( tan(gamma)^2 / tan(phi)^2 ) );
    thetaCR = thetaCR * k_gamma;
end
vsed = rho_S * ws * cnb / (rho_S * (1−n0−cnb));

phi_p = zeros(1,length(U));

for j = 1:length(U)
    u_star = sqrt(cf * U(j)^2);          % vloeistofmechanica(p.213)
    theta = u_star^2 / (Delta*g*D50);
    if U(j)<1
        %% Van Rijn
        if theta<thetaCR * k_beta
            ve(j) = 0;
        else
            phi_p(j) = 0.00033 * D_star^0.3 * ( (theta − thetaCR*k_beta) ...
             / (thetaCR*k_beta) )^1.5;
            ve(j) = ( phi_p(j) * sqrt(Delta * g * D50) ) / ( 1−n0−cnb );
        end
    else
        %% Van Rhee

        %% iteration to determine ve
        maxiter = 100; % maximum iteration steps
        ve_iter = zeros(1,maxiter); %0.0000001:0.0000001:0.01;
        ve_iter(1) = ve_initial;
        for m = 1: length(ve_iter)
            i = (ve_iter(m)/k) * ( (ni−n0) / (1−ni) );
            thetaCR1 = thetaCR * (sin(phi − beta)/(sin(phi) ) + A*(i/Delta));
```

```matlab
            if theta < thetaCR1 || thetaCR1<0
                phi_p(j) = 0;
            else
                phi_p(j) = 0.00033 * D_star^0.3 * ( (theta - thetaCR1) / thetaCR1)^1.5;
            end
            ve_iter2 = ( phi_p(j) * sqrt(Delta * g * D50) ) / ( 1-n0-cnb );

            if abs(ve_iter2-ve_iter(m)) < abs(0.01*ve_iter(m))
                disp(['Iteration stopped after ' num2str(m) ' interation steps '])
                ve(j) = ve_iter2;
                break
            elseif ve_iter2 < ve_iter(m)
                ve_iter(m+1) = ve_iter2 + abs( ve_iter2 - ve_iter(m)) /2;
            else
                ve_iter(m+1) = ve_iter2 - abs( ve_iter2 - ve_iter(m)) /2;
            end
            if phi_p(j) == 0
                ve(j) = 0;
                break
            end
            if m == maxiter
                disp(['The iteration could not finnish the iteration in ' ...
                 num2str(maxiter) ' interation steps '])
            end
        end
    end
    v_bed(j) = ve(j) - vsed;
end


end
```

funflow2

```
function [ Q, Fr, EL, hw, U, A_flow, width_water,  xi_outflow_dam ] = funflow2( g, cf, L, R, h_sea

H0 = max(h_basin,h_sea); %+ h_sill; % reference at N.A.P. - h_sill than highest of h_sea, h_basin
ht = min(h_basin,h_sea); %+ h_sill;
mu_in = 0.6;

if h_sea > h_basin
    xi_friction = 2 * cf(8) * 2 * L / R(8);
    if A_flow(BHP)/A_flow(BHP- 1) <= 0.01
        mu_dam = 0.60;
    elseif A_flow(BHP)/A_flow(BHP-1) <= 0.2
        mu_dam = 0.62;
    elseif A_flow(BHP)/A_flow(BHP-1) <= 0.6
        mu_dam = 0.7;
    elseif A_flow(BHP)/A_flow(BHP-1) <= 0.8
        mu_dam = 0.77;
    else
        mu_dam = 1;
    end
else
    xi_friction = 2 * cf(1) * 2 * L / R(1);
    if A_flow(EHP)/A_flow(EHP +1) <= 0.01
        mu_dam = 0.6;
    elseif A_flow(EHP)/A_flow(EHP +1) <= 0.2
        mu_dam = 0.62;
    elseif A_flow(EHP)/A_flow(EHP +1) <= 0.6
        mu_dam = 0.7;
    elseif A_flow(EHP)/A_flow(EHP +1) <= 0.8
        mu_dam = 0.77;
    else
        mu_dam = 1;
    end
end


xi_contraction_in = ((1 / mu_in) - 1)^2;
xi_outflow_out = 1;


if h_sea > h_basin
    xi_contraction_dam = ((A_flow(BHP)/(A_flow(BHP-1) * mu_dam)) - 1)^2;
    xi_outflow_dam = (1 - A_flow(EHP)/A_flow(EHP+1))^2;
else
    xi_contraction_dam = ((A_flow(EHP)/(A_flow(EHP+1) * mu_dam)) - 1)^2;
    xi_outflow_dam = (1 - A_flow(BHP)/A_flow(BHP-1))^2;
end

xi_total = xi_contraction_in + xi_contraction_dam + xi_outflow_dam + ...
    xi_outflow_out + xi_friction;

dHv_total = abs(H0 - ht);
U_el = sign(h_sea - h_basin) * sqrt(dHv_total * 2 * g / xi_total);
```

```matlab
    if U > 0
        begin = 1;
        finish = sections;
        step = 1;
        BHD = BHP;
        EHD = EHP;
    else
        begin = sections;
        finish = 1;
        step = -1;
        BHD = EHP;
        EHD = BHP;
    end
    Q = U_el * A_flow(finish);
for z = begin:step:finish
    if A_flow == 0
        Q = 0;
        break
    end
    if Q >0
        if z == begin
            EL(z) = H0 - (xi_contraction_in + (1/8)*xi_friction )  * U_el^2 / (2*g);
        elseif z > 1 && z < BHD
            EL(z) = EL(z-step) - ((1/8)*xi_friction) * U_el^2/(2*g);
        elseif z == BHD
            EL(z) = EL(z-step) - ((1/8)*xi_friction + xi_contraction_dam) * U_el^2/(2*g);
        elseif z > BHD && z <= EHD
            EL(z) = EL(z-step) - ((1/8)*xi_friction) * U_el^2 / (2*g);
        elseif z == (EHD+step)
            EL(z) = EL(z-step) - ((1/8)*xi_friction+xi_outflow_dam) * U_el^2 / (2*g);
        else
            EL(z) = EL(z-step) - ((1/8)*xi_friction) * U_el^2 / (2*g);
        end
    else
        if z == begin
            EL(z) = H0 - (xi_contraction_in + (1/8)*xi_friction )  * U_el^2 / (2*g);
        elseif z < begin && z > BHD
            EL(z) = EL(z-step) - ((1/8)*xi_friction) * U_el^2/(2*g);
        elseif z == BHD
            EL(z) = EL(z-step) - ((1/8)*xi_friction + xi_contraction_dam) * U_el^2/(2*g);
        elseif z < BHD && z >= EHD
            EL(z) = EL(z-step) - ((1/8)*xi_friction) * U_el^2 / (2*g);
        elseif z == (EHD+step)
            EL(z) = EL(z-step) - ((1/8)*xi_friction+xi_outflow_dam) * U_el^2 / (2*g);
        else
            EL(z) = EL(z-step) - ((1/8)*xi_friction) * U_el^2 / (2*g);
        end
    end
end
U = Q ./ A_flow;
for i = 1:sections
    hw(i) = ht + 0.5 * (H0-ht); % only for determination of flow is critical
    depth(i) = hw(i) + h_sill(i);
    width_water(i) = width_bed(i) + (hw(i) + h_sill(i)) / tan(gammaL(i)) + ...
    (hw(i) + h_sill(i)) / tan(gammaR(i));
    A_flow(i) = max(0,(hw(i) + h_sill(i)) * 0.5 * (width_bed(i)+width_water(i)));
    P(i) = width_bed(i) + (hw(i) + h_sill(i)) / sin(gammaL(i)) + (hw(i) + ...
    h_sill(i)) / sin(gammaR(i));
```

```
    R(i) = A_flow(i) / P(i);
    T(i) = A_flow(i) / width_water(i);
end
    Fr = abs(U) ./ sqrt( T .* g);
    kritSec = min(find(Fr==max(Fr)));
        if Fr(kritSec) > 1

            Ec = H0 + h_sill(kritSec);%EL(kritSec) + h_sill(kritSec);
            dc = max(0, 2/3 * Ec); % critical depth
            width_water(kritSec) = width_bed(kritSec) + dc / tan(gammaL(kritSec))...
            + dc / tan(gammaR(kritSec)) ;
            Ac_crit = 0.5 * dc * (width_bed(kritSec) + width_water(kritSec)) ;
            R_crit = Ac_crit / ( width_bed(kritSec) + dc / sin(gammaR(kritSec))...
             + dc / sin(gammaL(kritSec)) ) ;
            Ucr = sign(h_sea - h_basin) * sqrt(g*dc);
            Q = Ucr * Ac_crit;
            xi_hager = (H0+h_sill(kritSec)) / ( (H0+h_sill(kritSec)) + L );
            if ht > 0 - h_sill(kritSec)
                yL = 0.85 - 0.5 * xi_hager;
                yT = (ht+h_sill(kritSec)) / (H0+h_sill(kritSec));
                n = 7; % mag aangepast worden, zie artikel Hager
                psi = ( 1 - ( ( yT - yL) / (1 - yL) ) )^( 1/n);
                if psi>1
                    psi = 1;
                end
                Q = Q * psi;
            end
            for i = 1:sections
                 if i == kritSec
                    U(i) = Q / A_flow(i);
                    hw(kritSec) = dc - h_sill(kritSec);
                    width_water(kritSec) = width_bed(i) + (hw(i) + ...
                    h_sill(i)) / tan(gammaL(i)) + (hw(i) + h_sill(i)) / tan(gammaR(i));
                    A_flow(kritSec) = Ac_crit;
                 else
                    U(i) = Q / A_flow(i);
                    hw(i) = EL(i) - U(i)^2 / (2*g);
                    width_water(i) = width_bed(i) + (hw(i) + h_sill(i)) / tan(gammaL(i)) ...
                    + (hw(i) + h_sill(i)) / tan(gammaR(i));
                    A_flow(i) = max(0,(hw(i) + h_sill(i)) * 0.5 ...
                     * (width_bed(i)+width_water(i)));
                 end
            end
        else
            for i = 1:sections
                    U(i) = Q / A_flow(i);
                    hw(i) = EL(i) - U(i)^2 / (2*g);
                    width_water(i) = width_bed(i) + (hw(i) + h_sill(i)) / tan(gammaL(i)) ...
                     + (hw(i) + h_sill(i)) / tan(gammaR(i));
                    A_flow(i) = max(0,(hw(i) + h_sill(i)) * 0.5 * ...
                     (width_bed(i)+width_water(i)));
            end
        end
end
```